CHARACTERIZATION OF UNCERTAINTY IN MODEL PARAMETER AND PRECIPITATION DATA ACROSS SEVERAL HEADWATER CATCHMENTS IN THE CANADIAN ROCKIES: A LARGE-SAMPLE HYDROLOGY APPROACH

A Thesis Submitted to the College of Graduate and Postdoctoral Studies

In Partial Fulfillment of the Requirements for the

Degree of Master of Environment and Sustainability

In the School of Environment and Sustainability

University of Saskatchewan, Saskatoon

By

SAHAR SAFAEI

PERMISSION TO USE

In presenting this thesis in partial fulfilment of the requirements for a postgraduate degree from the University of Saskatchewan, I agree that the Libraries of this University may make it freely available for inspection. I further agree that permission for copying of this thesis in any manner, in whole or in part, for scholarly purposes may be granted by the professor or professors who supervised my thesis work or, in their absence, by the Head of the Department or the Dean of the College in which my thesis work was done. It is understood that any copying or publication or use of this thesis or parts thereof for financial gain shall not be allowed without my written permission. It is also understood that due recognition shall be given to me and to the University of Saskatchewan in any scholarly use which may be made of any material in my thesis.

Requests for permission to copy or to make other use of material in this thesis in whole or part should be addressed to:

School of Environment and Sustainability

University of Saskatchewan

Room 323 Kirk Hall, 117 Science Place

Saskatoon, Saskatchewan, S7N 5C8, Canada

College of Graduate and Postdoctoral Studies

Room 116 Thorvaldson Building, 110 Science Place

Saskatoon, Saskatchewan, S7N 5C9, Canada

ABSTRACT

Hydrologic modelling and prediction in the Canadian Rookies are hampered by the sparsity of hydro-climatic data, limited accessibility, and the complexity of the cold regions hydrologic processes. Previous studies in this region have mainly focused on very few heavily instrumented catchments, typically with limited generalizability to other catchments in the region. In this thesis, I adopt a "large-sample hydrology" approach to address some of the outstanding issues pertaining to data uncertainty, model parameter identifiability, and predictive power of hydrologic modelling in this region. My analyses cover 25 catchments with a range of physiographic and hydrologic properties located across the Canadian Rockies. To address forcing data uncertainty, which is commonly considered as the most dominant source of uncertainty in the hydrology of this region, I processed and utilized three different gridded-data products, namely ANUSPLIN, CaPA, and WFDEI. To make the problem tractable, I applied an efficient-to-run conceptual hydrologic model to simulate the hydrologic processes in this region under a variety of parameter and input data configurations.

My analyses showed significant discrepancies in precipitation amounts between the different climate data products with varying degrees across the different catchments. Runoff ratios were quite variable under the different products and across the catchments, ranging from 0.25 to 2, highlighting the significant uncertainty in precipitation amounts. To handle precipitation uncertainty in hydrologic modelling, I developed and tested two strategies: (1) implementing a correction parameter for each data product separately, and (2) developing and parameterizing a linear combination of the different data products to have a unified, presumably more accurate data product. These new precipitation-correcting parameters along with a selected set of the hydrologic model parameters were analyzed and identified via Monte-Carlo simulation, considering three model performance criteria on streamflow simulation, namely Nash-Sutcliffe Efficiency (NSE), NSE on log-transformed streamflow (NSE-Log), and Percent Bias (PBias). Overall, the hydrologic model showed adequate performance in reproducing observed streamflows in most of the catchments, with NSE, NSE-Log, and PBIAS ranging in 0.36-0.87, 0.43-88, and 0.001%-34%, respectively. However, most of the model parameters showed limited identifiability, limiting the power of the model for the assessment of climate and land cover changes. Overall, WFDEI climate data provided the best performance in parameter identification, while demonstrating a superior performance in reproducing observed streamflows.

ACKNOWLEDGEMENTS

I am foremost thankful to the NSERC (Natural Sciences and Engineering Research Council of Canada), CREATE for Water Security, Global Institute for Water Security, SENS (School of Environment and Sustainability), and The College of Graduate and Postdoctoral Studies for providing me financial support for my study and thesis work.

I would like to thank my supervisor, Dr. Saman Razavi for his constant encouragement to complete the research work. I am incredibly grateful for everything he has done in favor of my personal and professional growth.

I would like to express my deepest appreciation to my committee members, Prof. Howard Wheater, Dr. Alain Pietroniro, Dr. Warren Helgason, and Dr. Yanping Li for their guidance, motivation and reviewing my thesis.

I would also like to acknowledge Dr. Amin Haghnegahdar and Dr. Shervan Gharari for their help in solving many of my problems during my research. This work would not have been possible without their support.

I would also like to thank all my friends who helped and motivated me, specially Dr. Jeff Wong, Razi Sheikholeslami, and Fuad Yassin.

My beloved spouse Jamal Taghavimehr and my lovely parents, Masoud and Foroogh Safaei deserve special acknowledgement since they have always stood by me and given me strength to bear all hardships.

DEDICATION

This thesis is dedicated to

My spouse, Jamal Taghavimehr,

My father, Masoud Safaei, and

My mother, Foroogh Safaei

Table of Contents

List of Figures

List of Tables

1 Introduction

1.1 Motivation

Water is a critical natural resource that plays a vital role in public health, the economy, food production and the environment. Concurrent with a growing world population, the demand for water is increasing and the pressure on limited freshwater resources is escalating. It has been reported that global water use has more than doubled in the last 50 years (Wada et al., 2013).

The management of freshwater resources is becoming more challenging in the presence of climate change and increasing development. Effective freshwater management is of vital importance for Canada; reduced river flows, decreasing groundwater and lake levels and increasing water temperature in southern Canada have been associated with climate change and increasing water demand (National Water Research Institute, Environment Canada, 2004). Despite the demonstrated effects of climate change and development on water in Canada, water availability in the country remains the second-highest globally; yet, some communities are experiencing water supply shortages caused by decreasing water quantity and/or quality (Sullivan, 2002). Additionally, researchers have shown that as a result of climate change impacts, the frequency of extreme events, such as heavy precipitation events and droughts for example, is increasing (Karl, Knight, and Plummer, 1995; Tsonis, 1996). The increased frequency of extreme events translates to lower confidence in system prediction (Tsonis, 2004). Since extreme events can have devastating and long-lasting effects on communities and infrastructure, it is important that models for their prediction are improved.

By predicting future streamflow using hydrological models, hydrologists can provide estimates of future water supply. These estimates are important to manage and maintain existing water resources and to mitigate the impact of natural disasters (Razavi, 2014). However, there remains scope to reduce the uncertainty associated with hydrological models, thereby increasing the value of model predictions in water resources management. In particular, the reduction of uncertainty within hydrological simulations for mountainous headwater catchments that act as ‘water towers’, contributing the vast majority of flow in a river basin, would contribute greatly in

improving hydrological simulations. By characterizing the uncertainty within hydrological model parameter and precipitation data for mountainous headwater catchments, this study will hopefully contribute to reliable predictions of water availability in the future.

1.2 Problem Statement and Objectives

The Rockies act as 'water towers', and are therefore hydrologically very important for rivers that rise from this mountain range. For example, on an average year, the Rockies contribute 90% of the flow in the Saskatchewan River, which extends eastwards, supplying water to the Prairie Provinces. In recent decades, water demand has increased due to population and economic growth, thereby placing increasing pressure on this area (Wheater and Gober, 2013). Moreover, according to climate and land use change data, streamflow within the river is changing, thereby increasing concerns regarding the future capacity of the river to supply water and support economic productivity. Within the aforementioned context, the main objectives of this study are:

- Analyzing of the hydro-climatic data of the catchments falling within the Canadian Rockies using different database products. In addition, improving streamflow estimation using the semi-distributed HBV-EC model (Moore, 1993). The findings can allow us to quantify runoff components and to identify the dominant hydrological processes. Finally, the comprehensive information collected in basins can be used to provide a more accurate prediction of streamflow time series for both gauged and ungauged basins

- Investigating the parameter uncertainty and identifiability of HBV-EC model parameters using Monte Carlo simulation.

- Identifying and understanding the uncertainty related to the forcing data: (i) How accurate are the different precipitation datasets for streamflow simulations? (ii) What is the effect of uncertain input data (precipitation) on the streamflow estimation? (iii) How will the model components compensate for precipitation inaccuracy?

1.3 Thesis Layout

The thesis layout is as follows:

Chapter 2: Hydrology and Hydrological Modelling in a Changing World

Chapter 2 is a literature review, and provides a summary of hydrological modelling, different models and the distinction between conceptually- and physically-based, lumped and distributed models, with a focus on basins of the Canadian Rockies. A further literature review is provided regarding uncertainties of parameters and input precipitation data.

Chapter 3: Materials and Methods

This chapter presents the hydro-climatic information of the region along with physical characteristics, locations and land cover of the basins. The chapter also provides a detailed description of forcing data (precipitation, temperature and evapotranspiration) used to run the model and also a conceptual description of the semi-distributed HBV-EC model.

Chapter 4: Results and Discussion

Chapter 4 provides general results and discussion of hydrometric and climatic data analysis for 25 basins, with specific results discussed for five basins. The performance of model using different forcing data and results of parameter uncertainty and identifiability are also elaborated.

Chapter 5: Conclusions

Chapter 5 provides a summary of the main conclusions alongside with recommendations for future research.

2 Hydrology and Hydrological Modelling in a Changing World

Hydrology tries to answer the need for understanding water movement in the atmosphere and on the earth to help in solving water problems. Hydrological cycle is portrayed by a simplified diagram in figure 2.1; this process includes: evapotranspiration (water going into the atmosphere), condensation (forming of clouds); precipitation (in various form, such as rain, snow, sleet and hail), runoff (flow of rainwater on the earth's surface and in surface water bodies), and infiltration and percolation (water infiltrating into the earth and recharge groundwater bodies). The water movement from the earth's surface to the atmosphere is mainly driven by solar energy, while the water movement at and below the surface of the earth is mainly driven by gravity. Hydrological cycle maintaining the heat balance of the earth, trough moving and redistributing water masses (Blasone, 2007).

Understanding hydrological process (i.e. evaporation, infiltration, snowmelt, baseflow and peakflow) and climatic variability including streamflow, precipitation, and the temperature is an essential part of water resource and environmental sciences. For achieving sustainable land development and managing and maintaining the existing water resources, scientific research on the hydrological processes in space and time is crucial. Ever increasing anthropogenic changes across watersheds, together with the presence of climate change, results in non-stationarity of hydrologic processes. Significant research still lies ahead to properly address both the issue of "non-stationarity" and "uncertainty estimate" in the context of hydrology and eventually streamflow estimation.

Good progress has been made in the understanding of hydrological processes particularly after the development of the science initiative of predictions in the ungauged basins (PUB) that was proceeded by the International Association of Hydrological Science (IAHS) in 2003 (Hrachowitz et al., 2013; Sivapalan, 2003). The PUB initiative was created with the main purpose of reducing uncertainty in hydrological predictions. It addresses the streamflow prediction using new approaches which are based firstly on improved understandings and representations of physical processes within and around the hydrological cycle and improve their capacity to make

predictions in the ungauged basins (Sivapalan, 2003). Consequently, a decade of predictions in the ungauged basins has led to considerable advancement in scientific understanding of hydrological processes, new methods for data collection and model development, uncertainty analysis, classification of basins and progress of hydrological theories (Hrachowitz et al., 2013). And numerous researchers tried to find out the importance of additional data, new measurements, and modeling the hydrological processes at ungauged catchments (Fenicia, McDonnell, and Savenije, 2008; Hrachowitz et al., 2013; Lehmann et al., 2007; Son and Sivapalan, 2007; Uhlenbrook and Wenninger, 2006; Winsemius, 2009).

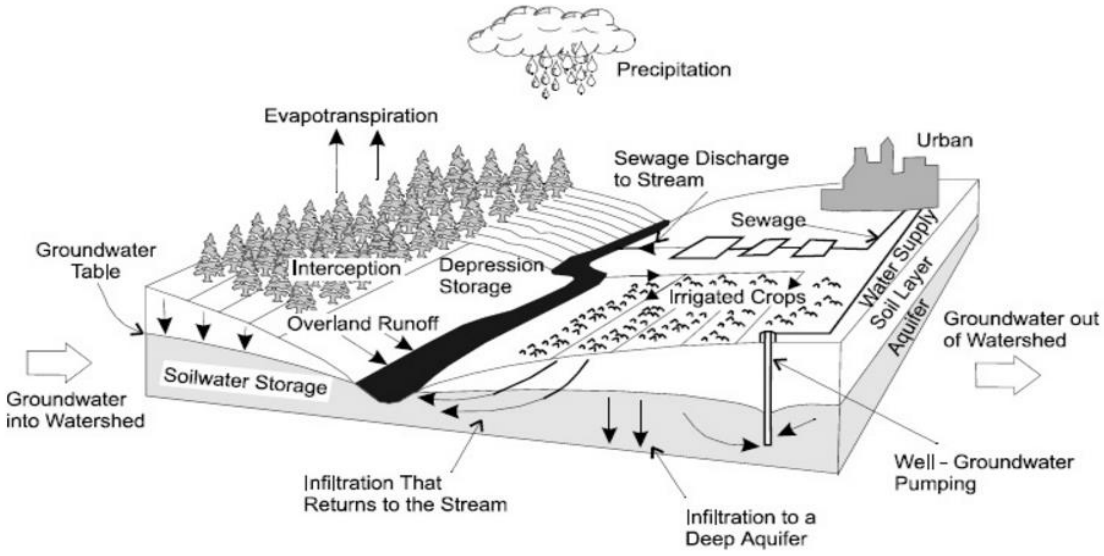

Figure 2.1: Schematic of hydrologic cycle (Ontario Stormwater Management Planning & Design Manual, 2003)

2.1 Hydrological Modelling

A model is a simplified representation of the real-world system and the ideal model is the one that generates results very close to reality using of least parameters and also model complexity. And hydrological modelling is the discipline that tries to quantitatively describe the terrestrial processes of the hydrological cycle (Singh and Woolhiser, 2002). Rainfall-runoff (or hydrologic) models simulate the hydrologic cycle using watersheds physical and climatological characteristics over a broad range of space, time and (potential) climate (Devia, Ganasri, and Dwarakish, 2015)

Hydrologic models are effective tools both for operational and research purposes. They have been applied extensively to investigate the impact of various water resource management scenarios. In addition, the need for accurate hydrological models has been increasing due to the growing complexity of operational hydrologic and hydraulic problems associated with population growth, quick urbanization and expansion of agricultural activities (El Hassan et al., 2013). In the recent decades, there have been significant developments in hydrological models, linking the process understanding to the structure and complexity of models. The modelling task is complicated as the development of hydrological models requires several steps which involve uncertainties. This uncertainty together with data errors and natural randomness can lead to increased uncertainty in model predictions (Butts et al., 2004). Hence, developing precise and reliable models remains one of the most challenging topics in hydrology.

2.1.1 Classification of hydrological models

Various hydrological models have been developed for different purposes. The data needed for hydrological models varies. A model, depending on its design, may need rainfall, air temperature, soil characteristics, topography, vegetation, hydrogeology and other physical parameters.

In the recent years different kinds of hydrological models have been introduced which all are useful but in the somewhat different circumstances; the choice of a model is determined by its purpose and data availability. Each model has its own effectiveness depending upon the objective of the study, the degree of complexity of the problem and the degree of accuracy desired. Models are not conflicting, they are rather a different level of approximation of reality (Xu, 2002).

Hydrologic models can be conceptual or physically based, lumped or distributed, which differ in data requirements, mathematical simulation of hydrologic processes and spatial representation of the simulated catchment.

In lumped models, the whole catchment is adopted as one unit and so spatial variability is ignored. In these models, the input data which is mainly precipitation and temperature and system output are related without considering the spatial processes, patterns, and organization of the characteristics governing the processes (Moradkhani and Sorooshian, 2008). A distributed model

is one in which parameters, inputs, and outputs vary spatially hence a model can make predictions that are distributed in space by dividing the entire catchment into small units, usually square cells or triangulated irregular network (Moradkhani & Sorooshian, 2008). A semi-distributed model takes a lumped representation for each sub-catchments. The advantage of the semi-distributed models are to have more detailed structures in contrast with the lumped ones, while, they need lesser amount of input data compared with the fully distributed ones.

All hydrological models are more or less lumped estimation of a heterogeneous world, therefore their equations illustrate the real world processes as being combined in space and time (Wagener and Gupta, 2005).

2.1.1.1 Empirical Models

Empirical models or data-driven models are observation oriented which take the information from the field measurement data without considering the hydrological processes. This kind of models make connections between input and output data through some statistical techniques (Devia, Ganasri, and Dwarakish, 2015). Hence the empirical models are inferred from data instead of representing detailed physical processes. Empirical models are generally less complicated than their physical and conceptual peers and acceptable results can be rapidly achieved by applying methods like regression and neural network (Aghakouchak and Habib, 2010). The SCS method (National engineering handbook, 1972) is a well-known example of a widely used empirical model for runoff prediction.

2.1.1.2 Physics-based modelling

Physically-based model is based on the best understanding of the physics of hydrological processes. The hydrological processes of water movement are represented by equations. The models are characterized by parameters that are in principle measurable and have a direct physical significance so they do not require extensive hydrological and meteorological data for their calibration. The evaluation of a large number of parameters describing the physical characteristics of a catchment requires data include boundary conditions, initial conditions, topography, topology, dimensions of river network etc. The physical model can overcome many defects of the other two types of models, empirical and conceptual, due to use of physical parameters. They can provide

large amount of information for a wide range of situations and an important advantage of these models is that if the physical parameters can be determined a priori, therefore they can be applied to ungauged catchments and the effects of catchment change can be represented (Devia, Ganasri, and Dwarakish, 2015). Nevertheless, most of the physically-based model are complex because of the spatial variability in the processes, and as a result they are generally described by a plenty of parameters. Spatial diversity between observed parameters and model parameters and differences between hydrological process scales and modelling scales is another problem with using physically based models (Shi et al., 2014).

2.1.1.3 Conceptual Models

Conceptual models are intermediate between physically-based models and empirical models while they generally consider physical laws but in a simplified fashion. In conceptual models, processes are estimated with simple equations rather than solving the governing equations differentially. In conceptual models, various kinds of parameters with no or little physically meaning are introduced to the model (Aghakouchak and Habib, 2010).

For applying conceptual models to a particular basin, the model must be calibrated, i.e. fitted to an observed data set to obtain an appropriate set of parameter values. Indeed the reliability of hydrological models is closely related to the calibration method. Model calibration is generally done either manually or automatically, using computer-based methodologies (Madsen, 2000). Manual calibration is very time-consuming. Moreover, it is hard to identify explicitly the confidence of the model simulations as it is based on hydrologists' judgment. On the contrary, for automatic calibration, parameters are adjusted automatically according to numerical measures of the goodness-of-fit in computer-based methods.

Using the conceptual models brings up different kinds of uncertainty that the main one may be conceptualization of reality, which reflects the modeler's, incomplete and/or biased understanding of significant processes in the natural system. The most challenging downside of using conceptual models is known to be "equifinality" (Beven, 1993). Equifinality refers to a case when a range of parameter sets can all lead to acceptable model results rather than a single "optimal" model result. These parameters cannot be linked to the basin if they are not uniquely

identified, hence it is difficult to apply the model for ungauged basins and also to track the basins changes.

In addition to parameter identifiability, other uncertainties can arise in (i) model context, (ii) model structure, and (iii) forcing data (Walker et al., 2003). The combination of these uncertainties in the modelling process produces its prediction error or predictive uncertainty (Todini, 2009). For instance observed flow (Hydrometric measurements) have an error range of ±5% in good conditions (i.e., well calibrated stage-discharge relationship, well maintained equipment, good river conditions for flow measurement, etc.) to as much as ±20% when the gauge is in a remote location and is not as well maintained on a regular schedule (Bohrn, 2012).

2.1.2 Monte-Carlo Simulation/ Model Parameter Uncertainty and Sensitivity Analysis

Monte-Carlo simulation is a robust stochastic technique for characterizing the response surface of a model (Kewlani & Iagnemma, 2008) in order to investigate model parameter uncertainty. Using Monte Carlo simulation, parameter values are randomly sampled from the feasible parameter space (conditioned on prior information, as available). And then parameter samples are applied into the model to generate simulated data. Based on this technique, Beven and Binley (1992) proposed the Generalised Likelihood Uncertainty Estimation (GLUE) procedure. GLUE groups the parameter sets into behavioral and non-behavioral ones given a threshold criterion for the objective function. The non-behavioral parameters describe parameter sets which return unacceptable model outputs and are eventually discarded (Beven, 2006). A further distinction is made between constrained and unconstrained parameters (Christiaens and Feyen 2002). Applying the uncertainty analysis in model parameters, rather than using point estimates, more information is provided to the catchment manager with respect to prediction error (Benke, Lowell, & Hamilton, 2008); in this case uncertainty related to model output can be represented as a probability distribution which can bring more helpful information about the degree of risk associated with particular actions (Benke, Lowell, & Hamilton, 2008). The level of improvement of the model by the GLUE approach depends on the used likelihood function threshold criterion and the number of sampled parameters. A number of likelihood functions have been applied: for example, the inverse error variance with a shaping factor (Beven and Binley, 1992), the Nash Sutcliffe model efficiency (Freer et al., 1996),

scaled maximum absolute residuals (Keesman & van Straten, 1989) and the index of agreement (Wilmott, 1981), model bias and coefficient of determination. The choice of the likelihood function itself has a strong influence on the results (He, et al. 2010). In general, the identifiability of parameters and uncertainties in conceptual hydrological modeling (i.e. HBV models) prove to be a challenging task (Ouyang et al., 2014).

In recent decades, Monte-Carlo-based approaches for uncertainty analysis has become an active area of research in hydrological modelling and various methods have been introduced. These techniques all have strengths and weaknesses and differ in their underlying assumptions and how the various sources of error are being treated and made explicit (Kuczeraa & Parent, 1998). Although it has been shown that Monte-Carlo-based methods have many privileges over conventional methods, the main downside of these methods is that they require a large number of model runs to make an accurate and reliable estimation of model uncertainty (Khu & Wernrr, 2003; Papadopoulos & Yeung, 2001).

In addition, reducing the number of parameters to a number which can be calibrated acceptably with limited data is a way to lessen the issue of parameter non-identifiability. One advisable strategy therefore is to use sensitivity analysis (SA) to identify the dominant parameters which define model behavior and have the most influence over model performance. Using SA, the structure of the model, major sources of model uncertainty and also the identification problem can be better figured out (Ratto et al., 2001; Razavi & Gupta, 2015). When the appropriate SA approach is applied, non-influential parameters can be recognized and fixed reasonably at given values over their ranges leading to simplification of the mathematical structure of the model without decreasing model performance. The more sensitive a model parameter for predicting a given target value is, the more constrained it becomes in the remaining behavioral parameter sets. Various SA procedures have been introduced which can be classified into two groups: Local SA and Global SA. A local analysis addresses sensitivity relative to point estimates of parameter values and in this category one the most common method is differential SA (DSA); this method is relatively simple, has limitations as it does not account for any interaction between model parameters and it measures only local sensitivity whose value is obviously location dependent (Gan, 2014).

Global SA (GSA) overcomes these limitations of local SA approaches. GSA characterizes the sensitivity of one or multiple model responses to model parameters across the entire feasible space of parameters, thereby providing a much more comprehensive assessment of sensitivity (Saltelli, 1999; Razavi & Gupta, 2015). There are a range of GSA methods in the literature based on different definitions and characterizations of "global sensitivity". Traditionally, most of these methods can be categorized under the families of derivative-based (e.g., the method of Morris, 1991) and variance-based (e.g., the method of Sobol, 1990) approaches. Recently, Razavi and Gupta (2016a) proposed a new, variogram-based approach that attempts to unify the theories of derivative- and variance-based approaches. Under this approach, Razavi and Gupta (2016b) developed an algorithm to implement a method called "Variogram Analsysis of Response Surfaces" (VARS) that generates a comprehensive set of global sensitivity metrics, including the Elementary Effects of Morris (1991) and Total-Order Effects of Sobol (1990), while being 1-2 orders of magnitude more efficient than the alternative methods.

Sensitivity analysis and estimation of uncertainty have become one of the main research topics in the hydrological modeling community and have been applied on many of both physically-based and conceptual models including HBVs. For this purpose, Spiegelhalter (2009) applied sensitivity analysis to the HBV-EC parameters in order to investigate the influence of climate change on the discharge of several watersheds in British Columbia. He concluded that most of the parameters were insensitive; meaning that reasonable simulation values were generated by using a parameter value out of the whole parameter range (e.g. Uhlenbrook, Seibert, Leibundgut, & Rodhe, 1999). However, they found that the climate and runoff parameters were rather sensitive, while the parameters associated with forest, soil and glacier routines were rather insensitive. Moreover, by comparing the catchments it was found that the sensitive parameters varied by catchment characteristics; for instance the number of sensitive parameters decreased with an increase in catchment size. However, the work of Seibert et al. (2000) resulted that catchment size does not control the number of sensitive parameters, and such an observation may be because of the differences in the characteristics of the catchment studied.

Other studies on the HBV model have also shown that most of the model parameters are not sensitive (Uhlenbrook, Seibert, Leibundgut, & Rodhe, 1999; Seibert, 1997; Harlin & Kung, 1992),

but the identification of the sensitive ones requires running GSA for each case and cannot be known a priori.

2.1.3 Effect of the forcing error/Precipitation uncertainty

An element of data uncertainty is introduced when a model is required to interpret the actual measurement such as precipitation data. Rainfall and snowfall are mostly the major driving force in hydrological models in runoff estimation. Therefore an accurate representation of the temporal and spatial variability of precipitation is of importance to achieve an accurate river basin model (Cho et al., 2009; Masih et al., 2011; Price et al., 2014). However in general input data applied to run the model may only be an approximation of the real-world forcing due to measurement errors and areal representativeness (e.g. precipitation uncertainty resulting from inadequate spatiotemporal network densities) (Wagener & Gupta, 2005). For example, one may have to deal with uncertainty in using radar measurements. They are measurements of reflectivity which are converted to precipitation estimates by applying empirical equations with calibrated parameters. This procedure is extremely uncertain (Wagener & Gupta, 2005).

Precipitation input uncertainty arises from various reasons: inadequate areal coverage of point-scale gauges, inaccurate spatial interpolation, mechanical problems of the gauges, wind speed and etc. (Guidice et al., 2016). Few methods have been developed to explicitly account for precipitation uncertainty and to propagate it through a hydrological rainfall-runoff model (Blasone et al., 2007). Uncertainty in precipitation data can substantially hamper the model's ability to present runoff where the assumption of spatially uniform precipitation is invalid (e.g. in mountainous regions, Cho et al., 2009; Giudice et al., 2016).

The impact of precipitation input on model performance is well documented (Fu, Sonnenborg, Jensen, & He, 2011; Kavetski, Kuczera, & Franks, 2006; Tuo, Duan, Disse, & Chiogna, 2016), as a function of catchment size (Moulin, Gaume, & Obled, 2008), rain gauge density (Bárdossy & Das, 2008) or using various geostatistical methods (Sun, Mein, Keenan, & Elliott, 2000). However, model robustness problems due to incorrect estimations of precipitation amounts are rarely reported in hydrological modelling, while it is well known that such errors

might have a significant effect on the final values of model parameters and resulting streamflows (Oudin, Perrin, Mathevet, Andréassian, & Michel, 2006).

However, the majority of the applications of uncertainty analysis techniques in hydrology assume error-free data and assess the uncertainty of the model output by considering only parameter variation (i.e., uncertainty in model parameters). This may be in part due to the computational complexity of including it in a likelihood function (Honti, Stamm, & Reichert, 2013; Kuczera & Williams, 1992; Sikorska, Scheidegger, Banasik, & Rieckermann, 2012). Kuczera and Williams (1992) have developed a method which accounts for the parameters and forcing data uncertainty separately for calibrated models. In this approach, the Monte-Carlo samples of spatially distributed rainfall fields and of parameter samples are generated and then the combined effect of precipitation and parameter uncertainty in the model output is assessed.

For this study, we have limited the investigation of forcing data to precipitation. Therefore, finding a robust method that can produce a reliable assessment of total output uncertainty and also the contributions of the parameter and input uncertainty has still room for research.

2.2 Investigating of hydrological process and runoff generation in the Canadian Rockies

Western parts of Canada is heavily dependent on water coming from the Canadian Rockies. A better understanding of hydrological processes and resilience of the Canadian Rockies headwater basins is curial due to increasing the change of the region including climate and forest cover change (Harder, Pomeroy, & Westbrook, 2015) that can lead to the extreme weather and extreme flooding; for instance flooding of 2013 in Marmot Creek.

Mountainous basins are mostly covered by seasonal snow and glacier and the main differences of the hydrological processes of these area with lower-elevation regions are sharp wet-dry seasonal changes, complex topographic and mixed landscape patterns, and steep changes of temperature and precipitation by elevation (Bales et al, 2006). One of the main purposes of understanding hydrological processes in such mountainous basins is to assess accumulation and ablation of snow as a main source of streamflow generation. The assessment and calculation of

snow melting can be challenging since it is significantly affected by many factors including, temperature, elevation, slope and aspect. For instance south facing slopes become snow free several weeks before north faces (DeBeer & Pomeroy, 2009). In addition, Needleleaf forest is the main vegetation cover of the mountainous area which disrupts the timing and melt of snow by dampening turbulent energy fluxes (Ellis, Pomeroy, Brown, & MacDonald, 2010; Harding & Pomeroy, 1996). Needleleaf forest also affects the interception process and as a result the snow accumulation. Intercepted snow is exposed to a higher rate of radiation which results in increased sublimation (Pomeroy, Parviainen, Hedstrom, & Gray, 1998) and a smaller snowpack on the ground for snowmelt (Pomeroy & Gray, 1995). The elevation is a major factor that influences temperature, the phase change of precipitation and precipitation amounts in mountain basins (Storr 1967).

Moreover, all these processes either in timing or in frequency, are changing because of climate change. The available documentation of Canadian Rockies shows the rising of air temperature and increasing precipitation (Harder, Pomeroy, & Westbrook 2015; Pomeroy, Fang, & Rasouli, 2015). Although in the Rockies basins melting water from snow pack and the glacier of mountains along with downstream processes such as groundwater recharge and interactions with ecosystems are the main water supplies of the residents, hydrological studies of some basins shows that streamflow is declining with time (Stewart, Cayan, & Dettinger, 2005; Valeo et al., 2007). For example Bow River at Banff has lost 11.5% of its mean annual flow over the period of 1910 to 2014 and the decline in summer flows is even more severe than the annual trend, with a 24.8% decline in August since the early 20th century (Pomeroy, 2009). In another example, consequences of hydrological changes of Marmot Creek, air temperature at low elevations, spring precipitation, inter-annual variability of precipitation, and groundwater levels of higher elevation are increasing. On the other hand, peak seasonal snow accumulation and groundwater levels at lower elevations are decreasing. However, other variables, i.e., streamflow volume, the timing of peak, and magnitude of the peak, are remained unchanged (Harder et al., 2015). In the other research on Canadian Rockies area, Larson et al. (2013) showed the other changes of streamflow including the date of peak snowmelt is occurring approximately 1 - 4 weeks earlier compared with the last half century. It is also documented that when the climate of basins in this area become wetter and warmer, the basin streamflow can be shifted to a more rainfall-dominated regime

(Whitfield, Cannon, & Reynolds, 2002), especially in areas west of the continental divide (Loukas, Vasiliades, & Dalezios, 2002).

However, the research of other basins of Canadian Rockies revealed other information about the hydrology changes of this region. For instance, Merrit et al. (2006) found that runoff at Okanagan watershed will increase in near future, however, it is likely that temperature increases will suppress the effect of precipitation increases, resulting in runoff decline in long term.

Besides the snow melting, glacier meltwater is another source of basins' discharge. Rockies glaciers flow into four major watersheds, those of the Mackenzie, Nelson, Fraser, and Columbia River basins and drain into the Arctic, Atlantic, and Pacific oceans, respectively (Tennant & Menounos, 2013). The contribution of glacier meltwater to total streamflow may be low, but glacier flows supplement summer flow and regulate stream temperature (Barry, 2006; Moore et al., 2009). Moore and Demuth (2001) showed that the presence of even a small amount of glacier cover in a basin can influence streamflow variability on a range of time scales. Many studies have focused on understanding of the processes governing glacier meltwater generation and drainage (e.g. Brazel, Chambers, & Kalkstein, 1992; Fountain, 1996; Gordon et al., 1998; Hock, 2005) while other studies have examined the variability of total annual or seasonal runoff in glaciated catchments (e.g. Fountain & Tangborn, 1985; Moore, 1992). However, relatively little research has focused on the effect of changes in glacier conditions on glacier discharge.

As glaciers retreat, the total volume of meltwater generation will be limited, even if high specific melt rates were sustained (Marshall et al., 2011; Moore & Demuth, 2001). Changes in glacier extent are inextricably linked with climate and a glacier's response to climate is complicated by local topography and by individual glacier attributes, such as elevation, slope, and aspect. Due to this complex system many other studies on large numbers of glaciers with different sizes and attributes are required to be monitored over periods of many decades to enhance our understanding of the effect of different parameters on glacier area, changes in the total glacier mass during the time and eventually streamflow rate in the future (Moore et al., 2009).

Another purpose of the investigation of hydrological processes in Canadian basins has been an attempt to predict flooding in the area. Flood events are the most visible expression of extreme weather in this region with recent catastrophic floods occurring in 1995, 2005, and 2013 (Harder

et al., 2015). Although, in many basins of this area constant or even declining annual peak flow has been observed, it needs to be distinguished from extreme flood events (Cunderlik & Ouarda, 2010). Flooding has attracted a great attention as it is a highly costly disaster and causes the most damages to inhabitants (Sandink, Kovacs, Oulahen, & McGillivray, 2010; Harder et al., 2015). However, it is one of the most difficult matter to investigate because of their infrequent occurrence and typically poor quality data (Whitfield, 2012). Due to mentioned reasons, useful data to determine frequency and magnitude of the flood is restricted (Harder et al., 2015). In addition, climate change has increased the uncertainty of prediction of this event. Whitfield (2012) and Pennelly, Reuter, and Flesch (2014) mentioned that climate change may increase the probability of extreme weather events that drive these floods. They also believe that extreme flood occurs because of various reasons and snowmelt alone is typically unable to generate sufficient runoff rates to cause large floods in this region.

Beyond all existing research, there is still a lack of understanding of hydrological processes, which along with limited observation networks restrict the ability to simulate and predict streamflow accurately. Therefore more investigation in hydrological processes and climatic data in the Rockies basins is required.

2.3 Hydrological models used to simulate Canadian Rockies basins

As mentioned before, snow and glacier melt, related energetics of phase change, along with other cryospheric processes and their contribution to streamflow volume are of the main processes of mountainous basins, which can be estimated through appropriate hydrological models if they are calibrated and validated properly. However, hydrological models especially conceptual ones such as HBV-EC face the basic challenge of model uncertainty due to the simplification of natural processes expressed in model structure and parameters (Finger, Vis, Huss, & Seibert, 2015). Therefore, selecting an appropriate model is one of the main step in studying the hydrological processes and stormflow generation in mountain area (Barnes, 1995). It is crucial to know the limitations and the requirements of the model to assess if the model is useful for the research and the study area at hand. A complex and physically-based model may not always be the best option and may not generate the better results rather than a simple model in all cases (Hirshfield, 2008). Finding an appropriate model is challenging and a number of previous studies in literature

summarize different models with their strengths and weaknesses (Barnes, 1995; El-Kadi, 1989; Sing & Woolhiser, 2002). Various kinds of hydrological models suitable for cold region climate (either conceptual or physical) have been used to simulate different hydrological variables of Canadian Rockies basins. Examples include MESH, RAVEN, CRHM and HBV-EC models that are described in the following paragraphs.

Environment Canada developed a coupled land surface and hydrological model known as the Modelisation Environmental Communitaire (MEC) – Surface and Hydrology (MESH). The MESH model is expanded from the MEC which created an environment to facilitate coupling between models focusing on different components of the earth system and eventually to produce operational forecasts (Pietroniro et al., 2007). MESH is capable of simulating runoff at any point within a watershed through the implementation of full hydrologic and hydraulic routing (Mengistu & Spence, 2016). However, it has been used for different hydrological aims in recent years such as promoting the transferability of vegetation parameters (Dornes et al., 2008) and simulating a number of hydrodynamic properties including lake level variation, ice concentration, and lake surface temperature (Dupont, Chittibabu, Fortin, Rao, & Lu, 2012).

Raven (Craig et al. 2008) is a flexible hydrological framework that can be used as an either lumped or semi-distributed model. Raven has been used to realize the hydrological behavior of a watershed and also to determine the potential impacts of environmental changes such as land use and climate upon watershed properties. Raven uses empirical relationships to simulate cold-regions processes, such as using temperature index model to calculate snowmelt (Rabiti et al., 2015).

Cold Regions Hydrological Model (CRHM), is a physically based model with a limited need for calibration (Pomeroy et al., 2007) developed at the Centre for Hydrology, University of Saskatchewan. This model aims to improve the understanding of hydrological processes in cold environments which are mainly controlled by snow, ice accumulation, interception, transport and melt, infiltration through frozen soils, and cold water bodies (Pomeroy et al., 2007). CRHM has been used in various hydrological studies such as understanding the dynamical processes of Canadian basins (Fang & Pomeroy, 2007), assessing the snowmelt and snow accumulation in

forest and clearing sites (Ellis et al., 2010), and simulating the impacts of forest disturbance in the basin hydrology (Pomeroy, Fang, & Ellis, 2012).

HBV-EC (Hydrologiska Byråns Vattenbalansavdelning-Environment Canada) have been applied frequently to investigate the snow and glacier related processes in different mountainous areas including Rockies basins (Mahat & Anderson, 2013; Chernos et al., 2016). Stahl et al. (2008) used HBV-EC in order to study the sensitivity of streamflow to climate and glacier changes over time for the Bridge River catchment in British Columbia. Uncertainty related to parameters controlling glacier melt generated uncertainty in future glacier retreat and streamflow response. They showed that although model fit to both streamflow and glacier mass balance was good and the model could reproduce the inter-annual variations in snowmelt and the glacial hydrograph, the model systematically underestimated of the (low) winter streamflows. However, winter streamflow values are usually affected by ice cover and the measurements are prone to significant uncertainty.

In order to quantify the contribution of glacier runoff to streamflow, Jost et al. (2012) applied HBV-EC in upper Columbia River Basin. Modelled results compared with observed data showed that Nash-Sutcliffe efficiency could reach to 0.95 and all the behavioral parameter sets produced the seasonal peak flows and low flows, but had a problem with modelling the intense precipitation events, especially during fall. However, they believed that since this problem was limited to rainfall-generated daily peak flows, molding result in estimation of glacier melt contributions to streamflow over the larger time scales (i.e. monthly) could be reasonable. In addition, a reasonable agreement was shown between the result of SWE (snow water equivalent) estimated by HBV-EC and observed values with linear regressions having average R^2 of 0.82 for three basins. Their result proved that the model also estimated the timing of the onset of snowmelt and the rate of reduction of SWE during the ablation stage precisely.

Other studies have focused on the comparison of HBV-EC with other hydrological models to assess whether the model is capable of producing reliable result and suitable for their study area. Bohrn (2012) compared the performance of HBV-EC and WATFLOOD hydrological models for Churchill River Basin with each other and also with observed streamflow data. WATFLOOD is a semi-physically based, distributed model developed by Nicolas Kouwen in 2011 (Kouwen, 2011).

Hydrograph generated by models showed that HBV-EC predicts an earlier spring freshet than the WATFLOOD. And latter predicted the freshet slightly earlier than the measured event. According to hydrographs, the annual peak value of measured data is lower than that estimated by HBV-EC and higher than the value of WATFLOOD. HBV-EC estimated slightly higher amounts of flow levels for the low-flow period of the year (late summer, fall and winter) and also higher average yearly flow in comparison with WATFLOOD. However both models compared well to the observed average flow. Overall, they concluded that HBV-EC is able to generate a reasonable results and also similar trends with WATFLOOD and observed data. And the discrepancy in the results is related to the fact that HBV-EC model was developed to model the hydrology of small mountainous basins that have high levels of relief.

In another research, Hirshfield (2008) compared several hydrological models including SWAT, HEC-HMS, GeoSFM, HBV-EC, and CRHM to identify the ones that are suitable to investigate the impact of climate change on streamflow in snow dominated mountain basins in British Columbia. They looked for the model which is able to run on limited input data and contains sufficient and appropriate snow routines to capture snowmelt hydrology. They used various evaluation criteria including: spatial scale, snow accumulation and melt, interception and infiltration, cost, the user-friendly quality, and technical support. Their comparison result showed that overall, HBV-EC and CRHM were the best selections for their study. However, the main advantage of HBV-EC is that the model is well-adopted for modeling streamflow especially in mountain region; it is fairly easy to use, and the set up time was less than 1 week for their watershed. Based on their research, CRHM is a supportive model for application in the diverse cold regions; it is able to simulate various snow processes including blowing snow transport, glacial melt, and permafrost. However, it may be overly complicated and time consuming and may not be a best selection for basins where data available are limited. On the contrary, HBV-EC is common because it is simple, easy to use and requires only daily/hourly precipitation and temperature data, and monthly/daily estimates of evapotranspiration as input to simulate daily/hourly streamflow (Mahat & Anderson 2013).

Accordingly, HBV-EC is used in our study since we aim to run the model for 25 basins using three different climate products, first, and then for 5 selected ones (4 times using three climate products and one combined precipitation data) for more rigorous investigation. The model

is needed to run 10,000 times for each basin, resulting in 950,000 total model runs. For such a large-sample hydrology approach, such a model appear to be the only option. Moreover, the amount of data for those 25 basins (which are mostly small basins with limited prior studies) are limited to temperature and precipitation, however in order to apply CRHM to its full extent, much more data is required (i.e. relative humidity, wind speed, and radiation). Therefore, the lack of data available for all basins and the running time are the main reasons that prohibit the use of a more complicated and physically-based model (i.e. CRHM) for this thesis. In addition, HBV-EC has shown to be capable of modelling glacial and snow processes and generating reasonable streamflow data.

3 Materials and Methods

3.1 Study area

The twenty-five Canadian Rockies basins (all in Montane eco-zone) were selected on the basis of having continuous and natural observed hydrometric data for more than 20 years.

Basins are located in Alberta and British Columbia provinces (figure 3.1) with areas ranging from 92.8 km^2 to 1150 km^2. Selected basins represent a wide variety of meteorological conditions with various precipitation values. Table 3.1 shows the percentages of four types of land use according to HBV-EC model land use classification, total area, and average elevation of basins.

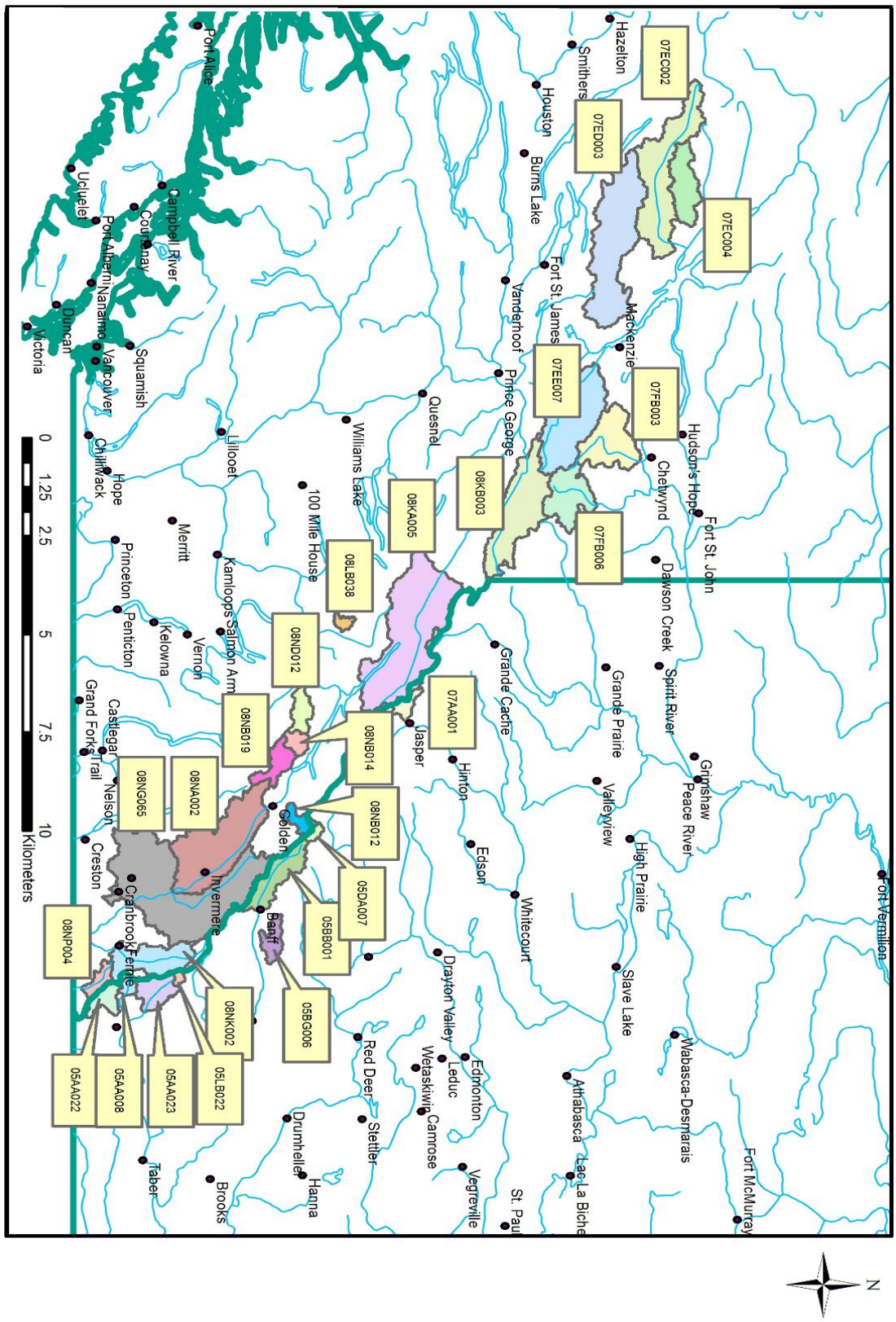

Figure 3.1: The Location of 25 basins in Alberta and BC provinces

Table 3.1: Basins information (ID, area, land use, and elevation)

Basin ID	Area (km^2)	Lake%	Glacier%	Forest%	Open%	Average Elevation (m.s.l)
08NP004	92.8	0	0	62.59	37.41	1792
08NK002	3090	0.3	0.65	67.9	31.16	1860
08NG065	11500	0.42	0.88	63.95	34.76	1790
08ND012	934	0.24	8.34	65.88	25.55	1713
08NB019	1150	0.34	11.68	52.85	35.13	1907
08NA002	6660	1.61	3.39	61.33	33.67	1784
08KB003	4780	0.89	5.74	65.5	27.87	1372
08KA005	6890	0.7	10.16	50.66	38.47	1849
08NB014	429	0.19	26.06	35.01	38.74	2119
08NB012	587	0.09	14.78	40.96	44.17	2018
08LB038	272	0.47	3.32	62.64	33.57	1560
07FB006	2370	0.6	1.83	76.63	20.94	1304
07FB003	2590	0.25	0.01	84.1	15.64	1199
07AA001	1940	0.2	0.7	57.88	41.22	1958
07EC002	5560	1.11	0.17	82.61	16.11	1281
07EC004	1950	0.42	0.3	72.63	26.65	1389
07ED003	6790	3.72	0	89.33	6.96	1089
07EE007	4930	0.74	0.28	86.33	12.65	1105
05AA008	402.7	0.67	0	71.08	28.25	1650
05AA022	820.7	0	0	59.41	40.59	1640
05AA023	1446.1	0.16	0	77.53	22.3	1848
05BB001	2209.6	0.85	5.71	44.7	48.74	2168
05BG006	332.5	0.24	0	68.51	31.24	1609
05BL022	165.5	0	0	78.11	21.89	2011
05DA007	248	3.6	19.6	25.6	51.2	2294

Land use classes are based on HBV-EC classification (will be described in 3.3.1 section) and include: 1) lake which is any kind of water body, 2) glacier, 3) forest and 4) open land that is any kind of land use that does not fall within other three groups and includes agricultural land, bare land, etc.

Referring the Table 3.1, these catchments show a variation of land cover. Forest is the most common one (except for four basins), varying from 25.6% for 05DA007 to 89.33% for 07ED003. Open land is the second most common type of land cover from 12.65% for 07EE007 to 51.20% for 05DA007.Glacier can be found in 22 basins with a coverage of 0.01% for 07FB003 to 26.06% for 08NB014. The lake area in the basins is relatively low, varying from 0.16% for 05AA023 to

3.72% for 07ED003, there are three basins without any water body (08NP004, 05AA022, and 05BL022).

3.2 Forcings and data

3.2.1 Meteorological Forcing data

Meteorological data consist of daily precipitation, temperature, potential evaporation, land use, and elevation. For precipitation and temperature three kinds of gridded data, ANUSPLIN, WFDEI, and CaPA, were used. Potential evaporation for different climate zone was calculated using Hamon's (1961) method. FAO, MODIS, and SRTM databases have been utilized for soil, land cover and digital elevation, respectively.

3.2.1.1 Precipitation and Temperature

The scarcity of gauge coverage in the Canadian basins has always been an issue for hydrological modeling purposes. The well-known Thiessen Polygon Method and inverse distance weighting are two of the few early attempts to interpolate precipitation from ground-based points to fill spatial gaps (Zhao, 2013). However, by the developments in computer technology, more advanced precipitation products and distribution methodologies such as gridded climate data have been introduced. Three different climate data products have been utilized in this study; each is described in the following sections.

3.2.1.1.1 CaPA

According to Bivand, Pebesma, and Gómez-Rubio (2013) and Boluwade et al. (2017), interpolation accuracy is only as good as the number of spatial points used in producing the resulting interpolated surface. In areas with a limited number of climate stations, there is a need for better methods of precipitation representation using more advanced datasets from weather prediction models at appropriate scales for hydrologic modeling applications. Therefore, Numerical Weather Prediction (NWP) models (Boluwade et al., 2017) provide a platform to predict precipitation for short time step. They use weather observation along with some 3-D

differential atmospheric equations to predict future events. NWP models can outperform gridded precipitation products constructed from satellite data (Kidd, 2012)

The Canadian Precipitation Analysis (CaPA) is a national project organized by the Meteorological Research Division (MRD) and the Meteorological Service of Canada (MSC) with the goal of producing near-real-time precipitation analyses over North America at fine temporal (6-h) and spatial (10 km) resolutions. CaPA combines precipitation observations with a background field obtained from a short-term NWP forecast in order to compensate the inadequate climate station network in Canada (Lespinas, Fortin, Roy, Rasmussen, & Stadnyk, 2015). These NWP data were generated by Environment and Climate Change Canada's Regional Deterministic Prediction System (RDPS), which in turn relies on the Global Environmental Multiscale (GEM) model (Côté, 1998). And GEM is an integrated forecasting system and data assimilation platform which is based on the hydrostatic primitive equations and two-time-level semi-Lagrangian procedure (Fortin, Roy, Donaldson, & Mahidjiba, 2015).

CaPA assimilates the GEM's short-term forecasts, radar precipitation estimates, satellite observation and point estimates from weather stations using an internal quality control procedure (Boluwade et al., 2017; Lespinas et al., 2015). Moreover, GEM takes into account topographic information for the mountainous area where weather stations are located in valleys and do not account for the orographic effects on precipitation (Mailhot et al., 2010). Performance evaluation of CaPA and GEM data is provided in Lespinas and Fortin (2015) and Boluwade et al. (2017).

3.2.1.1.2 WFDEI (WATCH)

The European Union Water and Global Change (WATCH) project sought to assess the terrestrial water cycle and hydrologically variables using land surface and hydrological models in the context of global change (Harding et al., 2011). Since such models require meteorological forcing data, WATCH Forcing Data (WFD) was created. WFD is based on the European Centre for Medium-range Weather Forecasts (ECMWF) ERA-40 reanalysis (Uppala et al., 2005) interpolated to 0.5 × 0.5 resolution with elevation correction of surface meteorological variables as well as monthly bias correction from gridded observation data. The WFD precipitation dataset has shown a good performance compared to TRMM satellite products and precipitation gauge data

(Li, Ngongondo, Xu, & Gong, 2013; Li, Xu, Zhang, & Jain, 2014). The WFDEI which stands for WATCH forcing data methodology applied to ERA-Interim data, uses the same methodology as the WFD, however with some differences including: (1) WFDEI data are derived from a different reanalysis with higher spatial resolution, (2) adjusted to updated monthly observational data, and (3) more appropriately adjusted in terms of shortwave fluxes in relation to the effects of aerosol loading and compared with satellite products (Iizumi, Okada, & Yokozawza, 2014; Weedon et al., 2014). This dataset contains the air temperature, precipitation (rainfall and snowfall separately) wind speed, surface pressure, specific humidity (2m), long and shortwave radiation (while the daily mean temperature is directly available). In this study, we extracted the daily minimum and maximum temperature (Tmin and Tmax) and took the average for running the model. The temperature data have been bias-corrected against CRU (Climatic Research Unit) mean monthly temperature and diurnal temperature range.

Rain and snowfall have been bias-corrected against observations by first correcting the number of dry days and then scaling the precipitation in each time step to make the monthly means match the observations. Finally, to consider the anticipated underestimation of precipitation in the observed data (Adam & Lettenmaier, 2003), the under-catch correction factor has been applied (Schneider et al., 2011).

Reanalysis datasets have been used recently for hydrological models in many research with various degree of success and they concluded that WFDEI improved streamflow simulation compared to WFD data (Nkiaka, Nawaz, & Lovett, 2017).

3.2.1.1.3 ANUSPLIN

Natural Resources Canada (NRCan) used the tri-variate thin-plate smoothing spline method along with some modifications to create gridded data of daily maximum and minimum air temperature (◦C), and total daily precipitation (mm) for the Canadian landmass south of 60◦ N at ∼ 10 km resolution (NRCan, 2014). This product is called Australian National University Spline or ANUSPLIN. Tri-variate thin plate splines allow for spatial dependence on the elevation, making the method suitable for applications across large heterogeneous areas (Hutchinson & Gessler, 1994; Stillman, 1996). Specifically, in this dataset, estimated local lapse rate is used to adjust

temperature data for elevation. In order to illustrate the changing temperature lapse rate in time and space, surfaces of temperature (minimum and maximum) along with precipitation data were fitted for each month separately. When the linear effect of elevation cannot be measured, the precipitation surface is fitted as an ordinary thin-plate spline. Therefore, the fitted surfaces can estimate the climatic variables for the places with available latitude, longitude, and elevation (Yan, Nix, Hutchinson, & Booth, 2005).

More detail of this approach can be found in several studies, including Hutchinson (1995) and Hutchinson and Bischof (1983). The ANUSPLIN software (Hutchinson & Xu, 2013) uses all available NCDA (National Climate Data Archive of Environment and Climate Change Canada) station daily data (ranged from 2000 to 3000 for any given year) as an input to the gridding procedure (Wong, Razavi, Bonsal, Wheater, & Asong, 2017). Hopkinson et al. (2011) subsequently extended this dataset to the period 1950 to 2011 and then has been updated by Canadian ANUSPLIN to 2013. It has recently been used as the basis of "observed" data for evaluating different climate datasets (e.g. Eum et al., 2012) and for assessing the effects of different climate products in hydro-climatological applications (e.g. Bonsal et al., 2013; Eum et al., 2014).

3.2.1.1.4 Potential and Actual Evaporation (PET and AET)

Potential Evaporation: Hamon's Equation

Hamon (1961) developed a simplified equation based on the mean air temperature to estimate potential evapotranspiration. It is widely used in different areas as well as Canadian Rockies as it is a simple method and has provided good results in several impact studies (Benninga, 2015; Singh, Rudra, & Gharabaghi, 2012; Spiegelhalter, 2010). Oudin et al (2005) recommended using a temperature-based potential evapotranspiration model in a daily rainfall-runoff model, among which Hamon is mentioned. According to Lu et al (2005) different evapotranspiration methods produce inconsistent results for some catchments and years therefore care have to be paid in selecting the method for study area. Hence he recommended using the Priestly-Taylor method if radiation data are available, otherwise Hamon method can be used. In using this method values of mean monthly temperature and the latitude of the site are required and then potential evapotranspiration (PET, mm day-1) is calculated as:

$$PET = C \times HPD^2 \times SVP \quad [3.1]$$

HPD (-) takes into account the possible hours of sunshine per day as a percentage of 12 hours, SVP (g m^{-3}) is the saturated water vapor density at the daily mean temperature and C is an empirical correlation coefficient, which has the value of 0.55 from comparisons with the results of the complex Thornthwaite (Thornthwaite, 1948) method and the Lowry-Johnson study (Lowry & Johnson 1942; Cruff & Thompson, 1967)

Hamon method is established based on the relationship between potential evapotranspiration, maximum possible incoming radiant energy, and the moisture-holding capacity of the air at the dominant air temperature (Cruff & Thompson, 1967). It also regards the influence of wind as insignificant and uses a constant value for this estimation. As a main heat source for the evaporation process, it considers the net radiation. Daily averages of the net radiation can be estimated by using the daily mean temperature and the average duration of day-time hours as a percentage of 12 hours (Spiegelhater, 2010).

Actual Evapotranspiration: MODIS Equation

The MODerate Resolution Imaging Spectroradiometer (MODIS) onboard NASA's Terra and Aqua satellites (EOS), provides unexampled information regarding vegetation and surface energy (Justice et al., 2002), which can be used for regional and global scale actual ET estimation in near real-time. MODIS is playing a vital role in the development of Earth system models in order to predict global change and protect our environment (Muhammed, 2012).

The main privilege of MODIS data is their resolution. They can be applied to estimate energy fluxes at any scales from regional to global and also at daily time intervals (Vinukollu, Wood, Ferguson, & Fisher, 2011), which is not possible with sensors such as Landsat TM and ETM (Lauer, Morain, and Salomonson, 1997). ET estimates of MODIS method have been shown to be accurate in numerous studies (Cleugh et al., 2007; Mu et al., 2007; Venturini, Islam, and Rodriguez, 2008; Mu, Zhao, and Running, 2011)

In this study, monthly average of MODIS actual evapotranspiration (MOD16A2) data with the resolution of 0.05 degree is utilized (data are available at http://files.ntsg.umt.edu/data/NTSG_Products/MOD16/MOD16A2_MONTHLY.MERRA_GMA

O_1kmALB/GEOTIFF_0.05degree/). It contains 1-km^2 land surface evapotranspiration data and covers 109.03 Million km^2 areas in 8-day, monthly and annual intervals (Mu et al., 2011). ET data of this dataset are generated using Mu et al.'s improved ET algorithm (2011) over previous Mu et al.'s paper (2007). This algorithm has used Penman-Monteith equation (Monteith, 1965) and has shown to be capable of generating accurate global ET data. It has also provided important information about global terrestrial water and energy cycles (Mu et al., 2009). The MOD16 evapotranspiration dataset calculates evapotranspiration as the sum of evaporation from wet and moist soil, interception, and transpiration. Transpiration stomatal conductance is specified by biome specific vapor pressure deficit and daily minimum temperature thresholds. However, the leaf area index is used to scale stomatal conductance to canopy conductance (Vanderhoof & Williams, 2015). Figure 3.2 illustrates the process of MODIS approach to estimate actual ET.

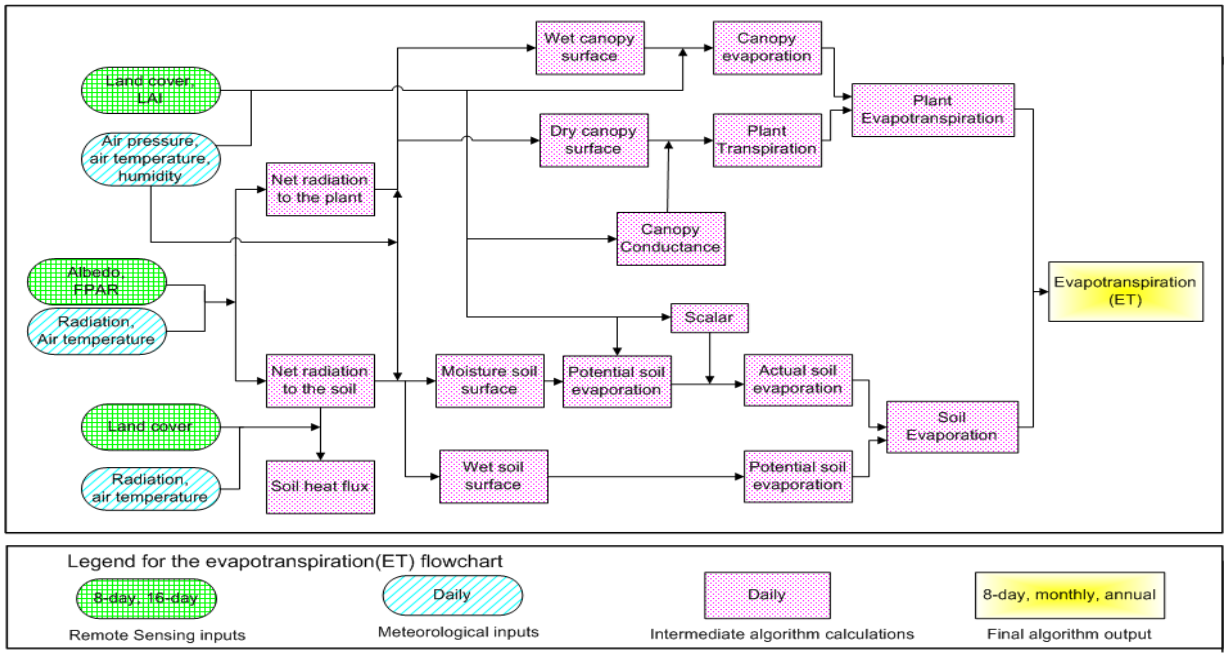

Figure 3.2: MODIS process in ET estimation (MODIS Global Evapotranspiration Project, available at http://www.ntsg.umt.edu/project/modis/mod16.php)

3.2.2 Hydrometric data

Hydrometric data for each basin consist of daily mean flows originating from the Environment Canada/Hydat database. Basins have a continuous daily time series data, however, there is missing data for some stations especially when the model was run for ANUSPLIN forcing data; since the period of this database is longer compared to other two forcings (1950 to 2013). In these cases, the missing days were ignored in calculating objective functions.

3.2.3 Land Cover

A number of national scale land cover database with the spatial resolution of 1-km has been produced by Canada Center for Remote Sensing. In this study, the most recent land cover database of Canada is used to determine the land cover classification of the catchments. This database is produced from 0.25-km spatial resolution MODIS (Moderate Resolution Imaging Spectroradiometer) data and contains two thematic layers based on the Federal Geographic Data Committee/Vegetation Classification Standard (FGDC/NVCS) modified for use in Canada and the International Geosphere Biosphere Program (IGBP) land cover classes. It has showed very good agreement with independent reference data (NRCan, 2008). This database has been used in previous research for different purposes including streamflow estimation (Mahaxay et al., 2016), estimation of nutrient concentration (Alarcon et al., 2010), and land cover characterization (Song et al., 2009).

3.2.4 Field Capacity

Field capacity (FC, mm) is the amount of water content kept in the soil after excess water drain by gravity. FC is one the soil module parameter of the HBV-EC model. To determine the range of this parameter in Monte-Carlo simulation, the Digital FAO-UNESCO Soil Map of the World (Fao, 1998) was used. Soil Map of the World (SMW) at 1:5,000,000 scale is known as the most comprehensive soil map with global coverage (Sombroek, 1989; Nachtergaele, 1996).

Development of the SMW was initiated in 1961, with the first hard copy map published in 1971 and the last map of the 10-volume series completed in 1981 (FAO-UNESCO, 1971-1981).

SMW units are divided into three textural classes of coarse, medium, and fine, which are defined by their relative proportions of clay (less than 2 micrometers), silt (2-50 micrometers), and sand (50-2000 micrometers) content. In this study, using the Digital SMW, the dominant topsoil class of each basin was found and then the FC range of each class was used in the model simulation. Regarding FAO classification, FC range of sand, silt, and clay are 25-100, 100-17, and 175-250 mm/m, respectively (http://www.fao.org/docrep/r4082e/r4082e03.htm#2.3.3 field capacity). The dominant soil of 25 basins of this research were placed into the two soil classes of silt and clay. However, the study of Hamilton, Hutchinson, and Moore (2000) showed that the optimum field capacity of HBV for their study area reached to 400 mm, as a result the range of this parameter was increased to 350 (instead of 250) for clay class in our study.

3.2.5 Digital Elevation Model (DEM)

Digital elevation model (DEM) is very important in hydrological modeling and in water resources management, as it can provide many hydrologically relevant parameters, such as drainage networks and catchment boundaries. In the HBV-EC model, DEM file provides the information of river network, aspect, slope, and outlet of basins. In practice, DEMs are often derived from stereo-photos or satellite imagery such as stereoscopic SPOT image and from the digitalized topographic contour. The resolution, quality, and availability of these derived DEMs are highly variable, leading to tremendous problems for research over large basins.

The SRTM (Shuttle Radar Topographic Mission) was launched (in February 2000) to catch the radar data of elevation on a near-global scale. Using these data, it produced a full high-resolution digital elevation database of the Earth. A survey of the land masses was made between 60° North and 58° South latitude and generated consistent, comprehensive, topographic data and radar images to model the terrain and map of the land of the most of the inhabited surface of the earth. The instrument used is the “Synthetic Aperture Radar” (SAR) applying interferometry techniques to make three-dimensional images of the surface with high resolution, no matter of sun’s position weather and surface contrast (De Ruyver, 2004). The single pass SAR

interferometry of SRTM made a coherent DEM measured by the single system within 11-day mission which is based on one geodetical reference system. Further information about this mission is available at https://www2.jpl.nasa.gov/srtm/. A DEM file generated by SRTM database was applied to HBV-EC model to generate the elevation and other related data of the basins.

3.3 Method

3.3.1 HBV-EC model

HBV model (Bergstrôm, 1976) is a conceptual model of catchment hydrology, originally developed for Scandinavian basins. During the last two decades it has been applied in more than 30 countries worldwide (Bergstrôm, 1992; Jia & Sun, 2008) and for different hydrological tasks, for instance, to compute spillway design floods or flood forecasting (Bergstrôm, 1992), to study the effects of changes in climate (Saelthun, 1996) and land use (Brandt, Bergstrom, Gardelin 1988); and different attempts have been made to relate the parameters of the HBV model to catchment characteristics for regionalization purposes (Braun & Renner, 1992; Seibert, 1999). Lindstrom et al. (1997) describe the HBV model as "a model of high performance" and characterize its structure as "very robust and surprisingly general, in spite of its relative simplicity".

The code of the HBV model has been rewritten in several versions. Its different versions provide examples of different decisions during the model development. Bergström (1995) completely described the application of the model and details on the basic internal routines.

HBV-EC was initially developed by Dan Moore in mid-1980s (Moore, 1993), and now has become one of the main models applied in British Columbia besides the UBC Watershed Model and the Distributed Hydrology Soil Vegetation Model (Rodenhuis, Bennett, Werner, Murdock, & Bronaugh, 2007). HBV-EC is semi-distributed allowing the basin to be divided into various HRUs based on land cover, elevation, slope, and aspect (Hydrological Response Unit). Moore (1993) added a glacier routine for the HBV-EC model and combined it with the EnSim Hydrologic modeling environment also known as Green Kenue (Canadian Hydraulics Centre, 2010). Cunderlik and Ouarda (2010) and Fleming et al. (2010) showed the capability of HBV-EC model to provide a precise streamflow prediction in British Columbia's mountain watersheds in an inter-

comparison study of watershed models for operational river forecasting. The algorithm and detail of the model are explained by Hamilton, Hutchinson, and Moore (2000) and Canadian Hydraulics Centre (2010).

HBV-EC is capable of modeling four land cover types: open, forest, glacier, and lake. The model allows a watershed to have different climate zones, thereby providing a better representation of lateral climatic gradients. Each climate zone is associated with one climate station and a unique parameter set; however in this study, no matter how many climate zones a basin has, a unique (universal) parameter set was used for different climate zones within the basin. HRUs created by the model is illustrated in figure 3.3.

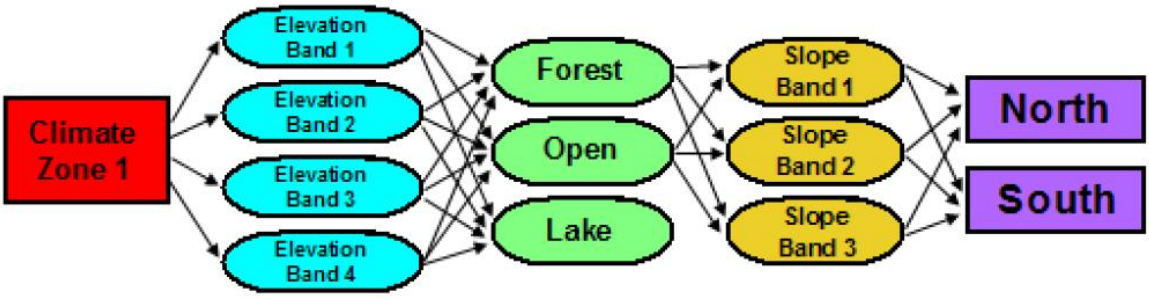

Figure 3.3: Schematic view of semi-distributed nature of the HBV-EC hydrological model (HBV-EC manual)

Within each of the climate zones (which are the grids of different products in this study) the user can identify a series of elevation bands based on the elevation values of DEM file. Consequently, each of the elevation bands are divided into one of the four land cover classes and then into the slope and aspect bands. As a result of this approach, the total number of areas is the product of the number of climate zones, the number of elevation bands, the number of land use types, the number of slope bands, and the number of aspect bands. Note that lake terrain is always considered to have a slope and aspect of 0. In this study, four elevation, two slope, and two aspect (0 and 180) bands were defined for each climate zone. The parameters of the outflow module apply to the entire watershed, regardless of the number of land classes or climate zones. On the other hand, the climate zone parameters including climate, forest, snow, soil, and glacier modules (provided in table 3.2) are specific to a single climate zone. Median value of each elevation band

is calculated and the differences of this value with elevation of stations is used to take into account the temperature lapse rate and orographic effects on precipitation.

Inputs to the HBV-EC model are the daily data of mean temperature (^{o}C), total rainfall (mm) and total snowfall (mm) (or total precipitation), and the mean monthly potential evaporation (mm). Daily evapotranspiration data can be applied instead of monthly average values, if available. The rainfall and snowfall correction factors (SFCF and RFCF) adjust recorded precipitation data in the presence of measurement errors. These include systematic errors due to missing evaporation from snow pack, gauge under-catch, and sublimation of deposited or drifting snow (Seibert, 1997). Climate data are adjusted for elevation, by applying a temperature lapse rate factor (TLAPSE) and separate gradients for precipitation below (PGRADL) and above (PGRADH) a threshold elevation (EMID). To calculate actual rainfall and snowfall from precipitation data the interval phase (TT ± TTI) is considered. Mixed-phase precipitation can occur within the interval, while above the interval there is only rain and below the interval there is only snow. In forested areas, interception loss is taken into consideration by a constant fraction of precipitation with separate fractions applied to rain (TFRAIN [-]) and snowfall (TFSNOW [-]).Table 3.2 shows the names, description, and units of the model parameters.

The HBV model has four main modules: (1) Snowmelt and snow accumulation; (2) Soil moisture and effective precipitation; (3) Evapotranspiration; and (4) Runoff response. The structure of the model is shown in figure 3.4.

3.3.1.1 Snow and ice melt Module

When the temperature is above the threshold temperature ($T_{0,}$ ^{o}C) precipitation is treated as rain, and snowmelt, M (mm), is calculated as equation 3.2.

$$M = C_m \times (T(t) - T_0) \qquad [3.2]$$

where C_m (mm $^{o}C^{-1}$) is melt factor and T(t) is the temperature at day t.

Refreezing of liquid water can occur when air temperature is below the melt threshold, at a rate governed by the parameter C_f (mm $^{o}C^{-1}$),

$$F = C_f \times (T_0 - T(t)) \quad [3.3]$$

If the calculated amount of refrozen water, F, exceeds the actual liquid storage, then F is set equal to the actual storage. The refrozen water, F, is added to the snowpack storage (Moore, 1993).

The melt factor varies from a minimum during the winter solstice, Cmin, (mm $^{o}C^{-1}$) to a maximum during the summer solstice in a sinusoidal way. The difference between the minimum and maximum values is the calibration parameter DC (mm $^{o}C^{-1}$). Snow melt factor (C_m) is only valid for open, flat areas. Therefore C_m changes as a function of aspect and slope of the basin. Equation 3.4 shows how C_m is calculated in HBV-EC:

$$C_m = MF_{FLAT} \times [1 - AM \times \sin(s) \times \cos(b)] \quad [3.4]$$

where s is a slope, b is an aspect, MF_{FLAT} is the melt factor computed for flat terrain (mm d^{-1}), and AM is a model parameter representing the aspect-slope reduction factor (dimensionless) varies between 0-1.

Moreover, in forested areas, the melt factor is further multiplied by MRF (ranging between 0 and 1) to account for the shading and sheltering effects of forest cover on melt rates (Stahl, Moore, Shea, Hutchinson, & Cannon, 2008).

3.3.1.2 Soil Module

Rain and snowmelt are added to the liquid water storage in the snowpack, and the excess in comparison to the water retention capacity is released to the soil moisture storage. This release is denoted WR (mm).

Soil moisture is modeled separately for forested and open areas within each elevation zone but the same parameter values are used for all zones (Stahl, 2008). The amount of water release that percolates through the soil moisture storage to become runoff RO (mm) is calculated by (Hamilton, Hutchinson, & Moore 2000):

$$RO = \begin{cases} \mathrm{WR}\,(\mathrm{SM}/\mathrm{FC})^{\beta} & \text{if } \mathrm{SM} < \mathrm{FC} \\ \mathrm{WR} & \text{if } \mathrm{SM} \geq \mathrm{FC} \end{cases} \quad [3.5]$$

SM equals to soil moisture storage (mm) for a particular land use class and elevation zone. FC is field capacity of the soil (mm), β is a parameter determined through calibration and controls the relationship between soil infiltration and soil water release. The difference between water release and runoff is added to the soil moisture storage. If the soil moisture exceeds the field capacity, all the water release becomes runoff.

3.3.1.3 Evaporation Module

Soil moisture and actual evapotranspiration calculations are connected by applying the L_p parameter. L_p is a soil moisture storage below which evaporation is limited. Equation 3.6 shows the relation between soil moisture and actual evapotranspiration (ET_a).

$$ET_a = \begin{cases} \text{PET}\ (\text{SM}/L_p) & \text{if SM} < L_p \\ \text{PET} & \text{if SM} \geq L_p \end{cases} \quad [3.6]$$

where PET is potential evapotranspiration.

Equation 3.6 shows that if the soil moisture is more than L_p value, the actual ET happens at the same rate as potential ET.

The HBV model is usually run with monthly data of long-term mean potential evapotranspiration and based on Penman equation (Penamn, 1948), however Paturel et al. (1995) and Nandakumar and Mein (1997) showed that compared to errors in precipitation data, PE errors made much smaller output errors, moreover a number of comparison studies have tested several methods of ET calculation such as a simplification of the Thornthwaite (1948) temperature index method or the Priestley-Taylor method (Priestley & Taylor, 1972), and none of these gave significantly better results than the other (Anderson, 1992; Gardelin & Lindstrrm, 1997). Obviously, HBV (or HBV-EC) is not sensitive to its ET computation routine and very simple temperature-based models are as efficient as more complex models such as the Penman model (Oudin et al., 2005).

3.3.1.4 Outflow Module

In the model, outflow from glacierized and non-glacierized HRUs is calculated separately. The runoff from all non-glacierized HRUs of all elevation bands is summed and afterward split by a factor FRAC (-) into two lumped reservoirs: a fast reservoir Q_f (mm) and a slow reservoir Q_s (mm). Outflow from the fast reservoir FR (mm d^{-1}) is computed as (Hamilton et al., 2000):

$$Q_f = K_f \times S_f^{(1+\alpha)} \quad [3.7]$$

where K_f is outflow coefficient ($mm^{-\alpha}$ d^{-1}), S_f is fast reservoir storage (mm), and α (alpha) is a parameter representing the amount of nonlinearity of the reservoir determined through calibration.

Outflow from the slow reservoir Q_s (mm d^{-1}) is calculated as:

$$Q_s = K_s \times S_s \quad [3.8]$$

where K_S is outflow coefficient (d^{-1}) and S_S is slow reservoir storage (mm).

The first reservoir represents the processes governing the near surface flow, whereas the second reservoir represents the processes governing the base flow (groundwater contribution). Two reservoir configurations (parallel vs. serial) are available in HBV-EC version, controlled by a variable. If the value of this variable is set to Parallel, the Runoff FRAC becomes a parameter and works as explained above; otherwise, the configuration of Runoff Perc will be used. FRAC defines the fraction of runoff directed to the fast reservoir. Basins that respond quickly to precipitation will tend to have higher values, while basins that show a delayed response will have lower values. On the other hand, Runoff Perc is the rate of percolation from the fast reservoir to the slow reservoir, per day. This simulates the effects of groundwater recharge on the slow reservoir.

To take into account the outflow from glacierized HRUs, the sum of water release from glaciers at all elevation bands is calculated and added to the glacial storage reservoir. Then the outflow Q_G (mm/d) of this reservoir is calculated by equation 3.9.

$$Q_g = K_{g,t} \times S_g \quad [3.9]$$

where S_g (mm) is the liquid water storage in the glacial reservoir for a certain HRU and $K_{g,t}$ (d^{-1}) is an outflow parameter that is time-dependent and changes in glacier development (equation 3.10) as

$$K_{g,t} = KG_{min} + dKG.\exp[-AG.SWE(t,g)] \quad [3.10]$$

where $K_{g,t}$ is the outflow coefficient for time t, KG_{min} (d^{-1}) is the undeveloped glacier situation where the drainage system is limited by deep snow lying on the top. dKG (d^{-1}) is the difference between KG_{min} and KG_{max}, and KG_{max} shows late summer situation with bare ice on the surface of the glacier and also drainage system is well-developed. AG (mm^{-1}) is a calibration parameter and SWE (mm) is the snow water equivalent for a certain glacier g at a certain time t.

The streamflow at the basin outlet is the sum of the outflow from the fast reservoir (Q_f), the slow reservoir (Q_s) and the glacier reservoirs (Q_g). The time dependency of the glacier drainage system is one of the main differences between the HBV-EC model and other versions.

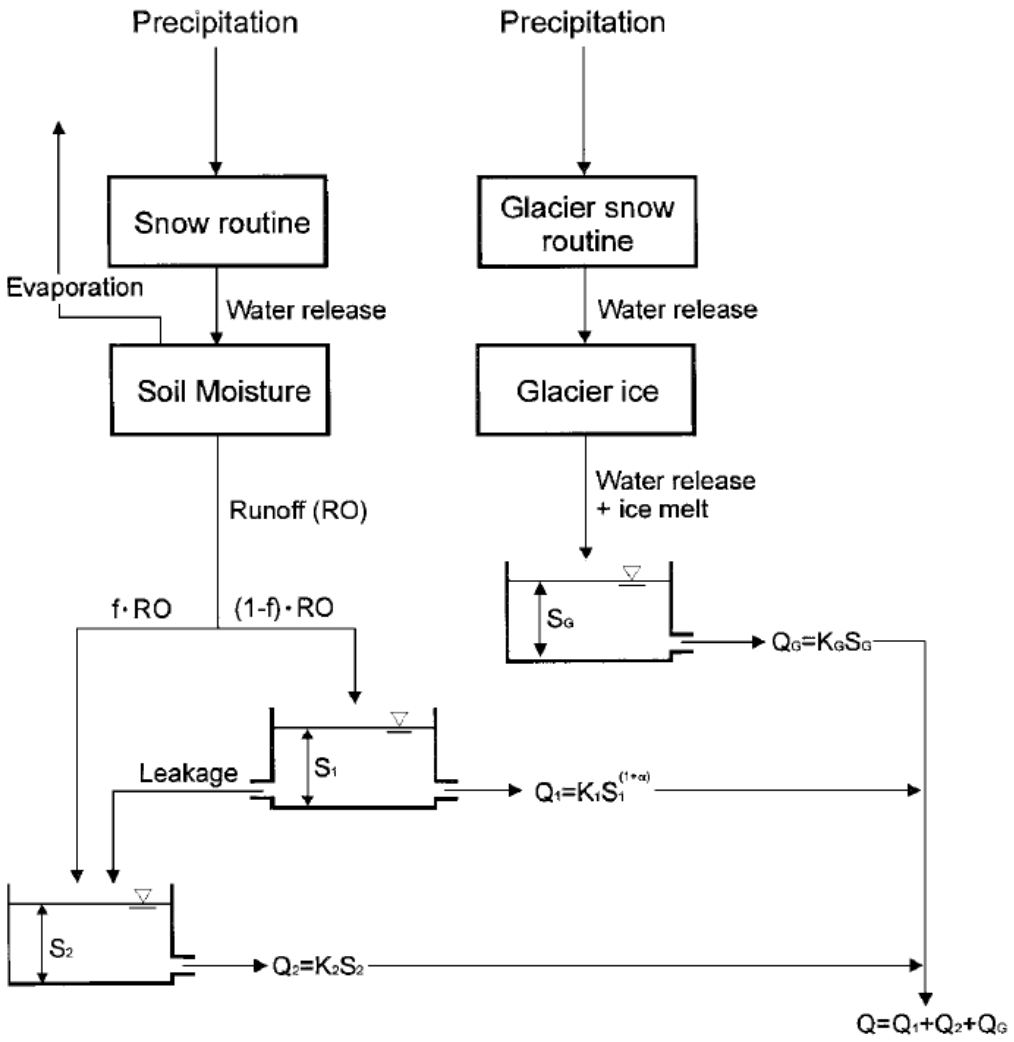

Figure 3.4: The structure of the HBV-EC model (Adopted from Hamilton et al., 2000)

Table 3.2: Model parameters (name, description, and unit)

Model routine	Name of Parameter	Description	Unit
Climate	TLAPSE	Temperature lapse rate	$^{\circ}C\ m^{-1}$
	ETF	Correction factor for potential evapotranspiration	-
	RFCF	Rainfall correction factor	-
	SFCF	Snowfall correction factor	-
	PGRADH	Fractional increase in precipitation with elevation, for elevations above EMID	
	PGRADL	Fractional increase in precipitation with elevation, for elevations below EMID	m^{-1}
	EMID	Mid-point elevation separating precipitation gradients	m^{-1}
	TT	Threshold air temperature for distinguishing rain from snow	$^{\circ}C$
	TTI	Temperature interval for mixed rain and snow	$^{\circ}C$
	EPGRAD	Fractional rate of decrease of potential evaporation with elevation	m^{-1}
Forest	TFRAIN	Fraction of rainfall reaching ground surface below the forest	-
	TFSNOW	Fraction of snowfall reaching ground surface below the forest	-
Snow	AM	Controlling the influence of the aspect on the melt factor	-
	TM	Threshold temperature for snowmelt	$^{\circ}C$
	CMIN	Value of the melt factor on the winter solstice for open areas	$mm\ ^{\circ}C^{-1}\ d^{-1}$
	DC	Increase in melt factor between winter and summer solstices	$mm\ ^{\circ}C^{-1}\ d^{-1}$
	MRF	Ratio between the melt factor in forest to the melt factor in open areas	-
	C_f	Controlling the rate at which liquid water refreezes in snowpack	$mm\ ^{\circ}C^{-1}\ d^{-1}$
	WHC	Liquid water holding capacity of snowpack	-
	LWR	Maximum amount of liquid water that can be retained by a snowpack	mm
Soil	FC	Field capacity of the soil	mm
	BETA	controlling the relationship between soil infiltration and soil water release	-
	L_P	Soil moisture content below which evaporation becomes supply-limited	-
Glacier	MRG	Ratio of melt of glacier ice to seasonal snow at the same air temperature	-
	AG	Controlling the relation between glacial snowpack water equivalent and runoff coefficient	mm^{-1}
	DKG	Difference between the minimum and maximum outflow coefficients for glacier water storage	d^{-1}
	KG_{min}	Minimum outflow coefficient for glacier water	d^{-1}
	K_g	Recession coefficient that is applied to the computation of the glacier outflow coefficient	d^{-1}
Runoff	KF	Fast reservoir coefficient	$mm^{-\alpha}\ d^{-1}$
	AlPHA	Fast reservoir exponent	-
	KS	Slow reservoir coefficient	d^{-1}
	FRAC	Fraction of runoff directed to the fast reservoir	-

3.3.2 Objective function

Assessing the performance of a hydrological model requires estimates of the goodness-of-fit of the simulated behavior of the model to the observations. Traditionally, the development of computer-based method has focused mostly on using a single overall objective function to measure the goodness-of-fit of the model (Madsen, 2000), Gupta, Sorooshian, and Yapo (1998) contended that considerable loss of information will appear if the differences between the measured and model output are captured using only a single objective. The multi-objective method makes it possible to find optimal parameter sets for different objective functions. Hence, multi-objective paradigm has been applied extensively in the literature to calibrate hydrological models for different flow segments of the hydrograph (for a review see Efstratiadis & Koutsoyiannis, 2010)

There is a large number of efficiency criteria used in hydrologic modeling studies and reported in the literature (Krause & Boyle, 2005; Nash & Sutcliffe, 1970). The selection and use of specific efficiency criteria and the interpretation of the results can be a challenge for even the most experienced hydrologists since each criterion may place different emphasis on the different types of simulation and observed behaviors (Krause & Boyle, 2005).

We used Nash-Sutcliffe efficiency (NSE), Nash-Sutcliffe efficiency on logarithm-transformed values (NSE-Log) and volume bias (BIAS) to describe the model fit with respect to the entire hydrograph. The combination of these three criteria is used in previous studies such as Tesemma et al. (2015) and Muleta (2012).

3.3.2.1 BIAS

Bias (BIAS) calculates the average tendency of the estimated data to be larger or smaller than the observed ones (Gupta, Sorooshian, & Yapo, 1999). The ideal value of bias is zero, with lower values indicating more accurate model simulations. Positive values indicate model underestimation bias, and negative values indicate model overestimation bias (Gupta, Sorooshian, & Yapo, 1999). Bias can show the model performance (Gupta, Sorooshian, & Yapo, 1999). Thus, it is a useful measure for assessing whether structural changes of the model equations are necessary for reducing the overall bias of prediction (Wallach et al., 2006). While this metric has been used in many previous research to provide information on model performance (Moriasi et al., 2007;

Houska, Multsch, Kraft, Frede, & Breuer, 2014; Moriasi & Gitau, 2015), it is not sufficient to evaluate model errors on its own, as a bias of zero could also be due to cancellation of large errors with different signs (Hiutska et al. 2014). The absolute bias which shows the magnitude of volume bias was calculated in this research (equation 3.11) as

$$BIAS = abs(\frac{\sum_{i=1}^{n}\left(Y_i^{obs} - Y_i^{sim}\right)\times 100}{\sum_{i=1}^{n}(Y_i^{obs})}) \quad [3.11]$$

where Y_i^{obs} and Y_i^{sim} are observed and simulated values at day i.

3.3.2.2 NSE

Nash-Sutcliff efficiency (NSE) proposed by Nash and Sutcliff (1970) is defined as one minus the sum of the absolute squared differences between the predicted and observed values normalized by the variance of the observed values during the period under investigation (equation 3-12).

This metric is sensitive to extreme values as the normalization of the variance of the observation series results in relatively higher values of NSE in the catchment with higher dynamics and vice versa. To obtain comparable values of NSE in a catchment with lower dynamics, the prediction has to be better than in a basin with higher dynamics. NSE ranges between $-\infty$ and 1.0, with NSE of 1 being the optimal value. Minus values demonstrates that the mean observed value is a better predictor than the simulated one that indicates unacceptable model performance (Moriasi et al., 2007). NSE is recommended for use by ASCE (1993) and Legates and McCabe (1999). Sevat and Dezetter (1991) concluded that NSE is the best objective function for reflecting the fit of a hydrograph. NSE is calculated as

$$NSE = 1 - \frac{\sum_{i=1}^{n}\left(Y_i^{obs} - Y_i^{sim}\right)^2}{\sum_{i=1}^{n}\left(Y_i^{obs} - Y^{mean}\right)^2} \quad [3.12]$$

where Y^{mean} is average of observed values in the period of study.

3.3.2.3 NSE-Log

The main disadvantage of the NSE is that high values are heavily weighted. Therefore, to reduce the problem of the squared differences and the resulting sensitivity to extreme values, the NSE is often calculated with log-transformed values of observation and simulation values (NSE-Log). In the process of logarithmic data transformation, the peak values of runoff data become flattened while the low flows are kept almost at the same values. Therefore, the effect of the low flow values is increased compared to the the peaks (Krause & Boyle, 2005). NSE-Log is calculated as:

$$NSE - Log = 1 - \frac{\sum_{i=1}^{n}\left(lnY_i^{obs} - lnY_i^{sim}\right)^2}{\sum_{i=1}^{n}\left(lnY_i^{obs} - lnY^{mean}\right)^2} \qquad [3.13]$$

3.3.3 Monte-Carlo simulation

The hypothesis that very different parameter sets can produce almost equally good fits between simulated and observed runoff was tested by using the following Monte Carlo procedure. Monte-Carlo algorithm is used to screen the high-dimensional parameter space for behavioral model runs and apply parameter identifiability method, to investigate model performance and parameter uncertainty. A number of studies applied the identifiability method to achieve a better understanding of rainfall-runoff models and their parameters (Lindstrôm, 1997). For the Monte Carlo simulations, 10,000 parameter sets were generated using random sampling from a uniform distribution within the given ranges for each parameter (table 3.3). For each parameter set, the model was run and the objective functions were computed. It should be mentioned that for running the model, the mean elevation within an elevation zone was used and also parameter values were not allowed to vary for the different climate zones. So the number of parameters and their values were equal for all zones within each basin. Models contain 32 parameters overall (table 3.2) for all modules. However, 11 parameters were analyzed in Monte Carlo simulation and the other 21 ones were kept constant at their default values. Table 3.3 summarizes values of parameters achieved by calibration or ranges used for either calibration or Monte-Carlo simulation, in previous studies. And the value used for fixed parameters are the default amounts of the model (table 3.4).

Reducing the number of parameters to be perturbed in the Monte-Carlo simulation was intended to reduce the dimensionality of the problem space and make the problem more tractable. The 11 parameters chosen were from different model routines and have been used frequently in model calibration in previous studies (Jost et al, 2012; Dakhlaoui, Bargaoui, & Bárdossy, 2012; Stahl et al 2008; Spiegelhalter, 2009 Bohrn, 2012; Mahat & Anderson, 2013). Most of these parameters are hardly identifiable without calibration, including: AM, DC (snow melting parameter), KF, ALPHA, Ks, FRAC, AG (outflow parameters), BETA, L_P (soil parameters) and ETF (ET parameter) (Spiegelhalter, 2009; Stahl et al. 2008; Mahat & Anderson, 2013). FC is a parameter which can be either measured or calibrated (Rusli, Yudianto, & Liu, 2015). However, because of the unknown spatial heterogeneity of the basins and the expenses involved, field capacity is mostly defined by model calibration (Raat, Vrugt, Bouten, & Tietema, 2004). Therefore, we included it in Monte-Carlo simulation and applied FAO soil properties data to define a reasonable range for each basin.

Some other parameters were kept constant with values given from previous studies (parameters such as TFRAIN and TFSNOW which are mostly fixed in the range of 0.8-0.9). For instance, it is recommended by Aghakouchak and Habib (2010) that 0 °C is a reasonable assumption for TT. Moreover TTI has been defined or calculated (in the calibration process) as 2 in some previous studies (Spiegelhalter, 2010; Heerema, 2013). Rainfall and snowfall correction factors (RFCF and SFCF) were fixed in the model in the first experiment. Later, however, I defined an external correction factor that as a multiplier for the precipitation data.

3.3.3.1 Progressive Latin Hypercube Sampling (PLHS)

The performance of a sampling strategy directly controls the efficiency and robustness of the associated sampling-based analysis. Different kinds of sampling strategies have been introduced over the past decades such as pseudo-random sampling, stratified sampling, fractional and full factorial design (Box & Hunter, 1961), regular grid sampling, orthogonal design (Owen, 1992), Latin hypercube sampling (McKay et al., 1979), and Sobol' sequences (Sobol, 1967). The proper choice of sample size which leads to a suitable distribution of the sample points in the input space can maximize the amount of information extracted from the model and also ensure sufficient

coverage of the output space which is required to characterize the complexity/nonlinearity of the response surface (Sheikholesalmi & Razavi, 2017).

In this study, a novel sampling strategy called Progressive Latin Hypercube Sampling (PLHS) method introduced by Sheikholesalmi and Razavi (2017) was used to generate sample points. PLHS is an extension of LHS (Latin Hypercube Sampling), developed by McKay et al. (1979) and Iman and Conover (1980) known as one of the most commonly used sampling approaches in environmental and water resources area. Because it is easy to apply (comparable with random sampling) and it ensures one-dimensional projection properties ("Latin Hypercube" properties). Sheikholeslami and Razavi (2017) showed some advantages of PLHS over LHS in terms of space-filling and one-dimensional projection properties (Sheikholeslami et al., 2017). The main differences of these two methods is that the original LHS generates the entire sample set in one stage while PLHS produces a series of smaller sub-sets (slices) such that (1) each sub-set is Latin hypercube and achieves maximum stratification in any one dimensional projection; (2) the progressive addition of sub-sets remains Latin hypercube; and thus (3) the entire sample set is Latin hypercube (Sheikholeslami & Razavi, 2017).

The performance of PLHS across several case studies and multiple applications including Monte-Carlo simulation, sensitivity and uncertainty analysis has shown superior efficiency, convergence, and robustness over alternative strategies. In this method unlike LHS, the new sample points can be added sequentially to the sample set. And in comparison with other sequential sampling approaches, it preserves projection properties along with other desired sample properties (Sheikholeslami & Razavi, 2017).

3.3.4 Forcing data combination

Previous studies have shown that precipitation products usually tend to underestimate or overestimate the real data. Negative or positive bias of a rainfall product in rainfall-runoff modeling can result in declining of modeling performance. Calibration based on such data leads to parameter values that are not realistic, as the model tries to compensate for the errors in precipitation data. Therefore, Artan et al. (2007), Behrangi et al. (2011), and Zeweldi, Gebremichael, and Downer (2011) recommended that precipitation products be corrected before

applying to the model. Some researchers have attempted to adjust the precipitation data for more accurate streamflow prediction (Habib, Haile, Sazib, Zhang, & Rientjes, 2014; Krogh, Pomeroy, & McPhee, 2015; X. Liu et al., 2017).

To adjust the precipitation data used in this study, two precipitation data sets which result in better objective function values (Product1 and Product2) were chosen to be combined in a linear fashion using two correction factors:

$$P = P_1 \times [(1 - P_2) \times Product1 \ + (P_2) \times product2] \qquad [3\text{-}14]$$

where P is combined precipitation, and P_1 and P_2 are precipitation correction factors.

Table 3.3: Range of parameters used in Monte-Carlo simulation or calibrated values

Name of Parameter	Ranges used in this study	Jost et al. (2012)	Hamilton, Hutchinson, and Moore (2000)	Stahl et al. (2008)	Przeczek et al. 2009	Hamilton (2001)	HBV-EC manual
ETF	0-1	-	0	-	-	0.5	0-1
AM	0-0.9	0-0.6	-	0.25	0.58	-	-
DC	0-3	0-1.2	2.55	2.08	0	2	-
FC	100-180, 180-350	-	400	-	-	100	-
BETA	0.8-2	-	1.81	-	-	1.3	-
L_P	0.5-1	-	0.599	-	-	0.7	-
AG	0-0.2	-	-	-	-	-	0-0.2
K_f	0-1	0.05-0.3	0.013	-	-	0.26	-
AlPHA	0-0.5	0.05-0.2	0.49	-	-	-	-
K_s	0.003-0.1	0.0005-0.015	0.00148	-	-	0.008	-
FRAC	0.4-0.9	0.7-0.9	-	-	-	0.57	-

Table 3.4: Values of fixed parameters

Name of Parameter	Value
TLAPSE	0.0065
RFCF	1
SFCF	1
PGRADH	0
PGRADL	0.0001
EMID	5000
TT	0
TT_I	2
EPGRAD	0.0005
TFRAIN	0.9
TFSNOW	0.8
TM	0
C_{min}	2
MRF	0.7
CRFR	2
WHC	0.05
LWR	2500
MRG	2
DKG	0.05
KG_{min}	0.05
K_g	0.7

3.3.5 Pareto Optimality

In many hydrological modeling applications, more than one optimization criteria (or objective functions) are used that measure various isaspects of the system behavior. These objectives are potentially conflicting, therefore, there is no feasible point that optimizes all of them simultaneously. A multi-objective calibration problem can be formulated as (Madsen, 2000):

$$\min \{F1(\theta), F2(\theta), ..., Fm(\theta)\} \text{ with } \theta \in \Pi \qquad [3.15]$$

where Fi (θ) (i=1, 2 . . . , m) are the objective functions and parameter set θ is restricted to the feasible parameter space Π.

Generally, the solution to the above optimization/calibration problem can consist of many (possibly unlimited many number of) parameter sets that all together will form Pareto optimal solutions (Gupta, Sorooshian, Hogue, & Boyle, 2003; Deb, 2001; Vrugt, Gupta, Bastidas, Bouten, & Sorooshian, 2003). Solutions laying on a Pareto front (also called trade-off curve) cannot be improved in one objective without worsening at least one other objective. This concept was proposed for the first time by Italian economist Vilfredo Pareto (1848-1923) in the Nineteenth Century in the context of optimal resource allocation (Pareto, 1896).

A schematic Pareto front is shown in figure 3.5, where two objective functions ‘a’ and ‘b’ are the axes, and the goal of the modeler is to minimize both. Dots show the values of objective functions related to different parameter sets. The black dots represent the Pareto-optimal set, and the curve connecting them is the Pareto front (Langenbrunner & Neelin 2017).

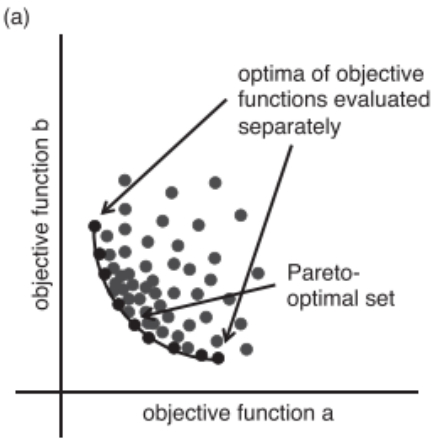

Figure 3.5: Schematic of Pareto front (adopted from Langenbrunner & Neelin, 2017)

All parameter sets that are non-dominated with respect to objective functions are equivalently optimal (in the Pareto sense) solutions to equation 3.15; however, all these solutions are not necessarily behavioral in the rainfall-runoff modelling context (Efstratiadis & Koutsoyiannis, 2010). And also the non-behavioral solutions might not always exclusively correspond to the extreme tails of the Pareto front. Thus, the principle of dominance needs acceptability thresholds to generate the behavioral solutions. This means that we need to identify a sub-set of Pareto-optimal solutions that are behavioral, by imposing cut-off thresholds to the Pareto front.

Figure 3.6 is a graphical example showing Pareto-optimal and behavioral solutions in the objective space, for two objective functions f_1 and f_2. Vector $e = [e_1, e_2]$ indicates cut-off thresholds for distinguishing behavioral and non-behavioral solutions (Efstratiadis & Koutsoyiannis, 2010; Gharari, Hrachowitz, Fenicia, & Savenije, 2013).

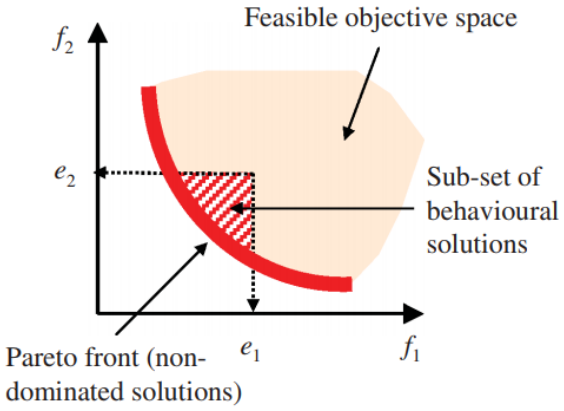

Figure 3.6: Pareto front and behavioral solutions (adopted from Gharari et al., 2013)

3.3.5.1 Cut-off thresholds

The challenge of how to keep the model parameters that have a consistent model behavior (or how to establish the cut-off threshold between behavioral and non-behavioral parameters) in a meaningful way requires further investigations (Gharari et al., 2013). To address this challenge, Gharari et al (2013) uses three approaches for the selection of behavioral parameter sets (figure 3.7): (I) Pareto optimal parameter sets, (II) Parameter sets within a pre-defined distance to the origin (which is the parameter sets with a distance smaller than 1.05 times of the closest Pareto member to the origin), and (III) Parameter sets that are contained within the quadrant determined by individual optimal solutions for each objective function.

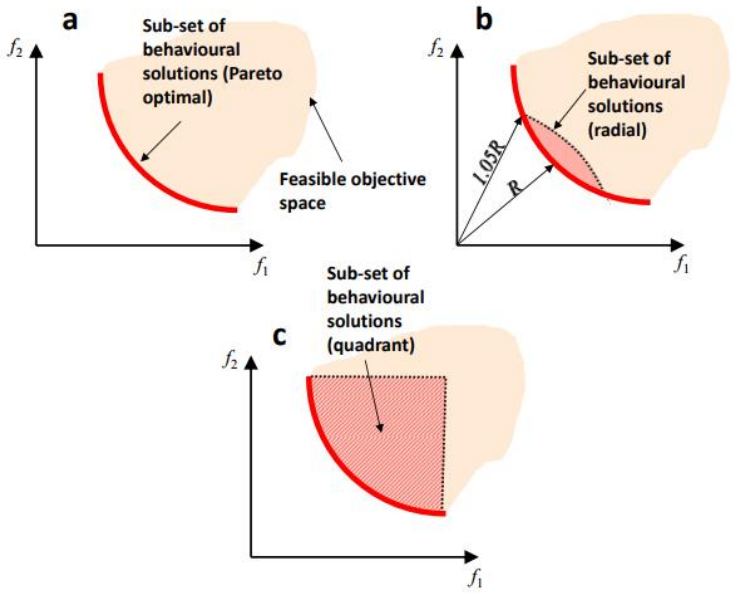

Figure 3.7: Different methods to select behavioral solutions; (a) Pareto optimal parameter sets, (b) parameter sets which perform closer than 1.05 of minimum distance of Pareto front to origin (radial), and (c) parameter sets which perform simultaneously better than the lowest performance of any dimension of Pareto front (quadrant) (adopted from Gharari et al., 2013)

In this study, two methods are applied to select 50 behavioral parameter sets (0.5 percent of all parameter sets generated), namely "Radial" and "Cut" methods:

1) Radial is the "b" procedure in figure 3.7. In this study, the pre-defined distance is set such that 0.5 percent of all parameter sets (50 numbers) are selected.

2) Cut is the "c" approach in figure 3.7. In this approach, 50 parameter sets are chosen by three criteria which are as follow; NSE and NSE-Log are higher than 0.5 and BIAS is the smallest value which leads to the selection of 50 parameters. BIAS changes for each case since this criterion is highly variable and cannot be fixed at a constant value, in order to select 50 parameter sets.

3.3.6 Flow Duration Curve for catchment selection

Flow Duration Curve (FDC) incorporates the relationship between the frequency and magnitude of streamflow (Vogel & Fennessey 1995). It integrates the combined impacts of climate, geology, geomorphology, soils and vegetation. Therefore, it is useful in comparing runoff characteristics of different catchments (Sugiyama, Vudhivanich, and Whitaker 2003; Pearce 1990; Searcy 1959). In general, FDC sorts out streamflow data by shifting high flows with high precipitation signals to one end of the curve, medium flows to the middle, and low flows (presumably with low precipitation signals) to the other end of the curve (Mahmoud, 2008). Normalized FDC (normalize the discharge by dividing to the drainage area) is more helpful in order to visualize the variation in hydrologic response of different drainage basins (Mahmoud, 2008) and therefore was utilized to select the basins (will be described in section 3.3.7).

A normalized FDC was constructed from normalized daily streamflow ($m^3\ s^{-1}\ km^{-2}$) for each study catchment, following the Weibull plotting formula (Sugiyama, Vudhivanich, and Whitaker 2003):

$$P = \frac{r}{(N+1)} \times 100 \qquad [3.16]$$

where P is the percentage of time that a given flow is equaled or exceeded, N is the total number of data points in the period of record, and r is the rank assigned to each streamflow value in the period of record.

3.3.7 Selection of Catchments under Investigation

In the first attempt, Monte-Carlo simulation experiments were carried out for the 25 basins with consistent parameter ranges. The Monte-Carlo simulation was applied three times for the three climate data sets, ANUSLIN, CaPA, and WFDEI (75 experiments overall).

In order to pick the five basins out of the 25 basins for more detailed investigation on hydrological processes and model parameters, the following criteria were considered: (1) the basins with no missing data in period 2002-2012 (which is the overlap period of the three databases), (2) the basins with maximum NSE and NSE-Log higher than 0.6, (3) the basins with

similarly-sized areas (to minimize the size effect on streamflow process), and (4) the basins with different shapes of flow duration curves (FDCs). An FDC integrates landscape–climate and hydrological influences and is applied as a hydrological descriptor to classify the basins into the different classes and then one basin of each class is selected (5 basins overall).

3.4 Boxplot

To display parameter identifiability of the model in different catchments, we generated boxplots using MATLAB for each model of the five basins, and three objective functions. The boxplot is a useful and standardized way of displaying the distribution of data (from min to max) based on the following summary statistics: minimum, first quartile (25th percentiles), median, third quartile (75th percentiles), and maximum. The ends of the whiskers show the position of the minimum and maximum of the data, whereas the edges and line in the center of the box show the upper and lower quartiles and the median.

The whiskers extend to the most extreme points are not taken into account as outliers. The outliers are illustrated individually by the '+' symbol (MATLAB manual). For symmetrically distributed data the mid-line (median) is half way between the upper and lower edges of the box (the upper and lower quartiles). A larger dispersion of the boxplot represents a lower identifiability of the associated parameter.

4 Results and Discussion

4.1 Data analyses of 25 basins

The average annual precipitation and temperature of the 25 basins for different climate products is illustrated in figures 4.1 and 4.2. Various products estimate different values for annual precipitation and temperature for each basin. The highest discrepancy for precipitation is 600 mm between CaPA and ANUSPLIN for basin 08KB003, which has an area of 4780 km^2 and an average elevation of 1372m. Some of the basins (08NP004, 08NB012, 07AA001, 05DA007, and 05AA022) which show agreement among the three precipitation products, at less than 77mm of precipitation in a year.

For temperature, ANUSPLIN and WFDEI show the maximum disagreement for basin 05BG006, which can be as high as 2.0°C (figure 4.3). CaPA and WFDEI show lower temperatures compared to ANUSPLIN in 22 out of 25 basins. Although the difference between CaPA and WFDEI may not be significant, a small change in temperature can cause snowmelt to start earlier or later. Thus, these slight shifts in temperature might have a significant impact on early spring flow.

Despite the differences of temperature values, some basins, including 08NP004, 07FB006, 07FB003, 07EC002, 07EC004, and 07EE007, show good agreement among the three products, with differences being less than 0.28 °C.

Results show that both precipitation and temperature data for the three products have good agreement for basin 08NP004 with an area of 92.8 km^2 and an average elevation of 1792m, which is amongst the smallest ones of the 25 basins.

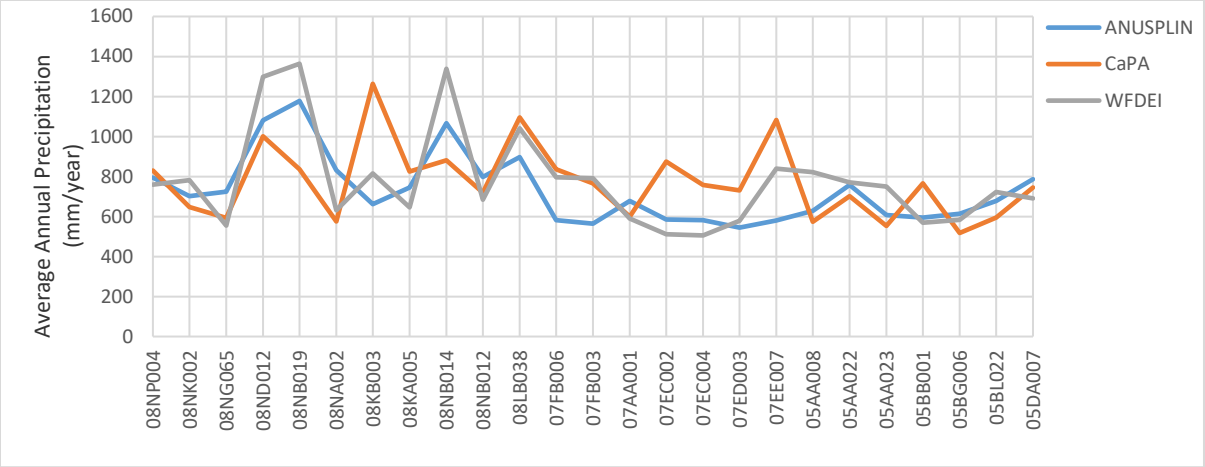

Figure 4.1: Average annual precipitation of all the basins for ANUSPLIN, CaPA, and WFDEI, for the years 2002-2012

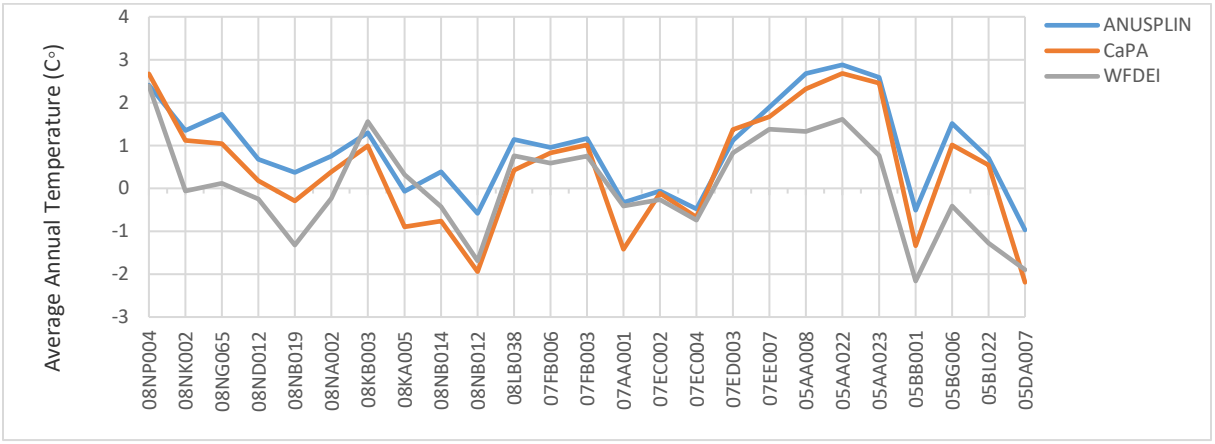

Figure 4.2: Average annual temperature of all the basins for ANUSPLIN, CaPA, and WFDEI, for the years 2002-2012

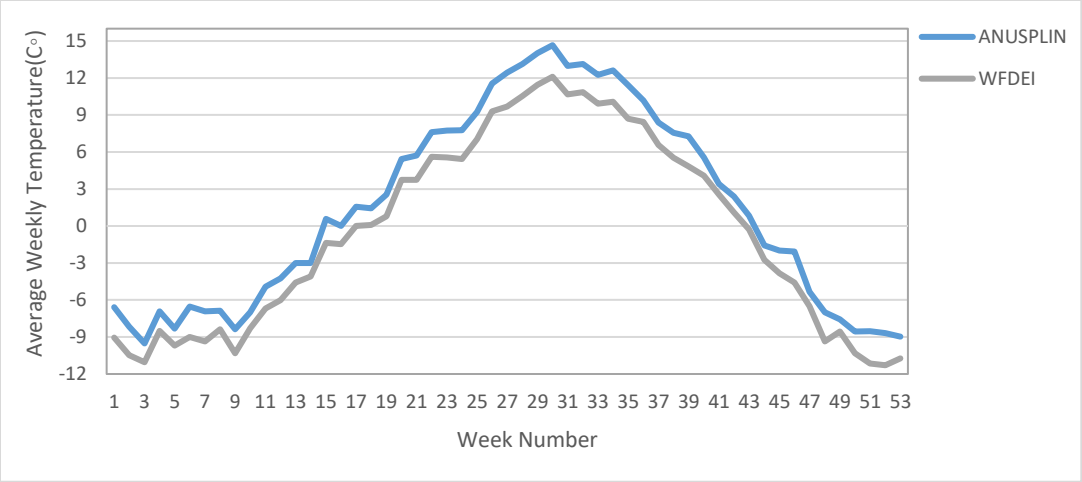

Figure 4.3: Average weekly temperature of 05BG006 for ANUSPLIN and WFDEI, for the years 2002-2012

4.1.1 Runoff ratio

The average values of the runoff ratio for the basins based on precipitation data are shown in figure 4.4. Percentage of glacier land cover for each basin is also illustrated in this figure. The runoff ratio is observed streamflow over average precipitation of the three products (ANUSPLIN, CaPA, and WFDEI).

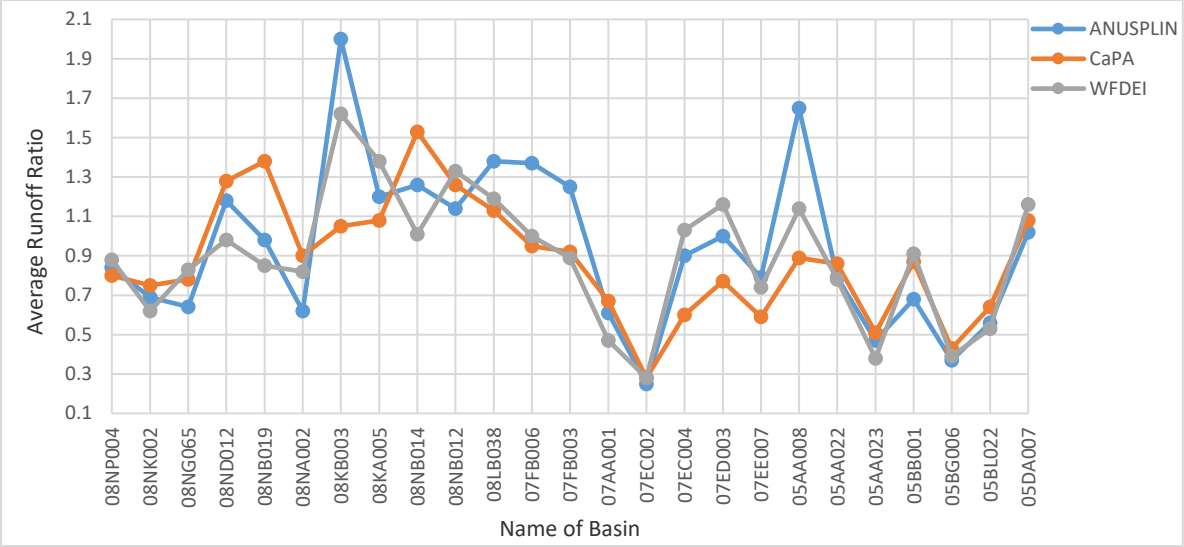

Figure 4.4: Average runoff ratio of basins for ANUSPLIN, CaPA and, WFDEI, for the years 2002-2012

Figure 4.4 shows that for several basins, for example, 08NB014, 05DA007, and 08NB012, runoff ratios are higher than one (by using any of three precipitation products). These results suggest two possible hypotheses: 1) the precipitation data is underestimated, or 2) significant glacier melt is contributing to the runoff ratio. Figure 4.5 shows the relationship of glacier percentage of watershed area and runoff ratio.

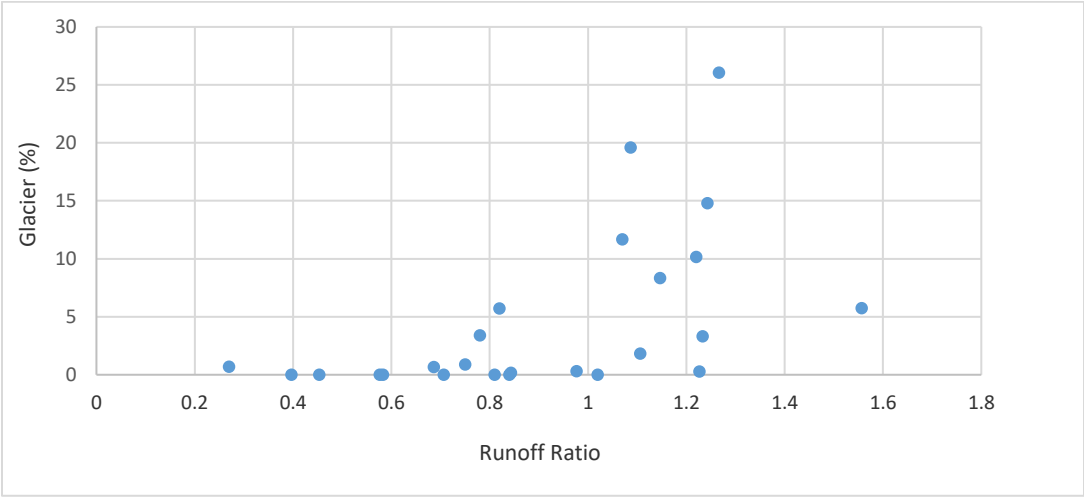

Figure 4.5: Scatter plot between glacier percentage and runoff ratio

Figure 4.5 shows that basins with a higher percentage of glacier are more likely to have a higher runoff ratio. Eleven of 25 basins have a runoff ratio of higher than one, and five of those 11 basins, have a glacier coverage of 10% or more. For instance, basins 05DA007, 08NB014, and 08NB012 with the highest amounts of glacier at 26%, 20% and 15%, respectively, show runoff ratios of 1.08, 1.24, and 1.08, respectively. These unexpectedly high runoff ratios could be related to the declining glacier mass in the Canadian Rocky Mountains. As mentioned, the Canadian Rockies have changed significantly during the last few decades. For example, icefield areas in the Athabasca, Saskatchewan and Columbia River basins have sharply declined (Reid & Charbonneau, 1979). Another change can be seen in the length, area, elevation, and volume of glaciers in the Rocky Mountains, which from 1919 to 2009 experienced substantial recession and mass loss (Tennant & Menousos, 2013). A third example of change in the Rockies is the Columbia Icefield, which, in the same period, decreased by 59.6 Km^2 (22%) (Tennant & Menousos, 2013). As a result of this evidence of declining glacier mass, it can be hypothesized that glacier melting contributes to streamflow generation and, consequently, a high runoff ratio. However, a high runoff ratio cannot be explained only by melting glaciers. For example, basin 07EE007 generates an average runoff ratio of 1.22, with the amount of glacier at just 0.28%. In this case, the underestimation of precipitation data seems to be a more plausible explanation for the high runoff ratio.

4.2 Data Analysis of 5 selected basins

In this section, the data is rigorously scrutinized for the five selected basins (refer to Section 3.3.7). Table 4.1 and figure 4.6 illustrate the name, ID and the coordinates of the hydrometric station for the basins and also the location of the basins in the Rocky Mountains. As can be seen, basin 05BB001 is in Alberta, while the others are in British Columbia. Table 4.2 shows the average elevation and slope of each basin. The average elevation of the basins ranges from 1713m for 08ND012 to 2168m for 05BB001. As for the slope, the maximum (24%) is seen in basin 08NB019 and the minimum (9.71%) in basin 08NK002.

Table 4.1: Hydrometric gauge information (Water Survey of Canada)

Station ID	Name	Latitude	Longitude
08NB019	BEAVER RIVER NEAR THE MOUTH	51°30'32.7¨ N	117°27'55.1¨ W
05BB001	BOW RIVER AT BANFF	51°10'20.0¨ N	115°34'18.4¨ W
08NB012	BLAEBERRY RIVER ABOVE WILLOWBANK CREEK	51°28'57.0¨ N	116°58'09.7¨ W
08NK002	ELK RIVER AT FERNIE	49°30'12.5¨ N	115°04'12.5¨ W
08ND012	GOLDSTREAM RIVER BELOW OLD CAMP CREEK	51°40'07.6¨ N	118°35'46.3¨ W

Table 4.2: The average elevation and slope of basins

Station ID	Average Elevation (m)	Average Slope (%)
08NB019	1907	24
05BB001	2168	10.9
08NB012	2018	14.9
08NK002	1860	9.71
08ND012	1713	15.8

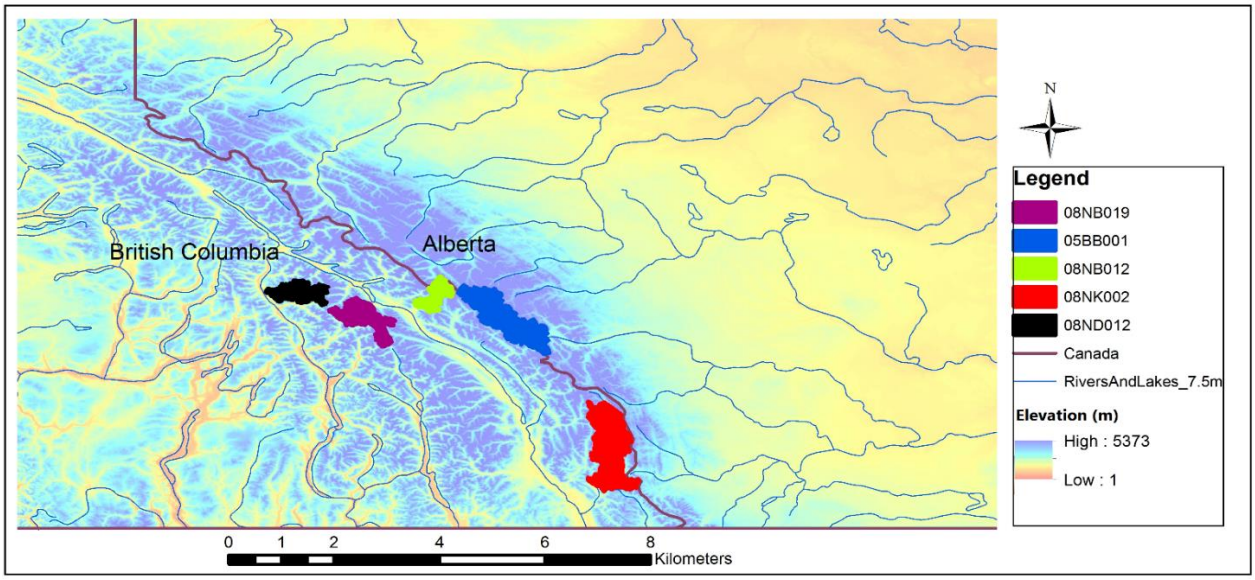

Figure 4.6: The location of selected basins on SRTM digital elevation model

4.2.1 Climate Zone

Figure 4.7 shows the gridded climate zone defined for model simulation. As mentioned in Section 3.3.1, the HBV-EC model requires the delineation of climate zones; each zone has its own time series of temperature, precipitation, potential evapotranspiration, and average elevation, all of which are used to drive the hydrological processes within the model. Grids of climate products were used as a climate zone (Figure 4.7), resulting in 20 climate zones for all 5 basins. Basin 08NB012 covers only two climate zones, while basin 08NK002 covers eight zones.

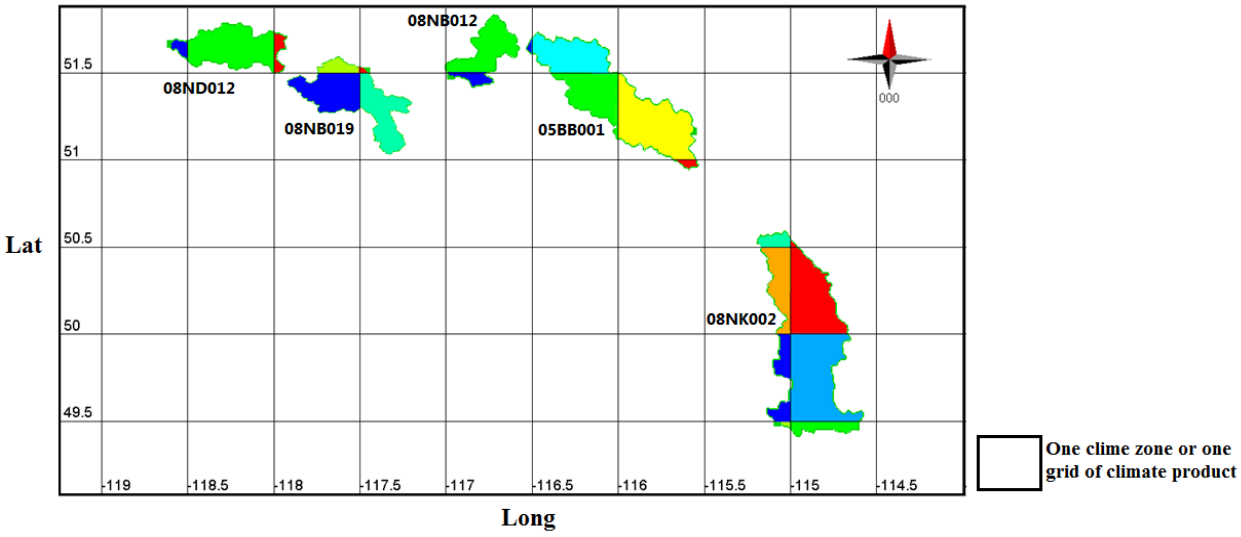

Figure 4.7: Gridded climate zones used in HBV-EC model

4.2.2 Land cover contrasts

The distribution of land-cover types using the HBV-EC classification for the basins are provided in figure 4.8 and figure 4.9. The basins are classified as mostly forested or open lands. Most of the areas classified as water are lakes with an almost negligible portion of 0-3.6%. For some basins, including 08NB012 and 08NB019, a substantial area is covered by glaciers, 15% and 12%, respectively. Since land cover directly impacts key aspects of hydrological processes such as ET, infiltration, and runoff, different combinations of land-cover types create different hydrological regimes for the river basins.

It has been found that under the same climate conditions (i.e., precipitation and temperature), higher ratios of open land (e.g., 05BB001 compared to 08ND012 in this study) lead to increased flow volume (Kundu & Olang, 2011). In contrast, more forested land cover (e.g., 08NK002 compared to 08NB012) reduces peak discharge (Kundu & Olang, 2011). Despite these findings, since the climate inputs of the above-mentioned sets of basins vary significantly, the differences of magnitude and timing of flow cannot be related only to the discrepancy in land cover.

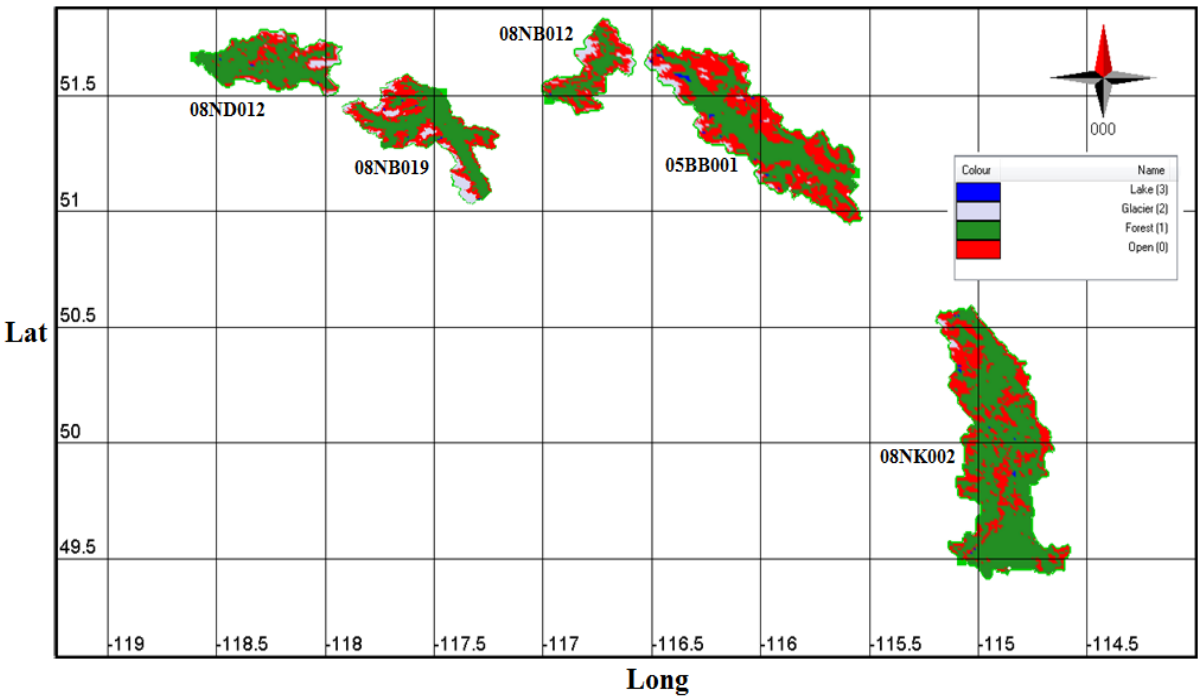

Figure 4.8: Land classification map for the basins used in the HBV-EC model

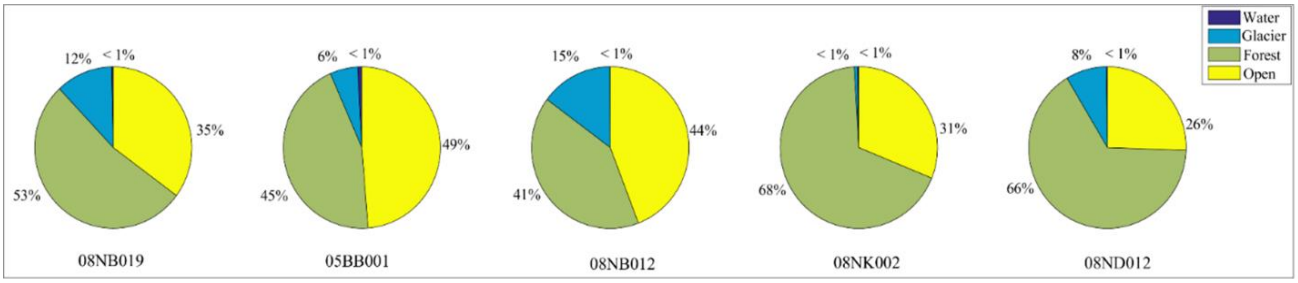

Figure 4.9: Land use percentage of basins

4.2.3 Hydrometric and Climate Data Analysis

Figures 4.10, 4.11, and 4.12 illustrate the average weekly precipitation, temperature and evapotranspiration of the basins. As can be seen in figure 4.10, basins 08ND012 and 08NB019 have the highest average weekly precipitation values for the entire period, with similar trends except for weeks 17 to 25 (May to the end of June), when basin 08NK002 reaches the maximum precipitation (for example 36.48 mm/week for week 24). 08NK002 with the elevation of 1860 has the lowest latitude compared to other basins.

The five basins receive the highest amounts of precipitation in different months. The highest amount of precipitation for basins 08ND012 and 08NB019 occurs in weeks 2 to 11 and 42 to 52, which correspond to January to March and the middle of October to the middle of December. For these two basins, snowfall is the dominant precipitation. For the other three basins, precipitation peaks occur from the end of May to the end of June. In these three basins, spring rainfall plays the primary role in precipitation peaks.

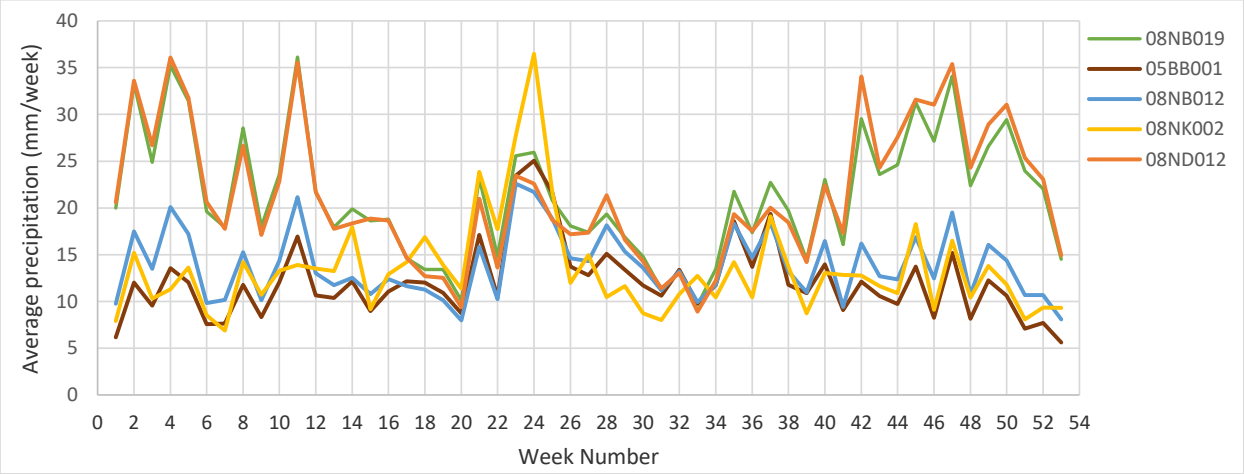

Figure 4.10: Average weekly precipitation of basins (observed data)

As shown in Figure 4.11, compared to precipitations trends, temperature trends and values are more uniform across the five basins. However, basin 08NK002 shows slightly higher temperatures, especially in warm seasons. Temperature peaks generally occur in week 30 (the end of July), and the lowest values are seen at the end of December. The noticeable differences among weekly temperature curves are the starting point of warm period and the length of this period. The

longest warm period is for basin 08NK002 that is 28 weeks (starts in week 16 and end in week 43), which may accelerate the initiation of snow melting. As a result, the peak of the hydrograph (figure 4.14) occurs earlier for basin 08NK002 (at week 23) than for the other basins (usually week 26).

The basins' average temperature and rain/snow ratio are positively related. Basin 08NK002 has the highest temperature, which results in a high rain/snow ratio (1.29). In contrast, basins 08NB012 and 05BB001 have lower rain/snow ratios (0.96 and 0.77, respectively), and their temperature is also lower compared to basin 08NK002 (figure 4.10).

The length of warming and the temperature values in this period can change the shape and peaks of the hydrograph by changing the duration of snow melting. Hence, the combined effect of both precipitation and temperature on the hydrograph should be taken into account.

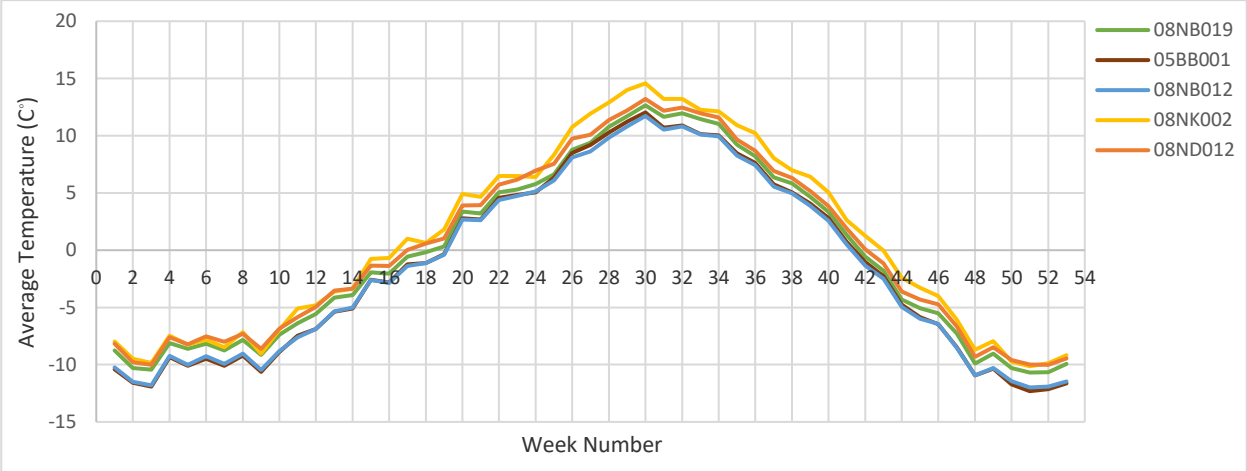

Figure 4.11: Average weekly temperature of basins

The actual evapotranspiration is another important process for these basins (figure 4.12). Based on the MODIS data a large portion of yearly evapotranspiration happens during the summer months (May to August). Basin 08NK002 has the highest temperature and also the largest percentage of forest, but it has the lowest portion of glacier, which generates more evapotranspiration during the cold season (January to April and October to December). However, for the warmer period from June to August 08ND012 as a second basin regarding to average temperature and also forest percentage, shows the highest amount of evapotranspiration.

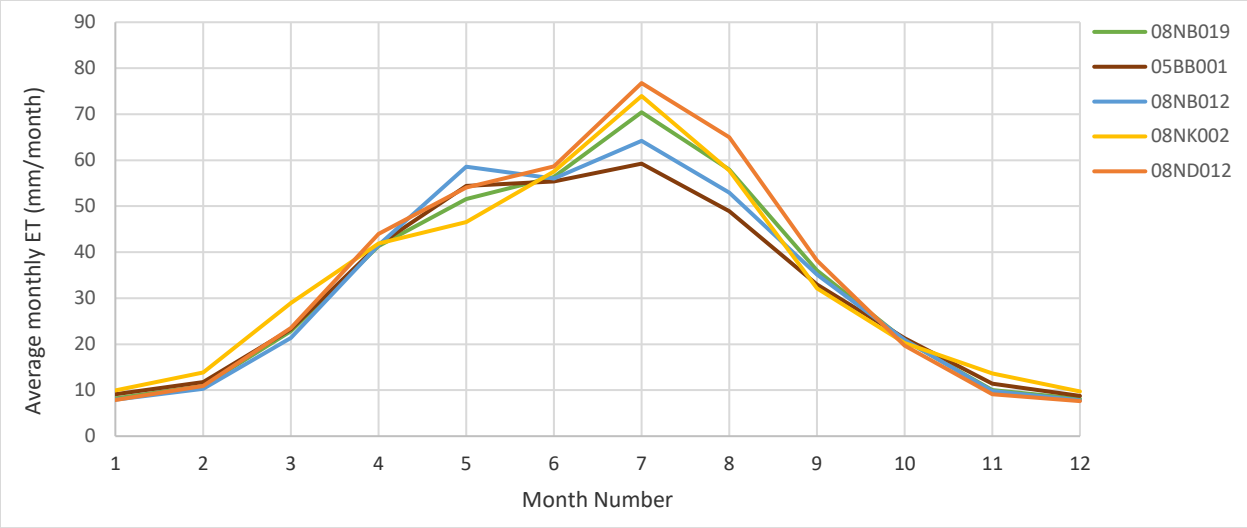

Figure 4.12: Average weekly ET of basins

Further, streamflow across the fine basins have been characterized via flow duration curves (a criterion used in selecting the five basins) in figure 4.13.

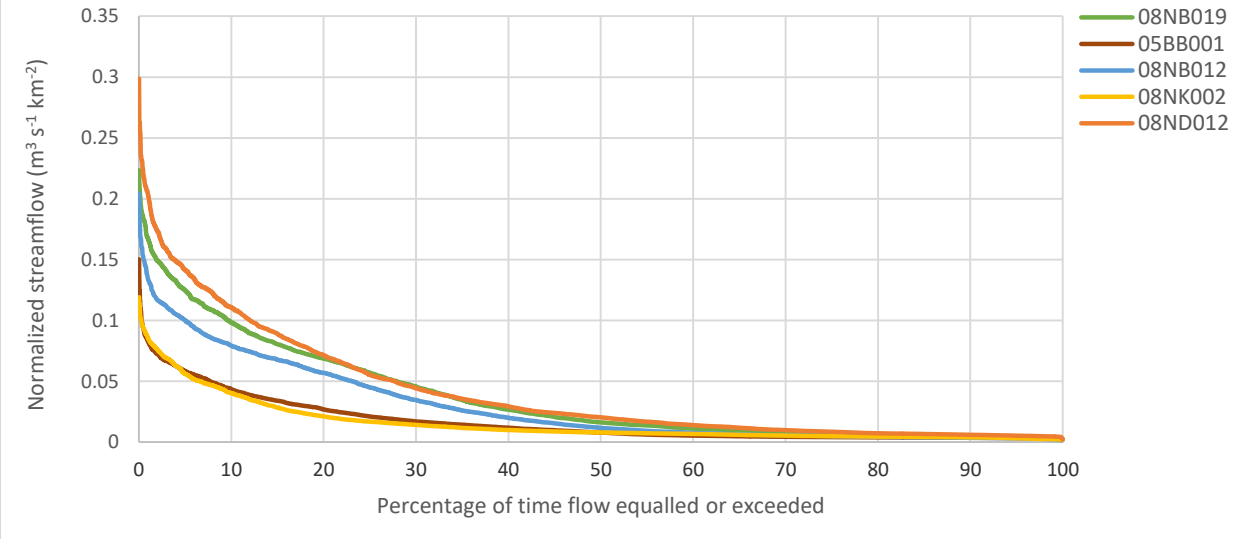

Figure 4.13: Flow duration curves of basins

All basins with a similar slope in the lower end of the flow duration curve show the same condition for their perennial storage; their gradual change is an indication of enduring storage over the year (Searcy, 1959). This gradual change in FDC (read as a flatter slope) may be the result of surface- or ground-water storage (basins 08NK002 and 05BB001). On the other hand, the steep

slope throughout the FDC is more likely to denote a highly variable stream, whose flow comes largely from direct runoff (basin 08ND012). Basins 08NB012 and 08NB019 show the property between these two conditions.

Previous research shows that streams with high flows produced by quick runoff from larger rainfall events have a steep slope at the upper end, while streams whose high flows come largely from snowmelt tend to have a flat slope at the upper (high flow) end (Searcy, 1959). Therefore, based on figure (4.13), basins 08NK002 and 05BB001 with a slightly steeper slope at the upper end show that heavy rainfalls are the main cause of quick flow in these basins.

A chronological sequence of long-term average daily flows is shown by a stream hydrograph (figure 4.14), which is a graph of the flow rate of a stream plotted against time.

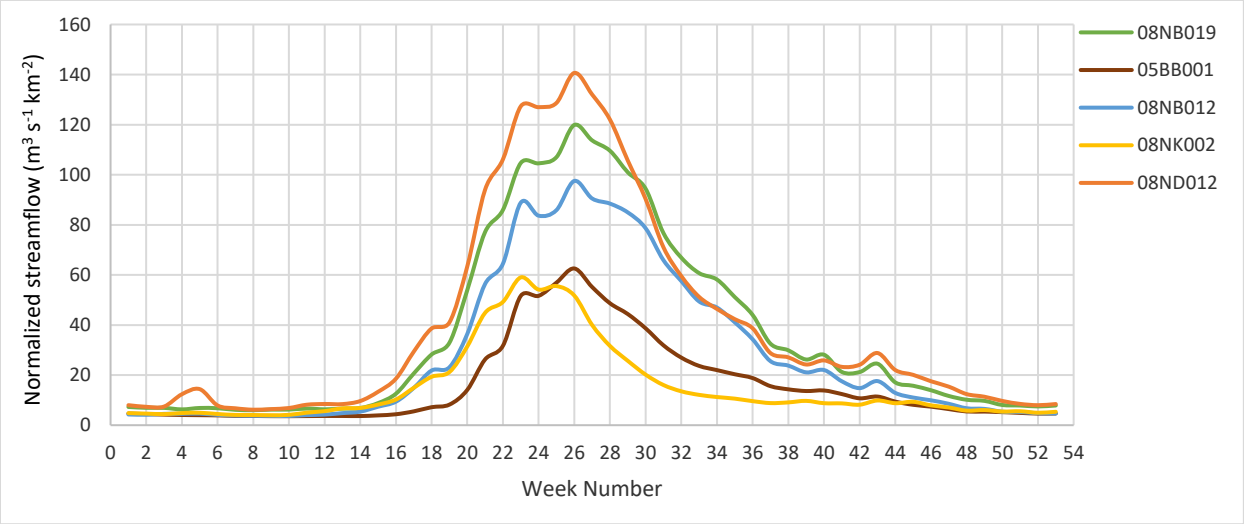

Figure 4.14: Average weekly observed streamflow of basins

A comparison of the average normalized streamflow shows that basin 08ND012 generates more streamflow except for the weeks 29 to 40. This greater flow in weeks 29-40 for 08NB019 might be due to the fact that the amount of precipitation for basin 08NB019 surpasses that of 08ND012 during this period.

In addition to climatic data, land use/land cover can be responsible for altering the hydrologic response of watersheds leading to impacting river flows and its hydrograph (Haile & Assefa, 2012). Agricultural or open areas are mainly covered by small plants, crops, and

herbaceous vegetation that have a shallow root zone. They intercept less precipitation than forested areas (Chow, 1964), resulting in increased flow volume and more flooding. In contrast, a more forested area can reduce peak discharges and direct runoff volume in the basin but increases the time of rise of hydrograph by affecting interception, snowmelt, soil moisture and the infiltration rate (Gray, 1964; Haile & Assefa, 2012; Sangvaree & Yevjevich, 1977). The percentage of glacier and its contribution to surface runoff, especially in warm seasons, is another important factor affecting the shape and timing of the hydrograph and should be taken into account when interpreting a hydrograph's characteristics. However, although 08NB019 contains a smaller portion of forest and a larger percentage of glacier compared to basin 08ND012, it shows a lower peakflow. This unexpected result may be related to an errors in precipitations and underestimation of data for 08ND012.

Regarding precipitation and its relationship to streamflow, the results from basins 05BB001and 8NK002 are inconsistent with those from basins 08ND012 and 08NB019. The hydrographs from basins 05BB001 and 08NK002 cross each other first in week 25 and second in week 45. They then continue with the same values to the end of year, a trend which is not in agreement with their precipitation curves. It can be attributed to their difference in the land use and/or temperature trend that changes the snowmelt timing.

When interpreting the shape of a hydrograph, the dominant soil texture and, therefore, infiltration rate should also be considered. Basin 08NK002 is mainly covered with clay, while for the other basins the dominant soil is silt. Regarding FAO (1998), silt has a higher infiltration rate than clay, leading to less surface runoff. Differences in soil properties and ratios of infiltration could be the main reason for the earlier peak flow (Hayes & Young, 2005) in basin 08NK002 compared to that of basin 05BB001, even though they have similar climate data and average slope.

4.3 Modeling result

4.3.1 Results of 25 basins

Table 4.3 shows the average of maximum NSE for each basin and using three products of ANUSPLIN, CaPA, and WFDEI. Maximum value of this objective function is higher than 0.7 for 14 out of 25 basins and it can reach to 0.81 for 05DA007. Model was not able to generate reasonable streamflow data for several basins including 07EE007, 08KB003, and 05BG006 therfore the NSE values are less than 0.5. Poor NSE values for these basins might be because of errors in the input data (i.e. precipitation data) and/or process representation in the model. It is not always an easy task to find the main reason of low objective function values or to make a connection between basin characteristics (i.e. elevation, vegetation cover, and size) and model performance. Nevertheless we used a hypsometric curve to find a possible relation between the NSE values of basins and their elevation (figure 4.15). A hypsometric curve is a histogram or cumulative distribution function of elevations within a catchment. This curve characterizes in part the catchment form and contains information on dominant runoff mechanisms (Vivoni et al., 2008). In figure 4.15 hypsometric curves of basins with maximum NSE values of higher than 0.7, between 0.5 and 0.7, and lower than 0.5 are illustrated in dark blue, green, and orange, respectively. Aforementioned figure shows that there is no obvious relationship between catchment elevation characteristics (hypsometric curves) and their NSE values. However, it is likely that most of the basins with high NSE (higher than 0.7) are more inclined to make a shift to the right side of the graph meaning higher elevation and most of the basins with low NSE (lower than 0.5) tend to stay on the left side meaning lower elevation.

Table 4.3: Best NSE of basins (the average result of three climate products)

Basin ID	Average of best NSEs
08NP004	0.41
08NK002	0.78
08NG065	0.75
08ND012	0.7
08NB019	0.77
08NA002	0.75
08KB003	0.4
08KA005	0.79
08NB014	0.79
08NB012	0.75
08LB038	0.73
07FB006	0.63
07FB003	0.48
07AA001	0.49
07EC002	0.71
07EC004	0.62
07ED003	0.68
07EE007	0.36
05AA008	0.57
05AA022	0.67
05AA023	0.75
05BB001	0.72
05BG006	0.4
05BL022	0.76
05DA007	0.81

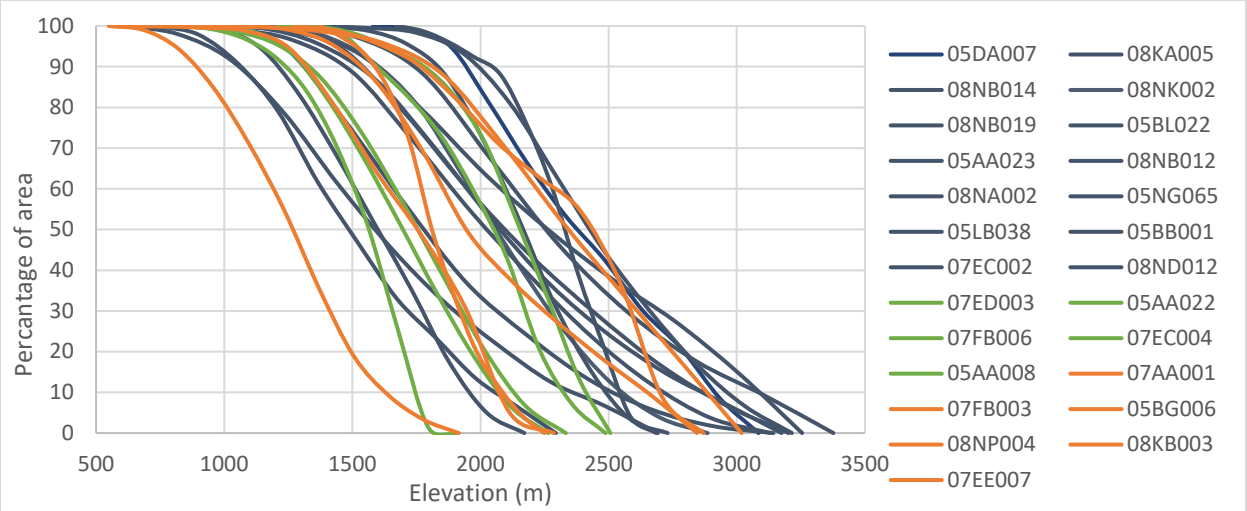

Figure 4.15: Hypsometric curves of 25 basins. Basins with maximum NSE values of higher than 0.7, between 0.5 and 0.7, and lower than 0.5 are illustrated in dark blue, green, and orange, respectively.

4.3.2 Results of 5 selected basins

4.3.2.1 Observed and simulated streamflow

Figures 4.16 to 4.20 show the observed and simulated streamflows for each basin. Only the simulated streamflows with the parameter values that resulted in in the highest NSE values are shown.

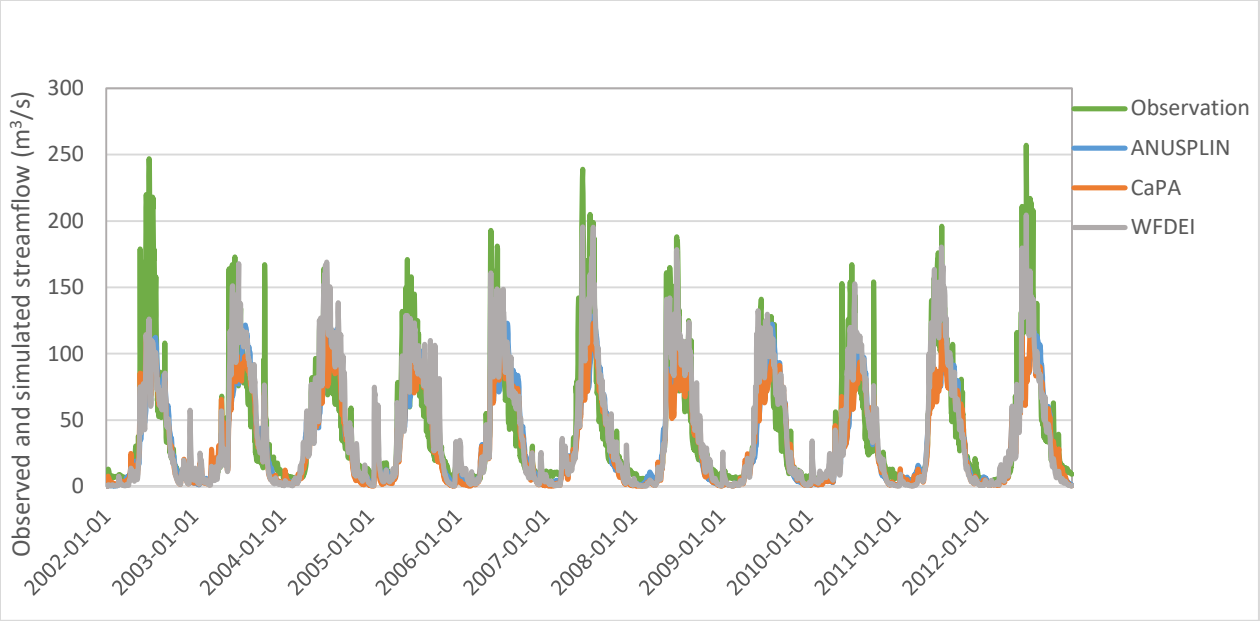

Figure 4.16: Observed and simulated daily hydrographs for 08NB019

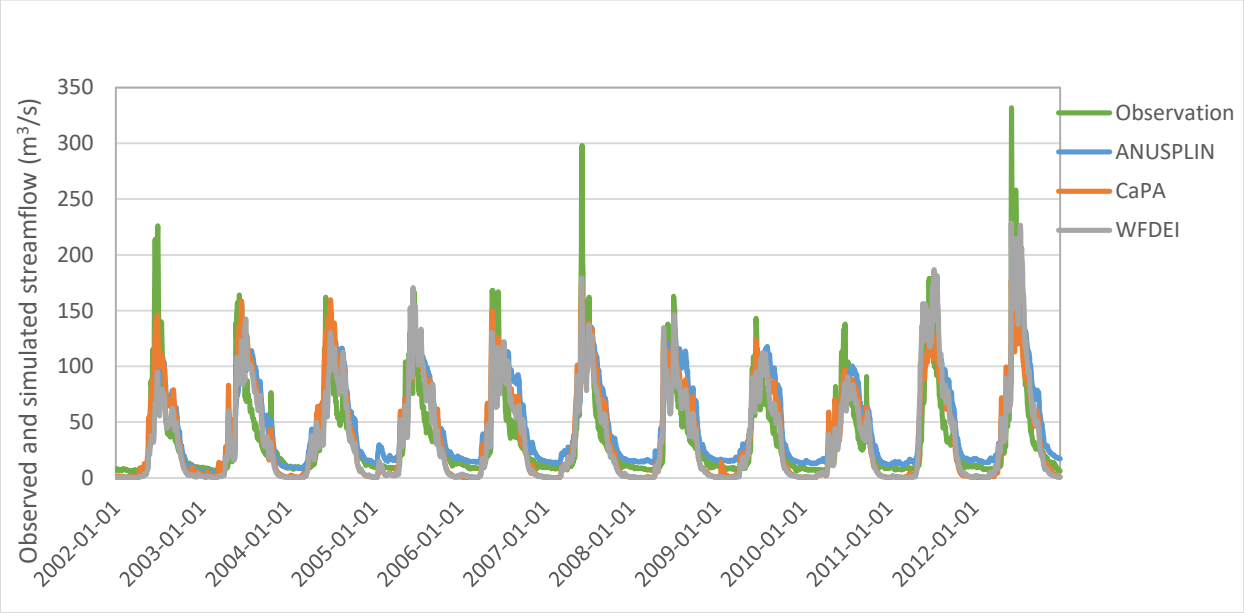

Figure 4.17: Observed and simulated daily hydrographs for 05BB001

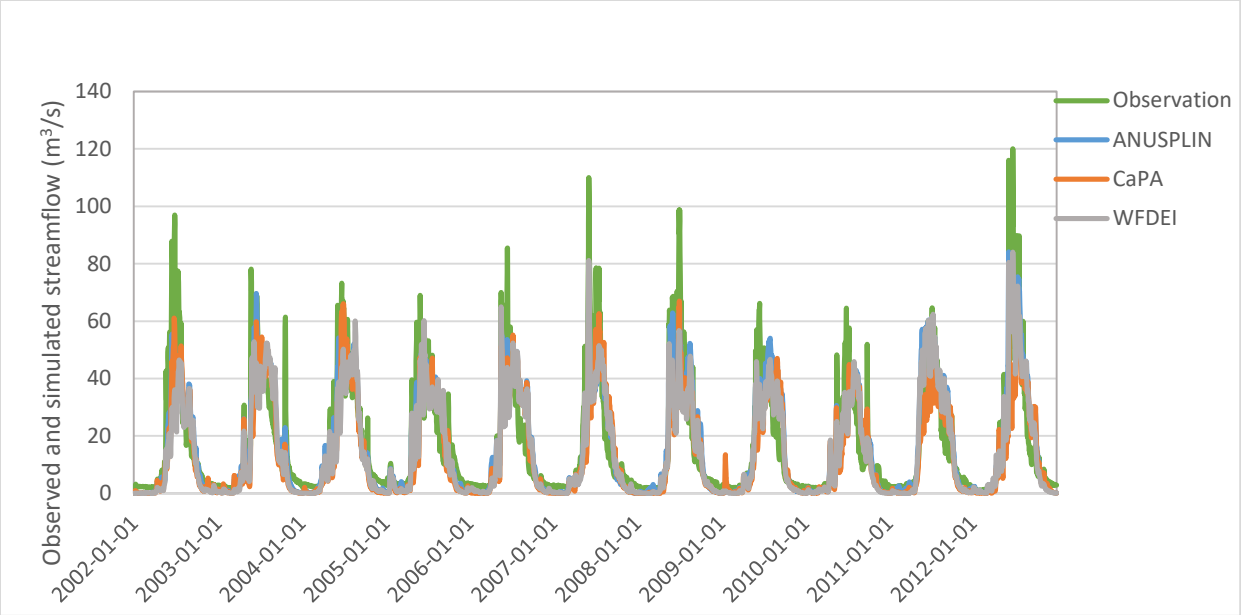

Figure 4.18: Observed and simulated daily hydrographs for 08NB012

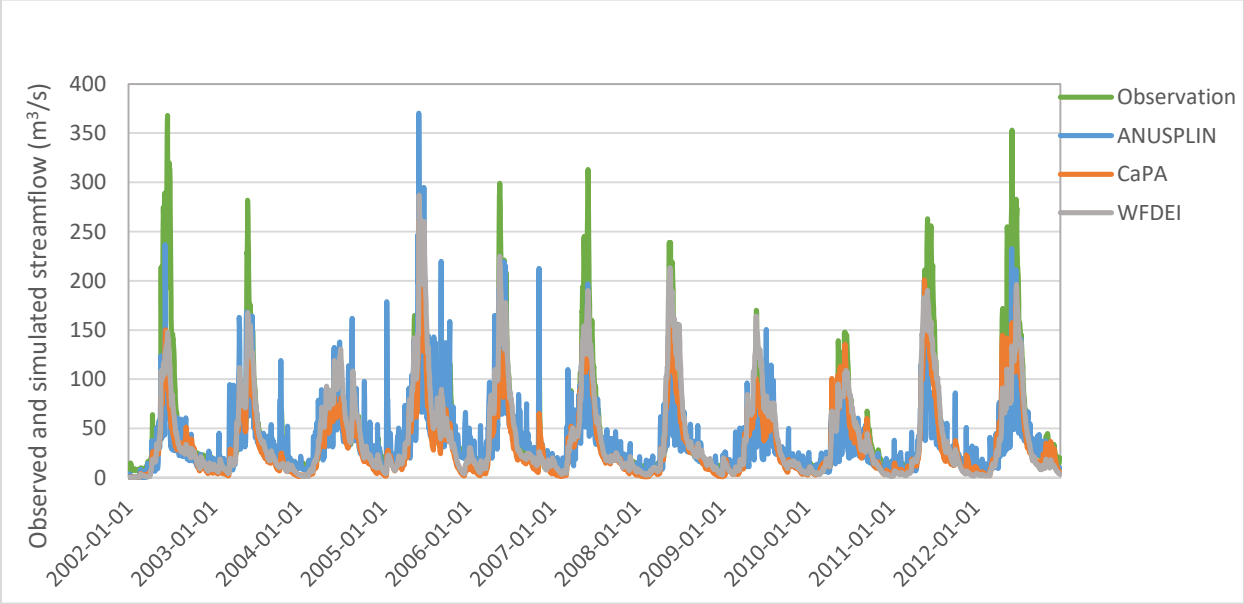

Figure 4.19: Observed and simulated daily hydrographs for 08NK002

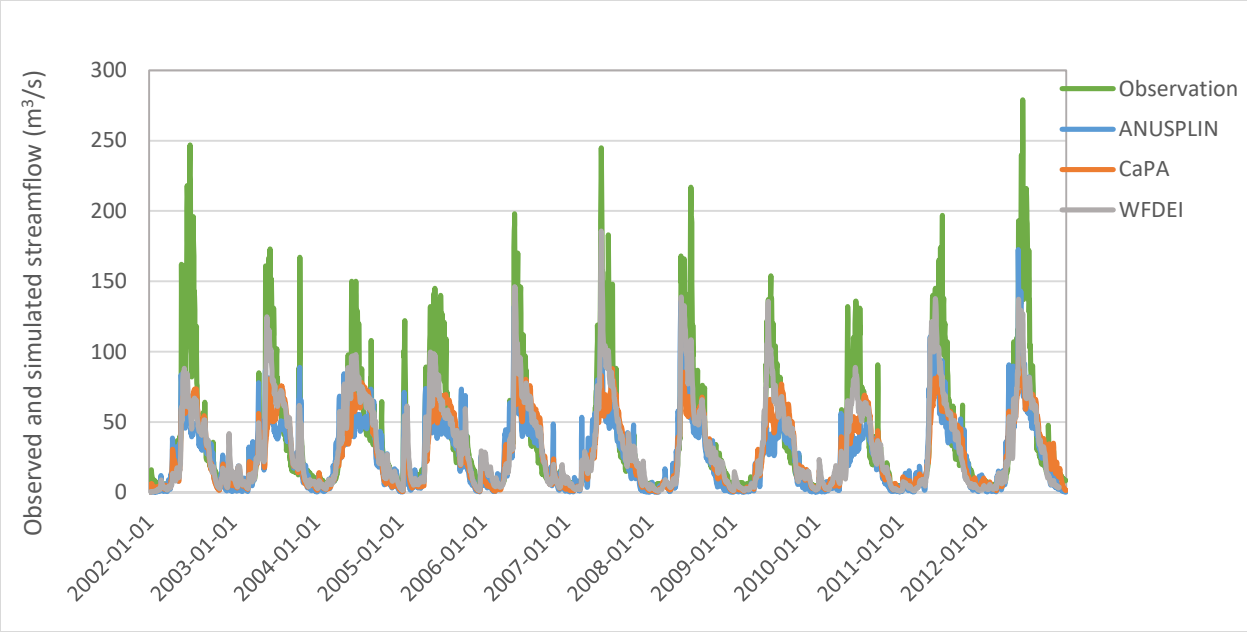

Figure 4.20: Observed and simulated daily hydrographs for 08ND012

The comparison of the observed and simulated daily streamflows shows that the model results using WFDEI data are more capable of capturing peak flows for basins 08NB019, 08NK002, and 08ND012. For 05BB001, the results of WFDEI capture the observed discharge variations and peakflows reasonably well. And for 08NB012, ANUSPLIN shows the best performance in simulating the high flows. Moreover, the timing of the flow events is better captured by WFDEI in almost all cases. However, the model tends to under-predict the very high flows of all five basins, especially when ANUSPLIN and CaPA are used. Model performance for each basin is investigated using different objective functions and results are provided in the following section.

4.3.2.2 The comparison of model performance

The performance of each climate product was assessed based on 10,000 Monte Carlo simulations using three objective functions, NSE, NSE-Log, and PBIAS (figure 4.21). PBIAS shows a superior performance for WFDEI compared to CaPA and ANUSPLIN for all five basins. CaPA and ANUSPLIN yielded the highest NSE and NSE-Log values for 05BB001 and 08NB012, respectively. However, for the other basins, WFDEI resulted in a higher performance. Overall, based on this hydrologic modelling results, WFDEI seemed capable of estimating climate data

more accurately than the other two products. Wong et al. (2017) drew similar conclusions, reporting that WFDEI, in general, provides the most consistent and reliable estimates for different metrics compared with other climate products, including ANUSPLIN. In Wong et al.'s research, WFDEI had over 65% of reliability over 15 terrestrial ecozones in Canada.

Figure 4.1 (p. 54) illustrates that for basins 08NB012, 05BB01, ANUSPLIN and CaPA and for other three basins WFDEI generated higher values for average precipitation respectively. This clearly demonstrates that higher precipitation estimation resulted in higher values for NSE and NSE-Log. The findings, therefore, suggest that all three products tended to underestimate total precipitation across the basins compared to real data. Wong et al. (2017) reported that these products overestimate precipitation in the west and underestimate it in the north and east compared to gauge stations. Wong et al.'s findings about precipitation are not consistent with the results of this study, which, as reported above, shows that precipitation was underestimated although our studied basins are located in the west area. However, the station data used in Wong et al.'s study are typically found to be at low elevations, which makes it almost impossible to produce a good representation of precipitation data. To support this claim, Gharari, Safaie, Razavi, & Wheater (2017) conducted a study that showed that rain gauge stations (used in Wong et al.'s research) are mostly located in lowlands and valley bottoms, which are almost 1000 m lower than the average catchment elevations. The cumulative distribution functions (CDFs) associated with gauge elevation and catchment elevation produced by Gharari et al. are shown in figure 4.22.

Other reports, however, indicate that the limitations and internal inconsistencies of the gridded datasets often lead to the underestimation of climate data, especially for areas with significant snowfall (Andermann, Bonnet, & Gloaguen, 2011). Models often compensate for underestimated precipitation with underestimated evapotranspiration and/or overestimated snow/glacier melt rates (Pellicciotti et al., 2012), reflecting a bias in estimating other components by models, which are more highlighted for small basins. In small catchments, precipitation is mainly influenced by topography, wind direction, hill aspects, and other factors. The development or reanalysis of precipitation data in small basin mostly needs more precise and comprehensive information in comparison with the data applied for large catchment (Ouyang et al., 2014). This error demonstrates the important role of orographic precipitation and topographic influence on precipitation quantity and distribution (Biemans et al. 2009), especially in mountainous and

relatively small areas; hence, the applicability of various gridded data to such basins requires further investigation (Yang, Wang, Wang, Yu, & Xu, 2014).

Figure 4.21: Best objective function values

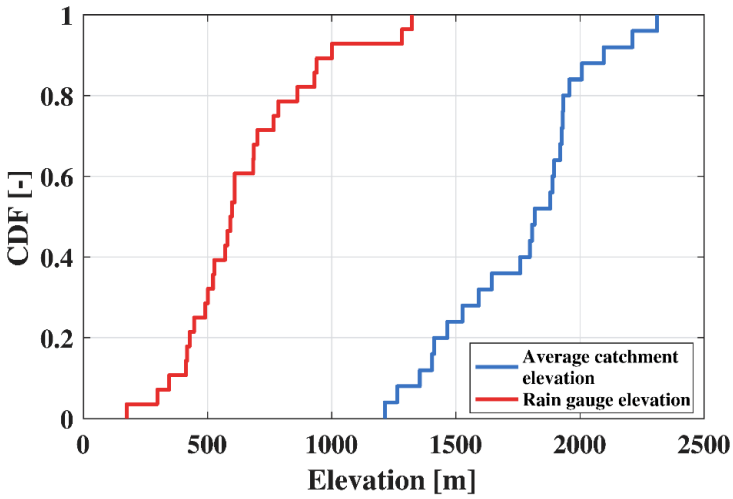

Figure 4.22: Elevation of catchments vs. rain gauges (adopted from Gharari et al., 2017)

4.3.2.3 Forcing data correction

The model evaluation of different data products in section 4.3.2.2, showed that WFDEI and CaPA are more reliable than ANUSPLIN in simulating streamflows for the basins of interest. Therefore, these two products are combined using equation 3.14 (p. 45).

A Monte Carlo approach based on PLHS was used to generate 10,000 random parameter sets. Each parameter set has 13 parameters (11 model parameters and two for precipitation correction). The model parameter ranges were the same as provided in table 3.3 (p. 46). The ranges of precipitation correction factors P_1 and P_2 were (0.5-2) and (0-1), respectively.

To keep the analysis of results less complex, we focused only on a combination of precipitation data, and for temperature and evapotranspiration inputs, we simply used WFDEI product.

4.3.2.3.1 Precipitation correction factors relationship

The meaningful relationship can be seen between precipitation correction factors (P_1 and P_2) for the best 50 parameter sets. Scatter plots of P_1 and P_2 for basins 08NB019 and 05BB001, for example, are provided in figures 4.23 and 4.24, respectively. The plot for basin 08NB019 shows that these two parameters are negatively correlated, which means that by increasing the P_1

parameter, P_2 decreases to gain higher objective functions. Increasing P_2 implies decreasing the ratio of CaPA to WFDEI in combined precipitation, indicating that WFDEI is overestimating precipitation compared to CaPA. The reverse is true for the plot of basin 05BB001, where a positive correlation demonstrates that increasing P_1 leads to a reduction of P_2, meaning that for this basin, CaPA estimated higher precipitation than WFDEI. This result is supported by average annual precipitation (figure 4.1 on p. 54), showing that the CaPA/WFDEI ratio is 0.61 and 1.04 for basins 08NB019 and 05BB001, respectively. Moreover, the correlation of P_1 and P_2 for basin 05BB001 (with a coefficient of determination or R^2 of 0.06) is not as strong as that for basin 08NB019 (with R^2 of 0.66) since the estimation of precipitation generated from two products (CaPA and WFDEI) were much closer for this basin rather than for 08NB019 (CaPA/WFDEI ratio of 05BB001 is closer to 1 compared to 08NB019 which are 1.04 and 0.61 respectively).

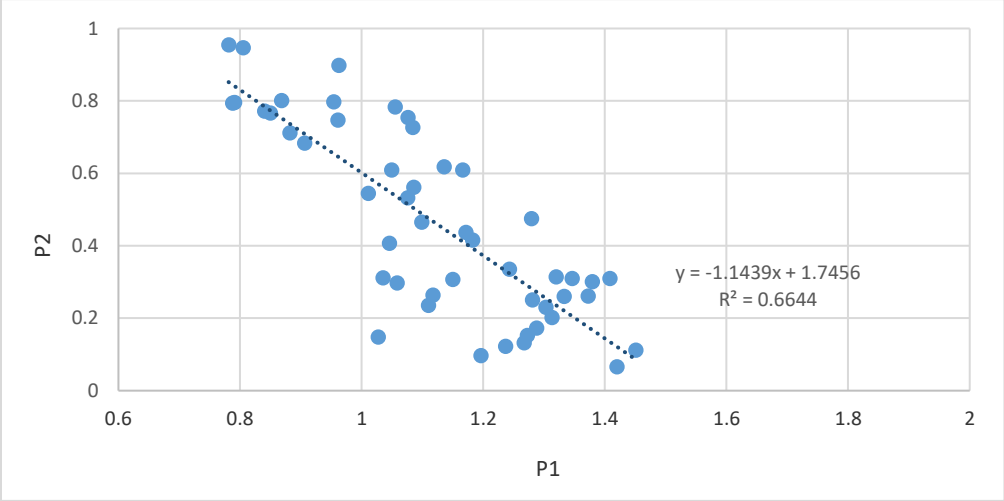

Figure 4.23: Relationship of precipitation correction factors for 08NB019

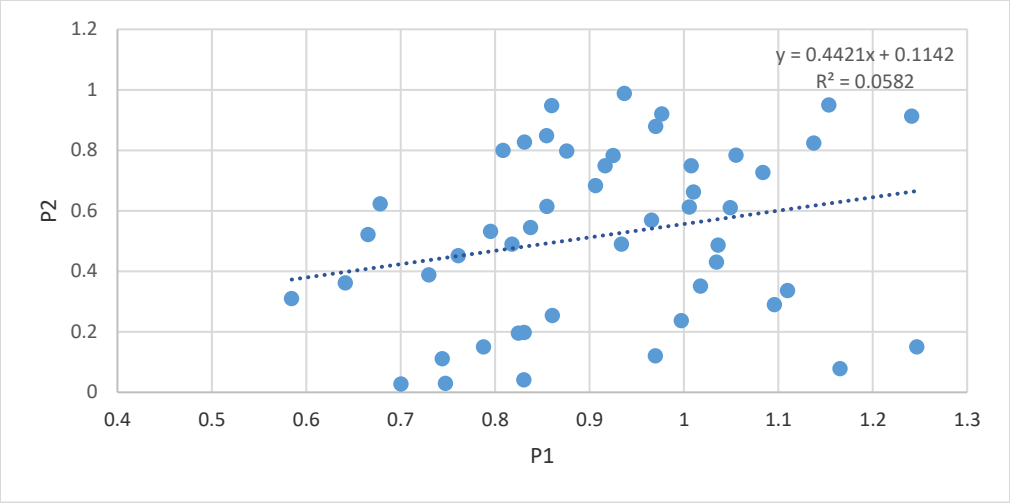

Figure 4.24: Relationship of precipitation correction factors for 05BB001

4.3.2.3.2 MODIS vs. Model AET

Conceptual hydrological models tend to compensate for the hydrological processes through the parameters. Evapotranspiration is mostly sacrificed in order to have a good estimation of observed discharges. The evapotranspiration process then acts as a buffer and compensates to close the hydrological budget (Minville et al., 2014). To investigate this compensation, monthly actual evapotranspiration estimated by the model was compared with the monthly MODIS actual ET estimates. The results of two basins, 05BB001 and 08ND012, for example, modeled using WFDEI data are illustrated in figures 4.25 and 4.26.

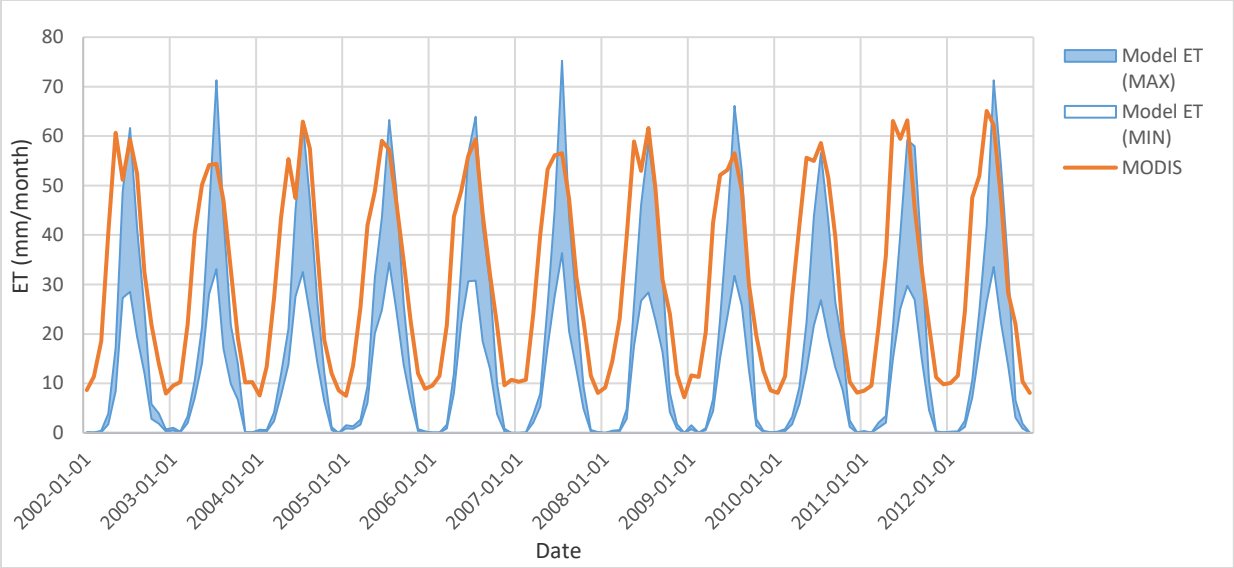

Figure 4.25: Evapotranspiration values simulated by model and MODIS for 05BB001

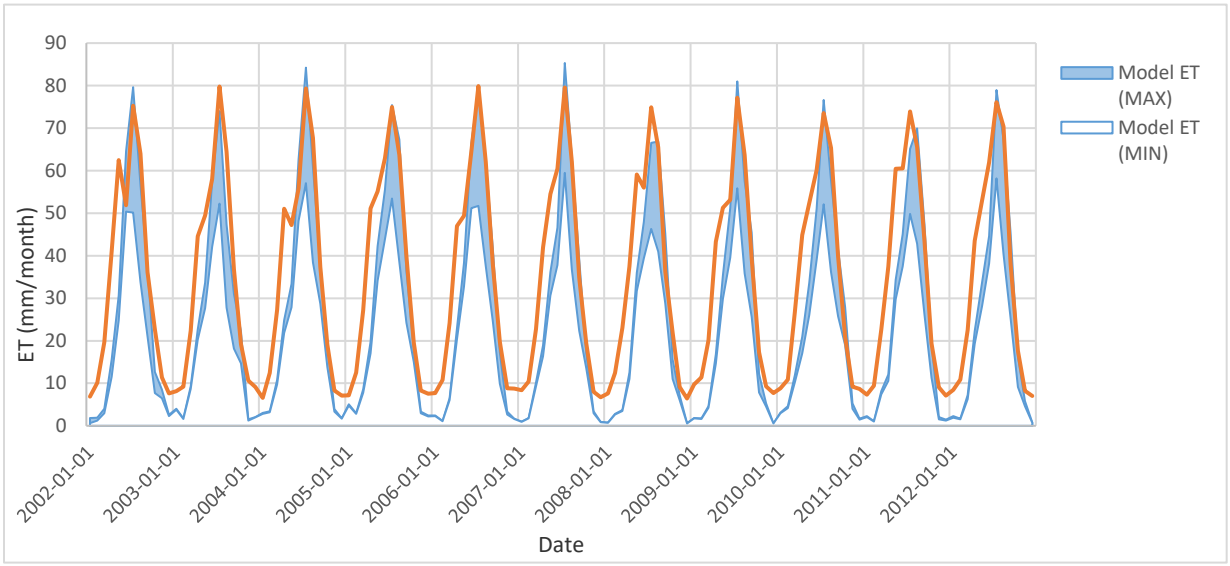

Figure 4.26: Evapotranspiration values simulated by model and MODIS for 08ND012

In figures 4.25 and 4.26, the blue band shows the range of evapotranspiration (maximum and minimum data) simulated by the model for each month, and the orange line refers to MODIS monthly data. The figures show that ET estimations by the model and MODIS are not in agreement with the rising limbs. However, for the falling limbs during the months of June to October, there is a better agreement between MODIS and the modelled evapotranspiration. Moreover, ET data driven from the model can reach zero (0.001mm and 0.5mm for basin 05BB001 and basin

08ND012) in the very cold period. However, the minimum ET generated by MODIS is greater than 7mm for basin 05BB001 and basin 08ND012. The reasons for this mismatch between the model evaporation and MODIS could be as follows:

1- The actual evapotranspiration of HBV-EC is based on either long-term monthly or daily potential evapotranspiration (in this study, daily potential evaporation was estimated using Hamon's equation), adjusted just for temperature. However, accurately estimating ET from complex landscapes can be data intensive since many other factors besides temperature are involved (Miranda, 2017). Evapotranspiration (ET) is a combined process of evaporation of liquid water from various surfaces, transpiration from the leaves of plants and trees, and sublimation from ice and snow surfaces (Rabiti et al., 2015). Nevertheless, actual ET estimated by Hamon's method (a temperature-based method) and HBV-EC equations can fail to include all the processes. For example HBV-EC model doesn't consider any sublimation and evaporation of snow across the basin is just taking into account by snowfall correction factor (SFCF). The MODIS model also does not bring in the sublimation process and makes no adjustments to account for the presence of snow cover since it assumes that bare soil evaporation is sufficient to calculate winter snow melt and subsequent evaporation as well as snow sublimation (Vanderhoof & Williams, 2015). However, the MODIS model relies on the energy flux approach and takes into account various parameters such as actual vapor pressure, relative humidity, and incoming solar radiation (figure 3.2, p. 28) for calculating evapotranspiration, which creates differences in ET values compared to the modeled ET, especially in cold periods.

2- These different ET values probably occurred because the model is trying underestimate evaporation to get water balance right. As mentioned, precipitation products are underestimated for our study area, and, consequently, evapotranspiration must necessarily be underestimated as well to compensate for the missing water input (Oliver & Oliver, 1995). Compared to the MODIS equation, the model gives lower evapotranspiration estimations not only in cold conditions but also over the summer months.

The ET data of parameter set which resulted the highest correlation coefficient (R) with MODIS data was selected and their relationships with MODIS values ae illustrated in scatter plots

of (4.27) and (4.28). The linear fits have R^2 value of 0.79 and 0.87 for 05BB001 and 08ND012 respectively.

Although WFDEI underestimated precipitation probably for all basins, basin 08ND012's estimations might be closer to real data since WFDEI shows significantly higher precipitation values compared with ANUSPLIN and CaPA. The WFDEI precipitation product also results in better and higher NSE and NSE-Log values compared to other products. However, for basin 05BB001, higher values for precipitation and, therefore, NSE and NSE-Log values were estimated by CaPA, meaning that CaPA is more capable of estimating accurate precipitation in this basin. The better estimation of precipitation resulted in higher consistency, higher R^2, between the modeled evaporation and MODIS evaporation. In other words, when precipitation estimations were closer to real values, the model provided a better estimation of evaporation. This, to some extent, supports the hypothesis that the modeled ET might be underestimated to compensate for precipitation underestimation.

With all these interpretations, the results of the relationship between these two products may change if the monthly comparison of evaporation is replaced with daily comparisons. Miranda et al. (2017) showed that when two different evapotranspiration products are compared, greater R^2 values will be reached for the monthly scale than for the eight-day scale.

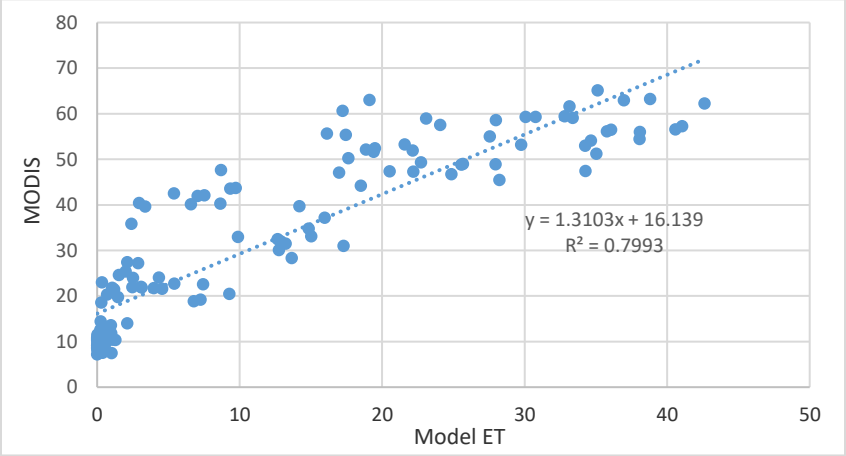

Figure 4.27: Model and MODIS ET relationship for 05BB001

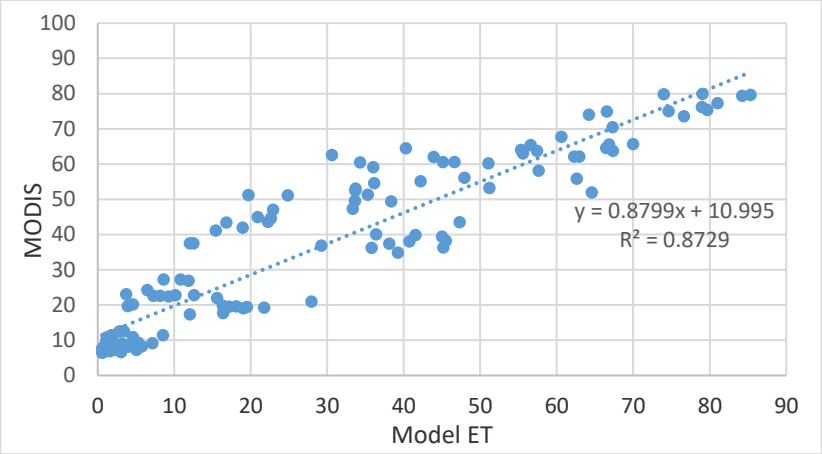

Figure 4.28: Model and MODIS ET relationship for 08ND12

4.3.2.4 Objective Function values

Figures 4.29 to 4.32 present the distribution of three objective functions pertaining to 50 behavioral parameter sets and for ANUSPLIN, CaPA, WFDEI, and combined data, respectively. The left column of each figure shows the result of the "Cut" method, and the right column is related to the "Radial" method for distinguishing behavioral and non-behavioral parameter sets.

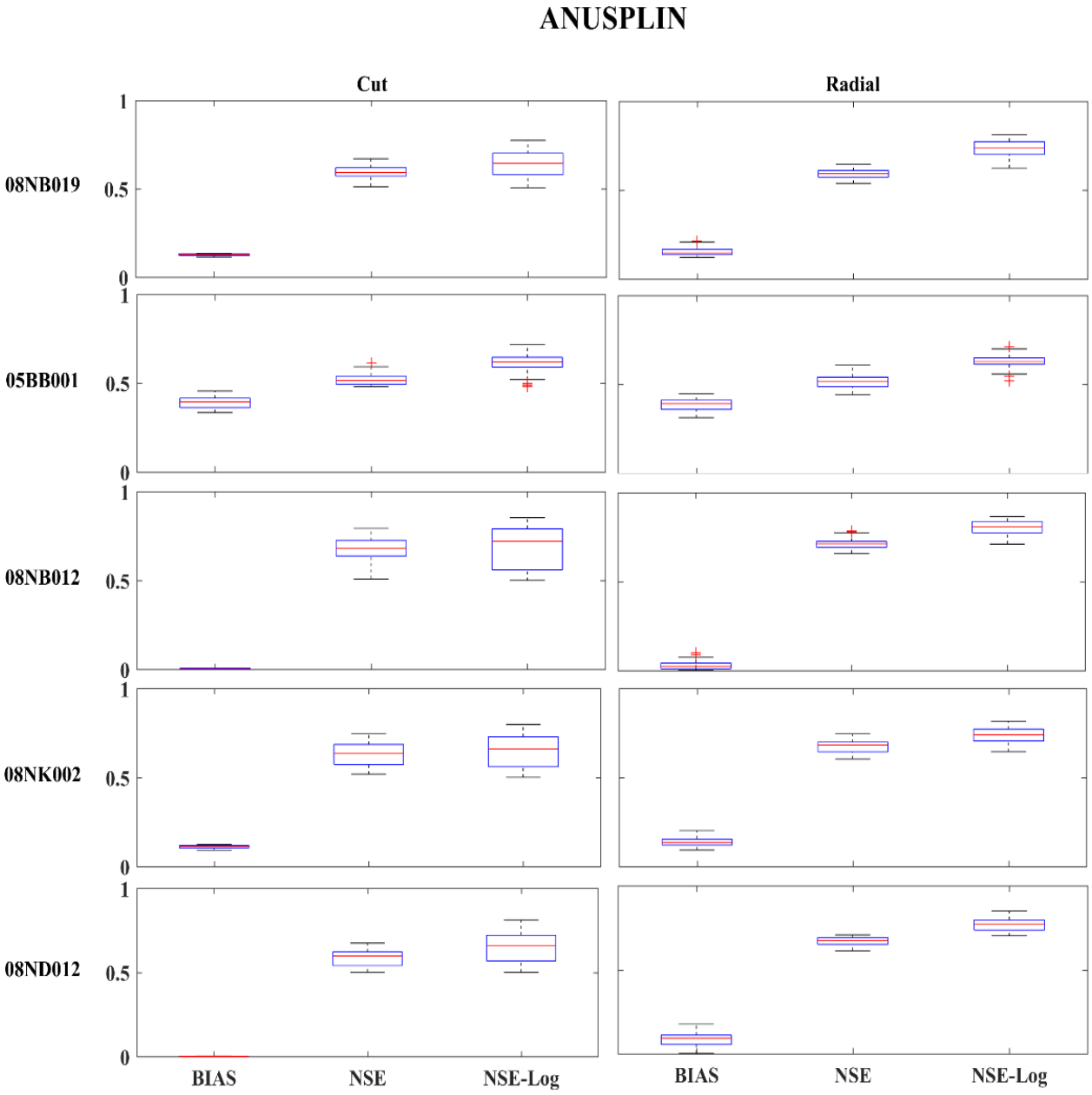

Figure 4.29: Boxplots of the model performances for the behavioral parameter sets selected by "Cut" and "Radial" methods, using ANUSPLIN data

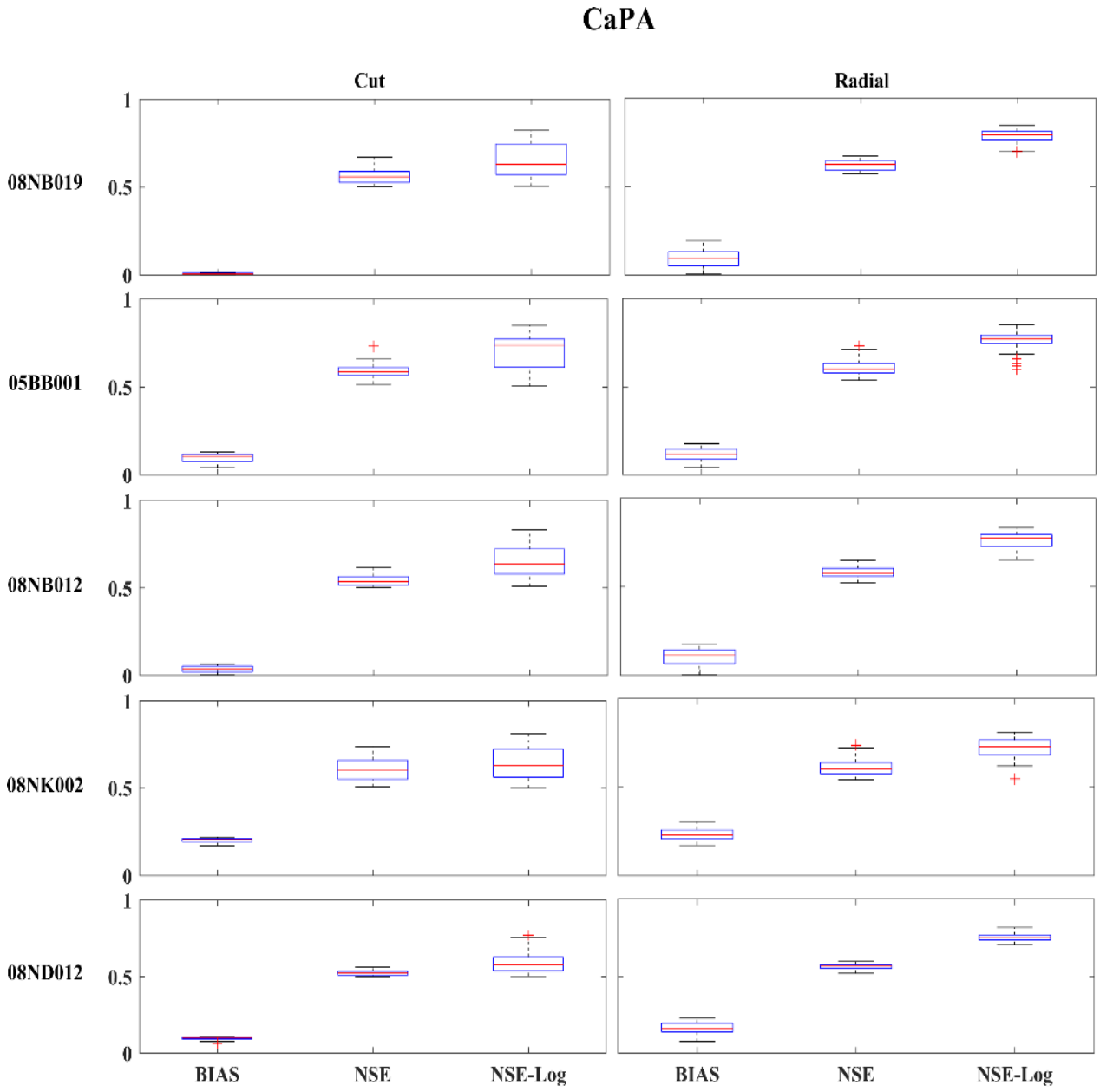

Figure 4.30: Boxplots of the model performances for the behavioral parameter sets selected by "Cut" and "Radial" methods, using CaPA data

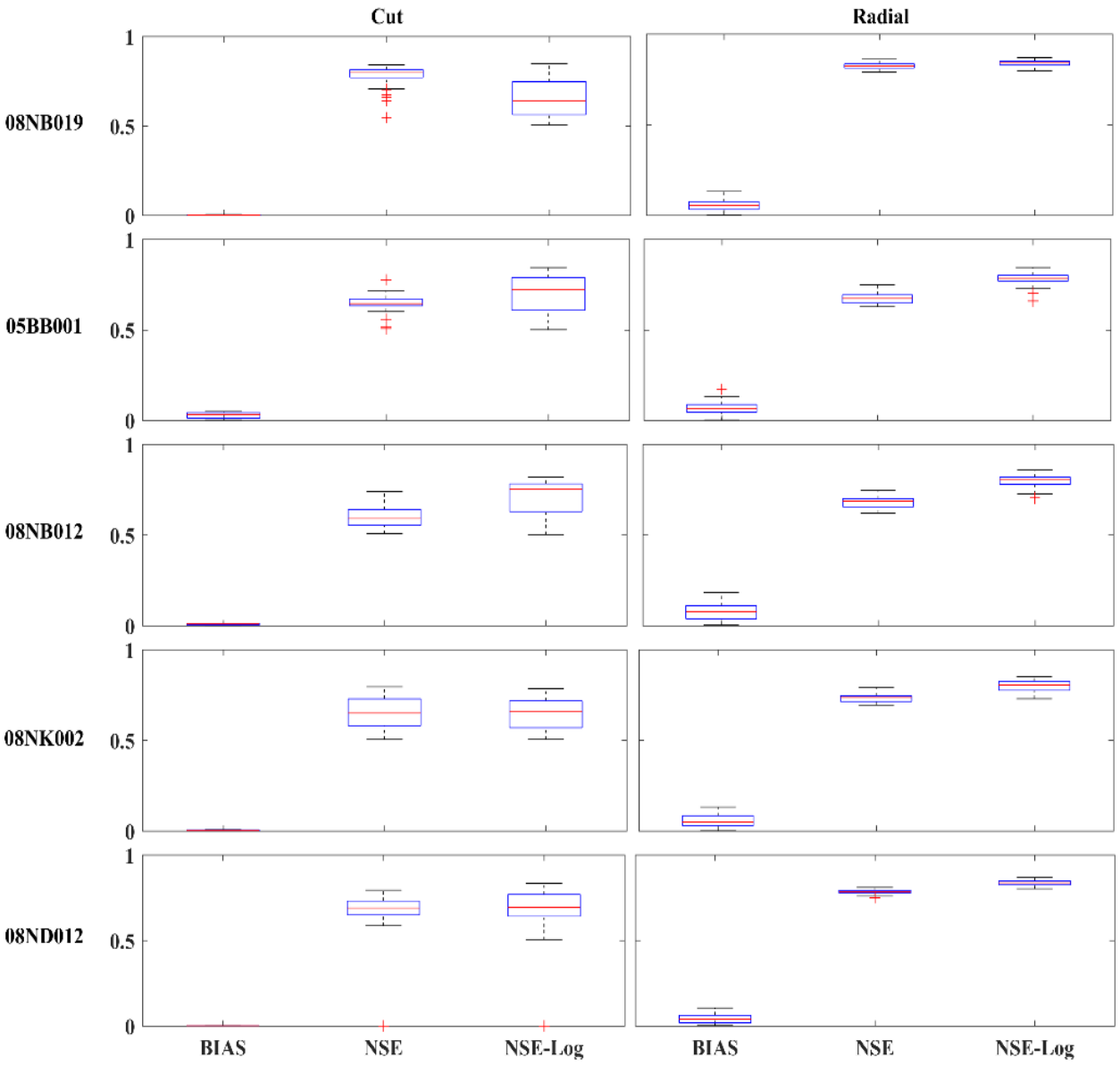

Figure 4.31: Boxplots of the model performances for the behavioral parameter sets selected by "Cut" and "Radial" methods, using WFDEI data

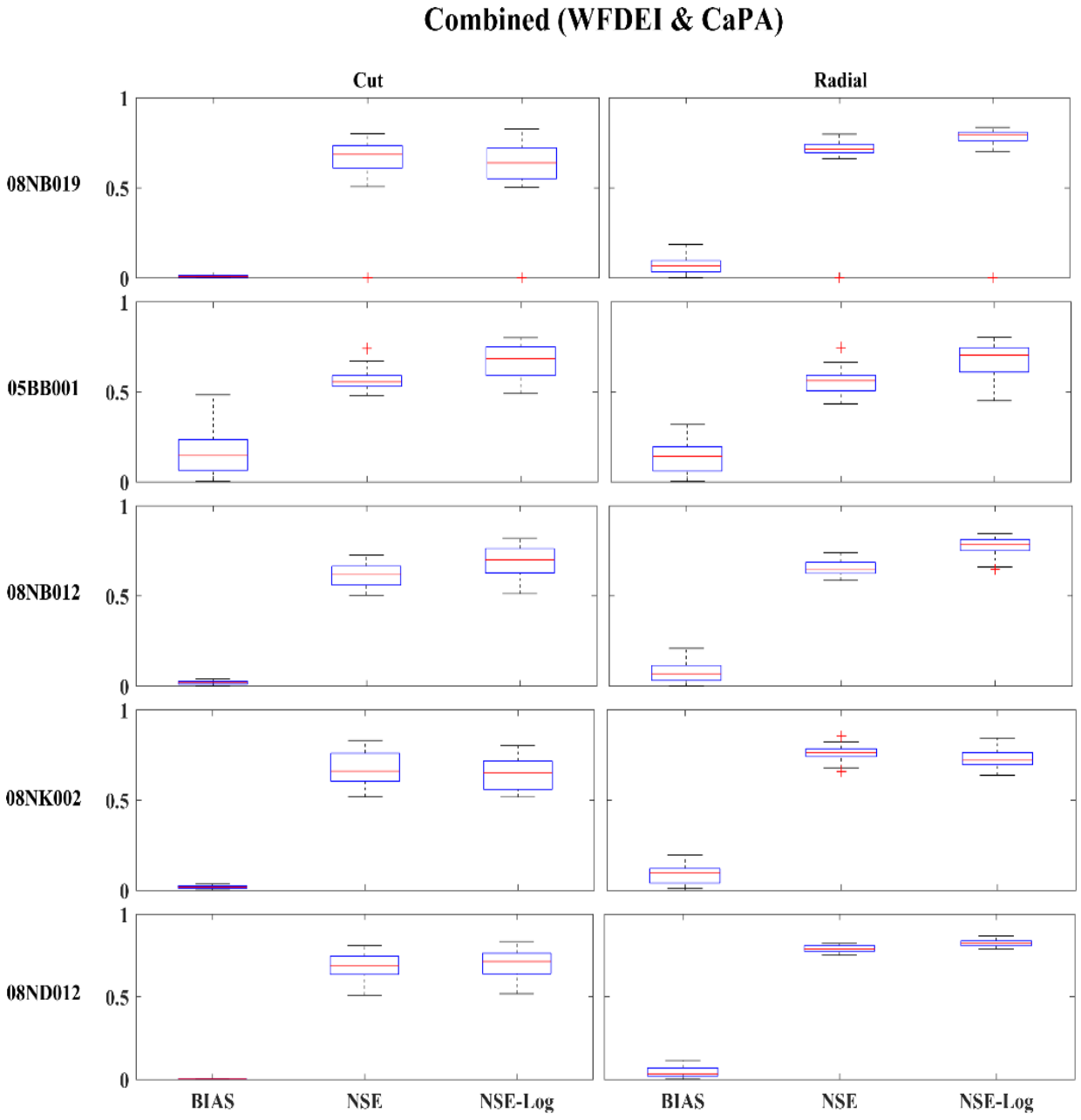

Figure 4.32: Boxplots of the model performances for the behavioral parameter sets selected by "Cut" and "Radial" methods, using combined data

The first point of these figures is about the differences between the “Cut” and “Radial” methods for selecting behavioral parameter sets. The NSE and NSE-Log values related to parameters chosen by “Cut” shows larger variation of the boxplots compared to “Radial,” meaning that “Radial” was more stable in selecting behavioral parameters for these objective functions.

The second point is that the median NSE and NSE-Log value in “Radial” is higher than that for “Cut,” which means that parameter sets resulting in higher NSE and NSE-Log values were chosen by this method; however, the reverse is true in the case of BIAS objective functions. In most cases, boxplots of BIAS are narrower in the “Cut” method and also have lower values for the median.

Valuable results were produced by comparing the boxplots of different basins. As seen in figure 4.21 (p. 74) , basins 08NB012 and 05BB001 had a relatively better model performance for ANUSPIN and CaPA, which is consistent with the above figures, showing that these two basins boxplots (ANUPLIN and CaPA, respectively) are narrower and have higher median values for the NSE and NSE-Log. Basin 08ND012 shows a narrower boxplot in almost all cases, especially over NSE and NSE-Log objective functions; hence, when high flow and low flow were investigated, the model had better prediction ability for this basin.

In addition, comparing the results of different forcing data indicates that for WFDEI, preferable results came not only in terms of objective functions (both maximum and median values) but also in the width of boxplots. The boxplots of the NSE and NSE-Log values of the “Radial” column and the BIAS of the “Cut” column are considerably narrower for WFDEI compared with those for other forcing data.

Figure 4.32 shows the results of the model using a combination of WFDEI and CaPA as forcing data. By applying the combined forcings to the model it is expected to catch the best result of WFDEI and CaPA when they are applied individually. However, when a large enough number of parameter sets are run by the model, all the parameter sets of CaPA and WFDEI can be contained as well. Figures 4.30 to 4.32 show that some cases (basin 08NB019 in the “Radial” column, for instance) show better results for WFDEI than the best results of the combined data and also with the narrower boxplots. These findings suggest that if a higher number of parameter sets were run by the model, more acceptable results would be achieved by combining precipitation products.

However, regardless of the values of objective functions, the narrower boxplots of the “Radial” method for WFDEI indicated a better performance of WFDI than for the combined data. Overall, the “Radial” method was better than the “Cut” method in finding the behavioral parameter sets. Therefore, to further investigate the model performance and parameter uncertainty, the “Cut” method was discontinued. Only the results of the “Radial” method are provided.

4.3.2.5 Model Validation

In order to evaluate the model performance we used calibration and validation procedures for all five basins. The record of simultaneous forcing and observed streamflow data was split into a calibration (2002-2008) and validation (2009-2012) periods for each basin. We used one-year spin-up period (year 2002) to reach an equilibrium model state for initialization of our runs.

Model was run (10,000 times) for period 2003-2008 and the behavioral parameter sets using radial method were picked in the calibration procedure. Subsequently model was run again for these parameter sets for period 2009-2012. Figures 4.33 and 4.34 show the objective function values of behavioral parameter sets for calibration and validation periods and for each product. Results show that model performance is generally well at the validation stage as revealed by the outcome of NSE, NSE-Log and BIAS of behavioral parameter sets for both CaPA and WFDEI forcings.

In order to make sure that parameters sets selected in calibration period reasonably generate the streamflow for the validation period, we compared the best objective function values of behavioral parameter sets with the ones for all parameter sets (10,000 ones) of this period (figures 4.35 and 4.36). Results show that best objective function values for parameter sets selected in calibration are very close to the best values for all parameter sets specifically for basins 08NK002 and 08ND012 indicating that parameter sets picked from calibration period are able to produce reasonable results for validation period as well.

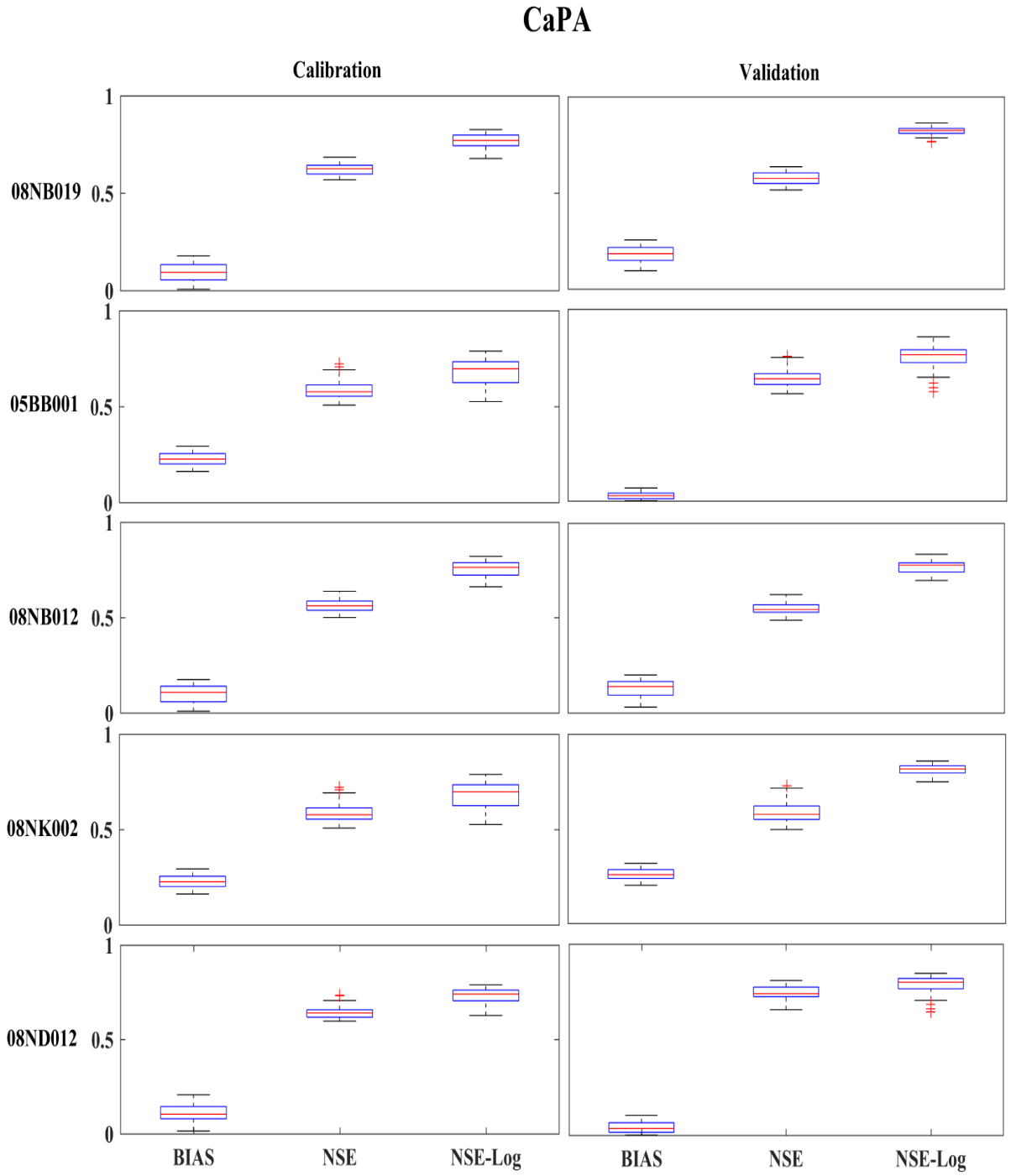

Figure 4.33: Boxplots of the model performances for calibration and validation period, using CaPA data

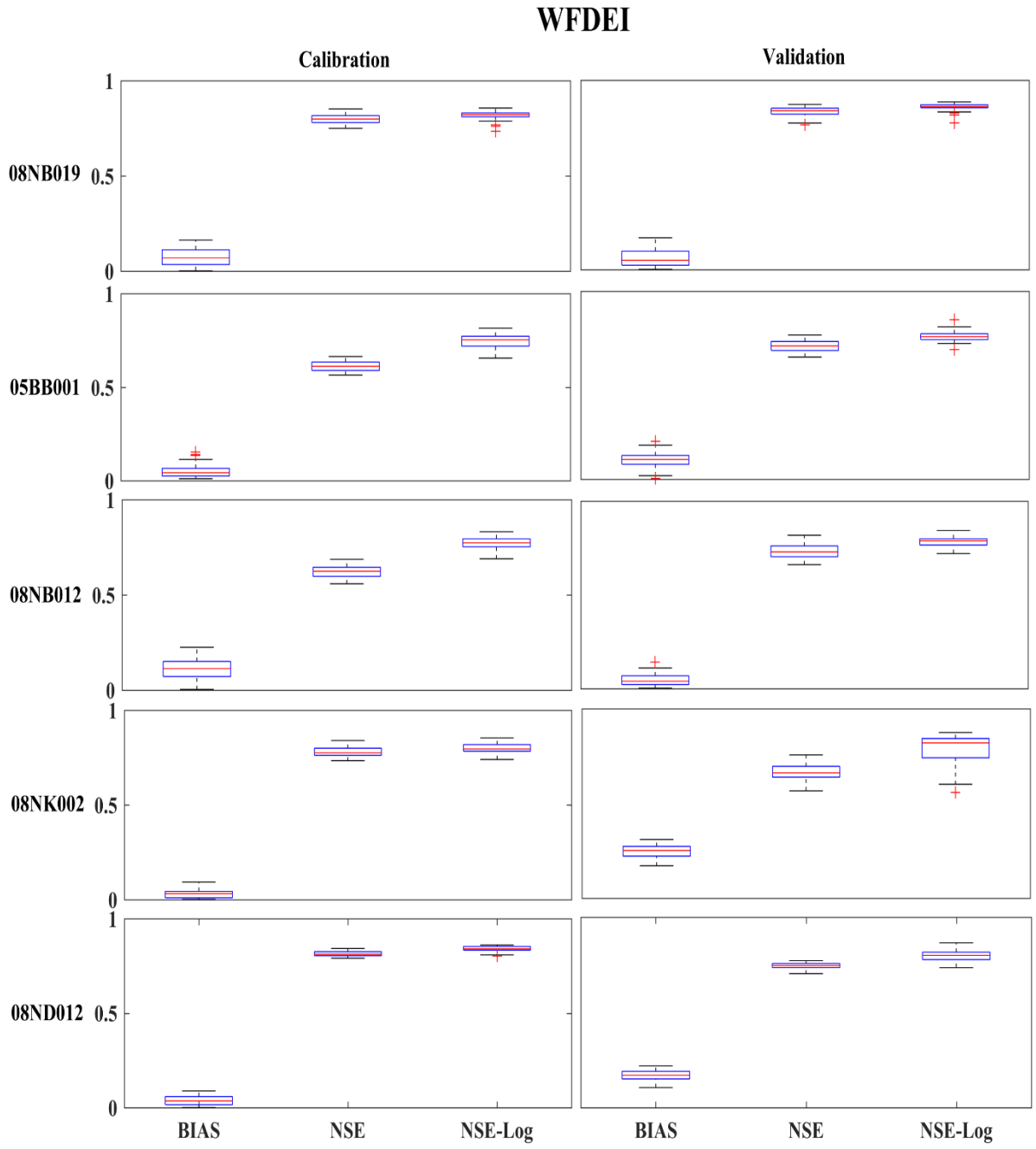

Figure 4.34: Boxplots of the model performances for calibration and validation period, using WFDEI data

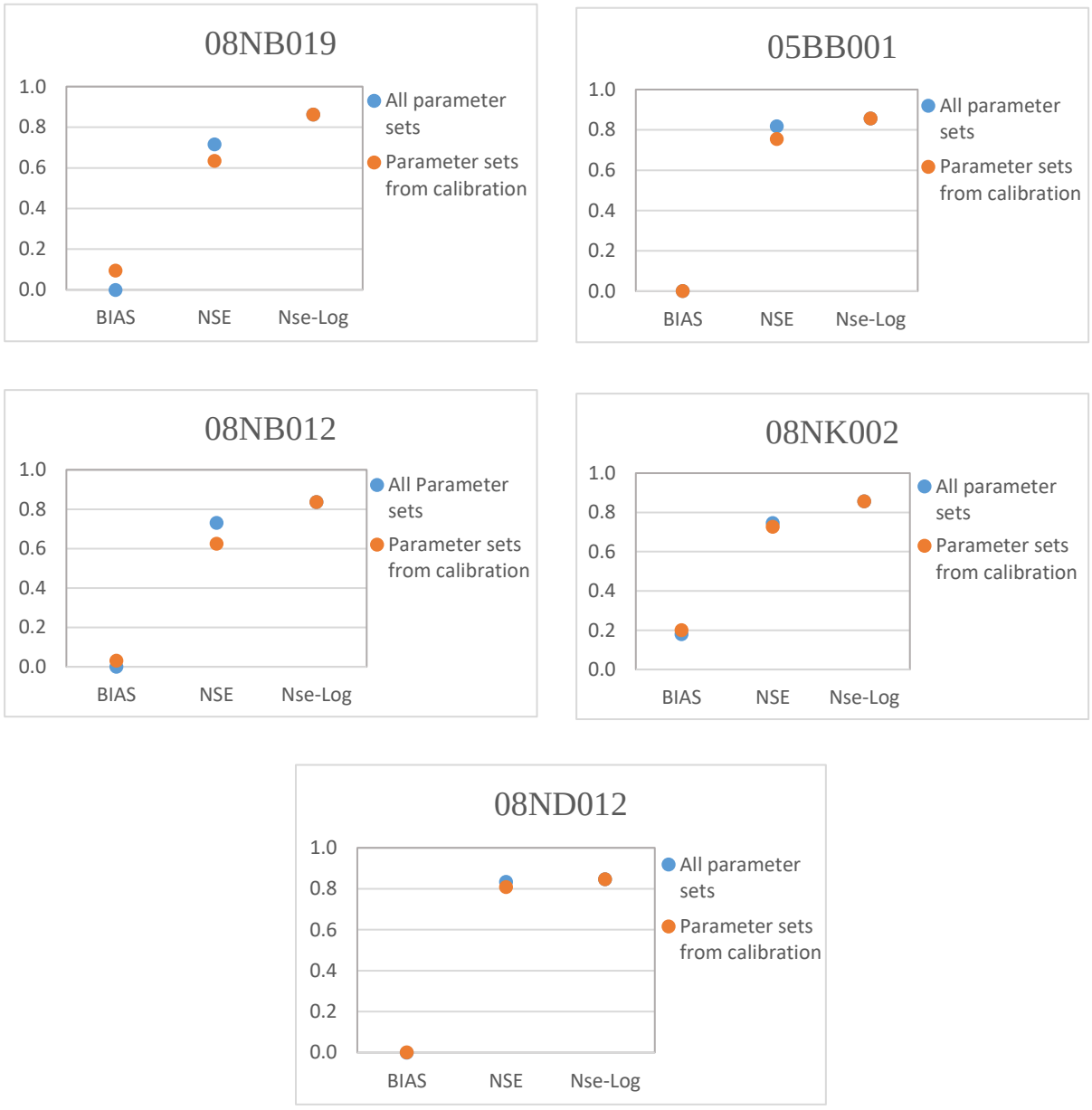

Figure 4.35: Best objective function values for validation period, using CaPA data

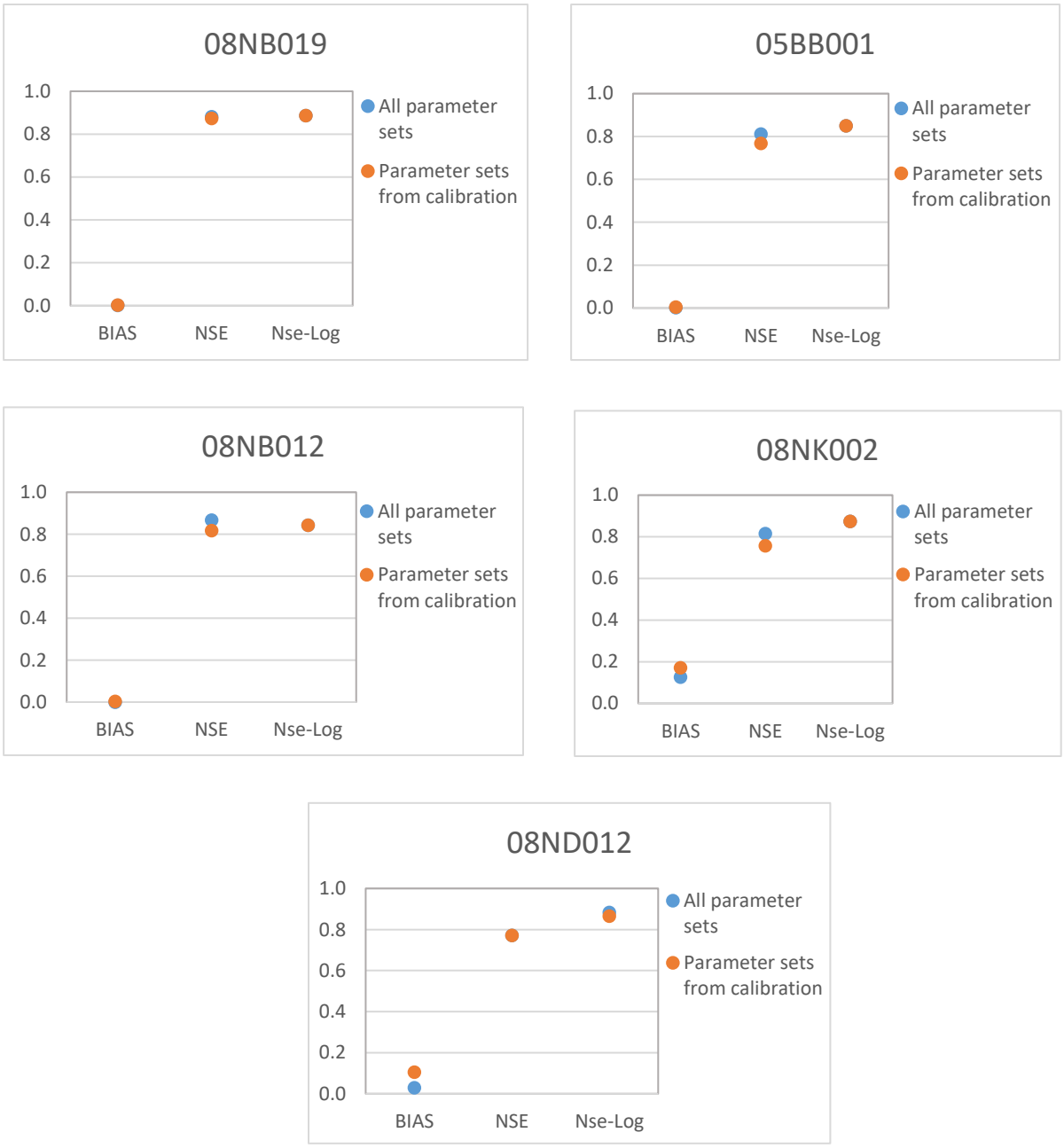

Figure 4.36: Best objective function values for validation period, using WFDEI data

4.3.2.6 Precipitation Correction factor impact on model performance

In this part, we attempted to mitigate the bias problem of WFDEI and CaPA data by adjusting the daily data and using a precipitation correction factor (P_1). WFDEI and CaPA data were used to run the model by applying a multiplicative correction factor. 10,000 parameter sets each containing 12 parameters (11 model and one correction factor, P_1) were generated and applied to the model. The range of parameters were consistent with the previous sections.

Figures 4.37 and 4.38 demonstrate the performance of the model for WFDEI and CaPA, respectively, when the data were multiplied by the P_1 correction factor.

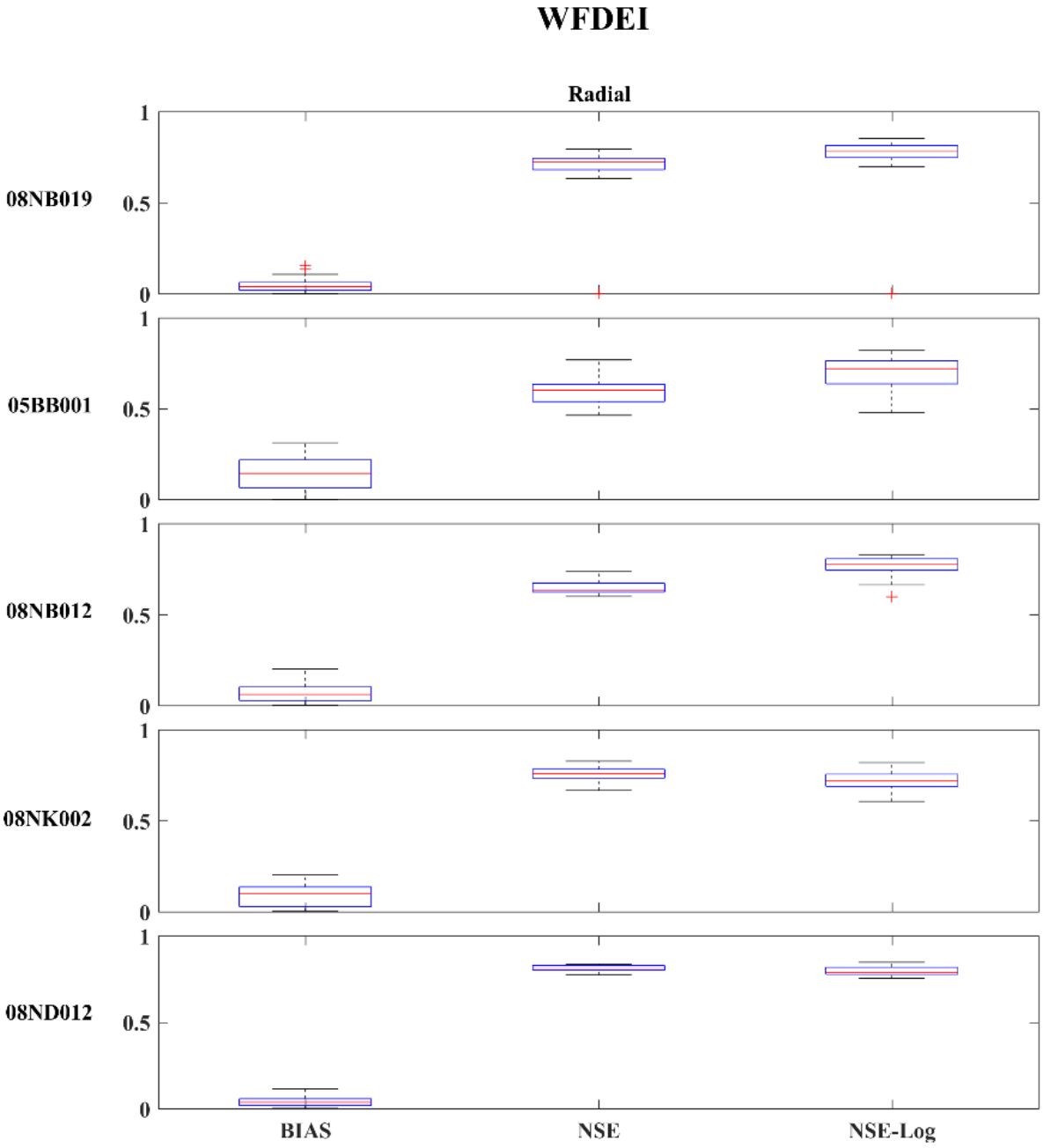

Figure 4.37: Boxplots of the model performances for the behavioral parameter sets selected by "Radial" methods, using WFDEI data

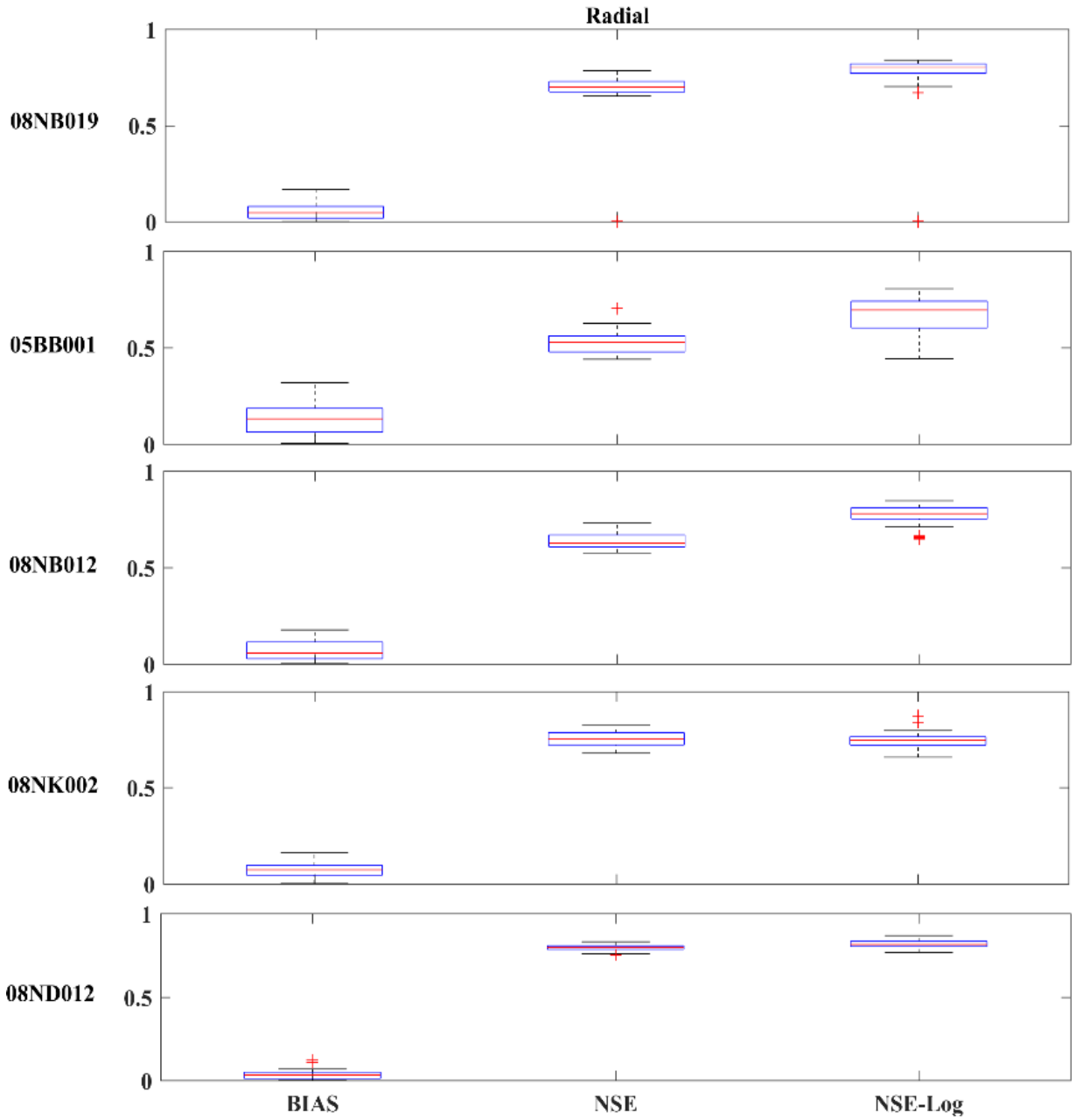

Figure 4.38: Boxplots of the model performances for the behavioral parameter sets selected by "Radial" methods, using CaPA data

A comparison of figures 4.37 and 4.38 with figures 4.30 and 4.31 shows that the differences of model performance with and without the precipitation correction factor are more pronounced for CaPA. Changing the WFDEI precipitation factor slightly alters the best value of objective functions compared with CaPA. This result suggested that although the NSE values of all basins (except basin 08MB019) were increased for WFDEI figures, these changes were not more than 0.02 (which corresponds to basin 08NK002), while the maximum change was 0.23 for CaPA (the NSE values of basin 08ND012 increased from 0.6 to 0.83). The other important effect of the P_1 factor on CaPA precipitation data was that it decreased both minimum and median values of the BIAS criterion for all five basins. In some cases (especially for WFDEI) the best NSE-Log values using P_1 factor, are lower than those with no correction parameter. This result brings us back to the number of parameter sets that were not large enough to cover all parameter combinations. Nevertheless, both sets of precipitation data, to some extent, benefited from a correction factor to better represent the actual precipitation.

4.3.2.7 Parameters Identifiability

Figures 4.39 and 4.40 display the parameter identifiability of the model corresponding to CaPA and WFDEI (with the P_1 correction factor) data, and figure 4.41 shows the identifiability of parameters when a combination of products was used. To compare different model parameters, the original values are normalized.

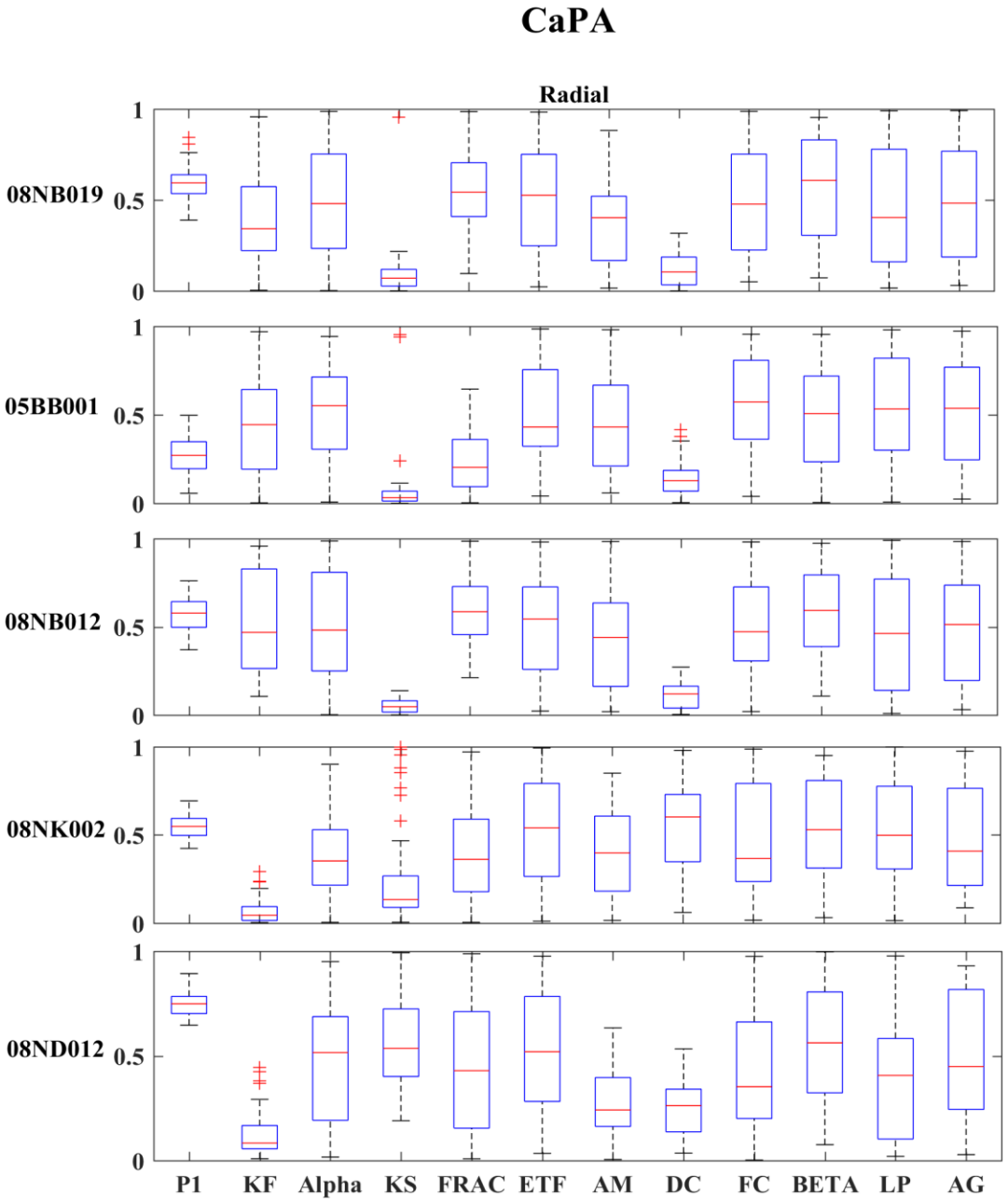

Figure 4.39: Identifiability of model parameters, using CaPA data

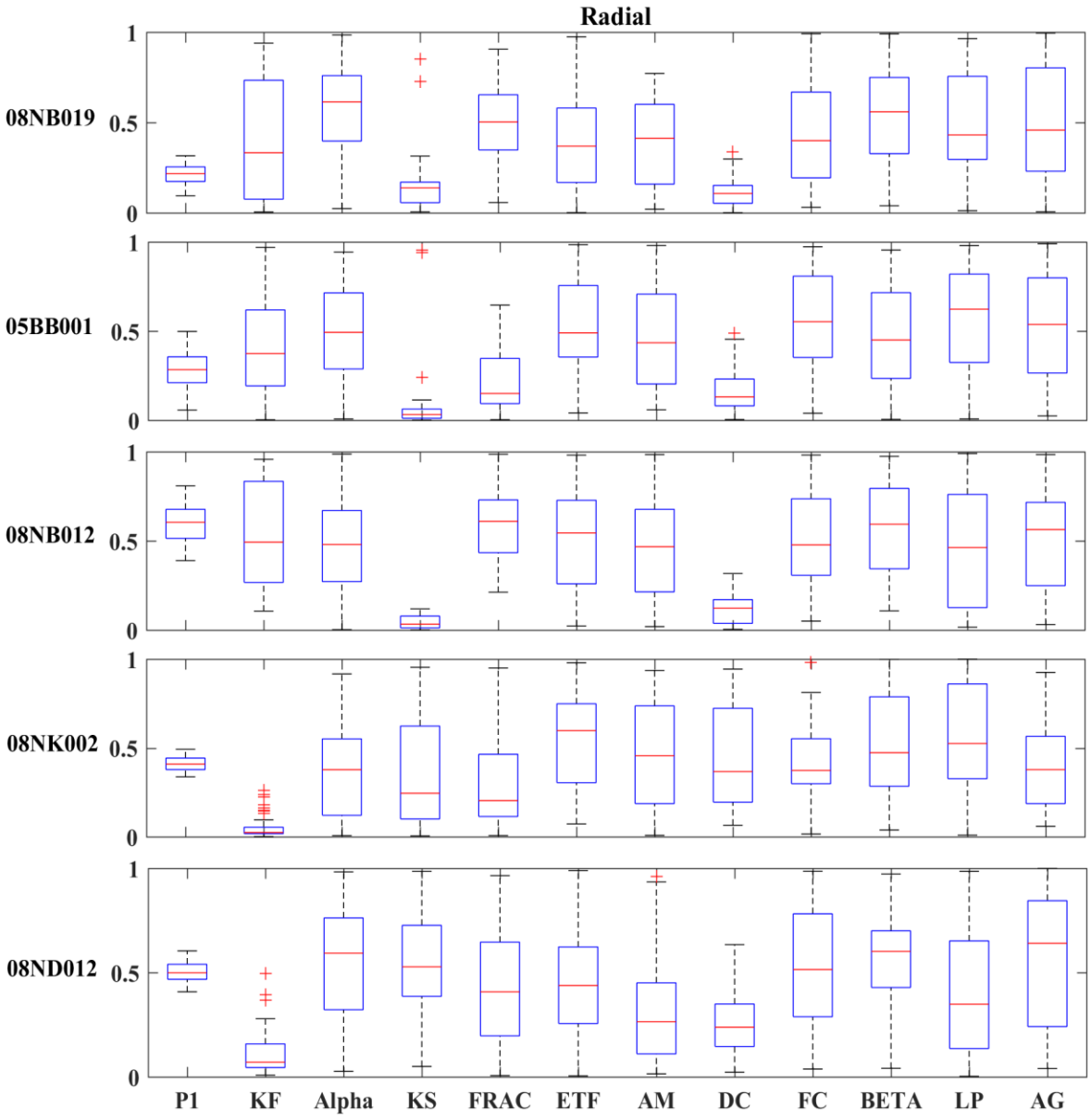

Figure 4.40: Identifiability of model parameters, using WFDEI data

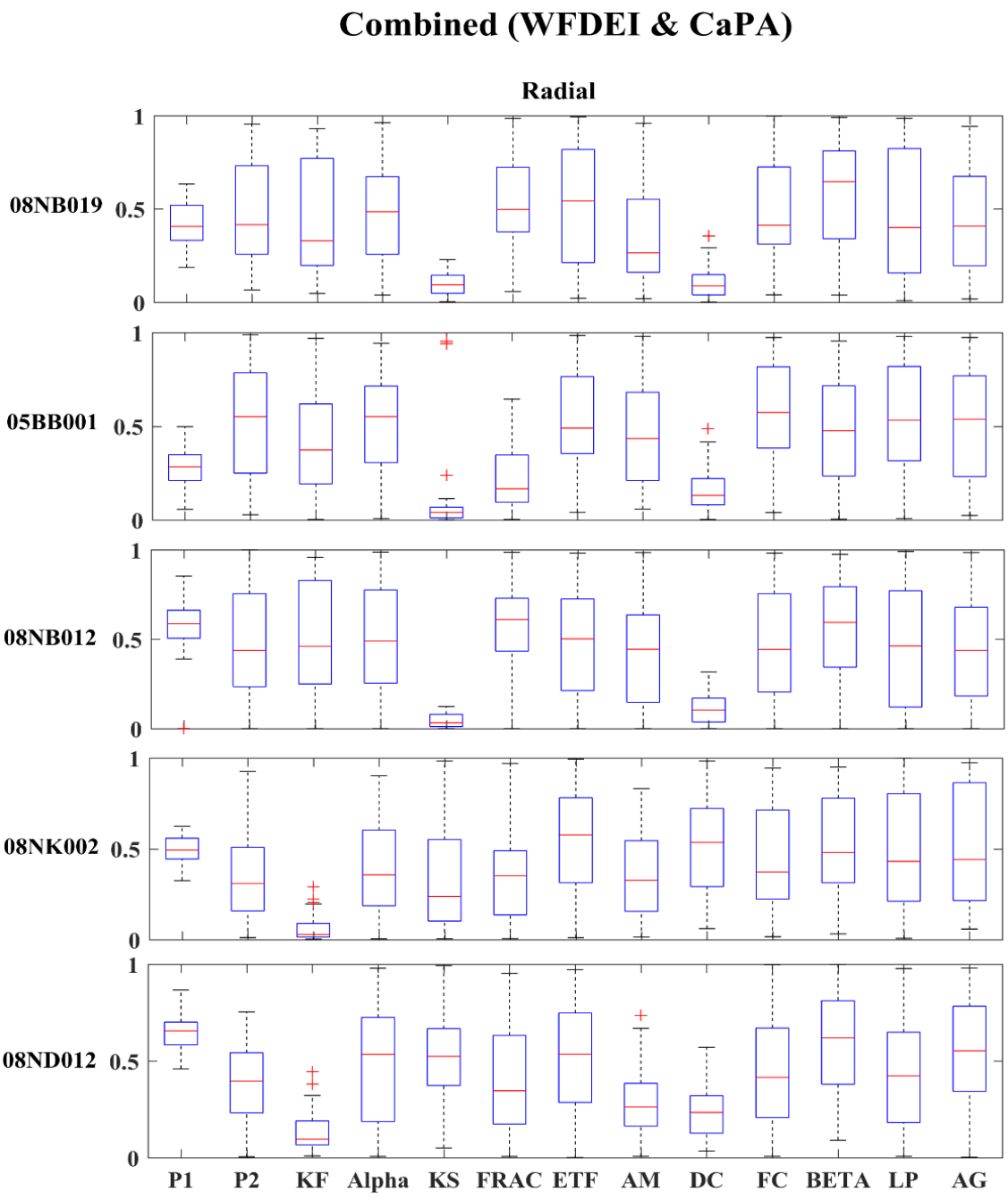

Figure 4.41: Identifiability of model parameters, using combined data

All three figures show similar patterns in terms of parameters that were identifiable, however, with the various median, maximum, and minimum values. The only noticeable differences in the constraining of the parameters are found between the CaPA and WFDEI boxplots showing that the parameters of WFDEI (figure 4.40) tend to be more constrained.

Some parameters are well-defined, since the behavioral parameter values lie in a narrow region of the parameter range, such as P_1, DC (except for basin 08NK002), K_f (or K_s), whereas other parameters are spread across the entire range.

The boxplots of K_f and K_s illustrate that for each basin, only one of these two parameters can be identified. The identified parameter can compensate for the unidentifiable parameter. Additionally, in some cases, basin 08ND012, for example, higher values were assigned to K_s compared to K_f, which contrasts with the nature of the two parameters. These higher values indicated errors in the structure of the model or pointed to some important processes that are not involved in streamflow estimation. To prevent these errors, more accurate ranges could be applied in the Monte-Carlo simulation, especially K_f and K_s. In other words, in this study if there were no overlap between their ranges, K_f would not reach higher values than K_s.

The identifiability of P_1, DC and K_f/K_s means that among the different model parameters, model results were largely dependent upon three: P_1 (precipitation correction factor), K_f or K_s (runoff routine), and Dc (snow routine). Parameters of other routines (soil, evapotranspiration, and glacier) could be compensated in the model by other parameters. Runoff is highly influenced first by precipitation inputs and then by snow melt. Therefore, the dominant role of the climate (P_1) and snow routine (DC) parameter for the model performance was not surprising. Figures 4.39, 4.40, and 4.41 show that among the non-identifiable parameters some parameters appear to be more constrained than others. For instance, for basin 08NK002 when WFDEI was used, parameter FC exhibits a somewhat higher identifiability than BETA in soil routine parameters (soil routine contains three parameters of FC, BETA, L_P). This higher identifiability occurred because the model was more sensitive to FC compared to the other two parameters in this area. Previous studies of parameter identifiability on HBV have shown that FC has a larger impact on the model performance than BETA (Ouyang et al., 2014) and L_P, has the least sensitivity (Ouyang et al. 2014).

In the other studies of HBV model, different parameters were found to be well or badly defined (Ouyang et al., 2014; Uhlenbrook, Seibert, Leibundgut, & Rodhe, 1999). Non-identifiability of parameters can result from either over-parameterization or model structure errors (Pokhrel, Gupta, & Wagener, 2008; Sorooshian, Duan, & Gupta, 1993). These findings suggested that it is difficult to know in advance whether a specific parameter will be well defined or not.

4.3.2.8 P1, P2 range

Figure 4.42 shows the values of precipitation correction factors (without normalization) of behavioral parameters correspond to WFDEI and CaPA data. And figure 4.43 shows a range of P_1 and P_2 values of behavioral parameter sets when combined data were used. A value closest to 1 indicates that the raw precipitation product performed well in approximating the streamflow.

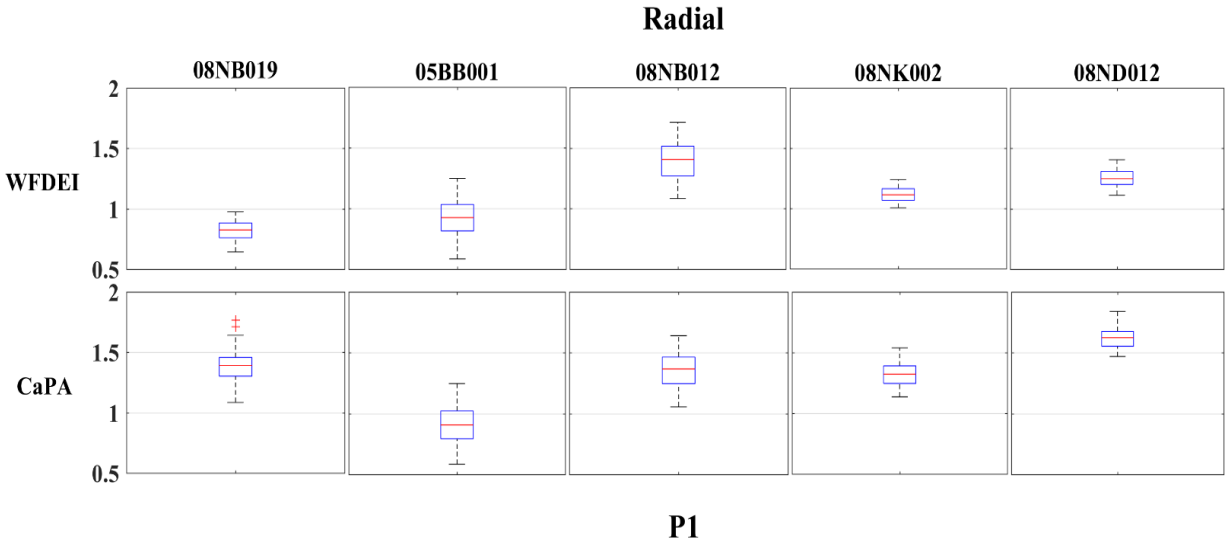

Figure 4.42: Range of precipitation correction factor (P_1) for WFDEI and CaPA data

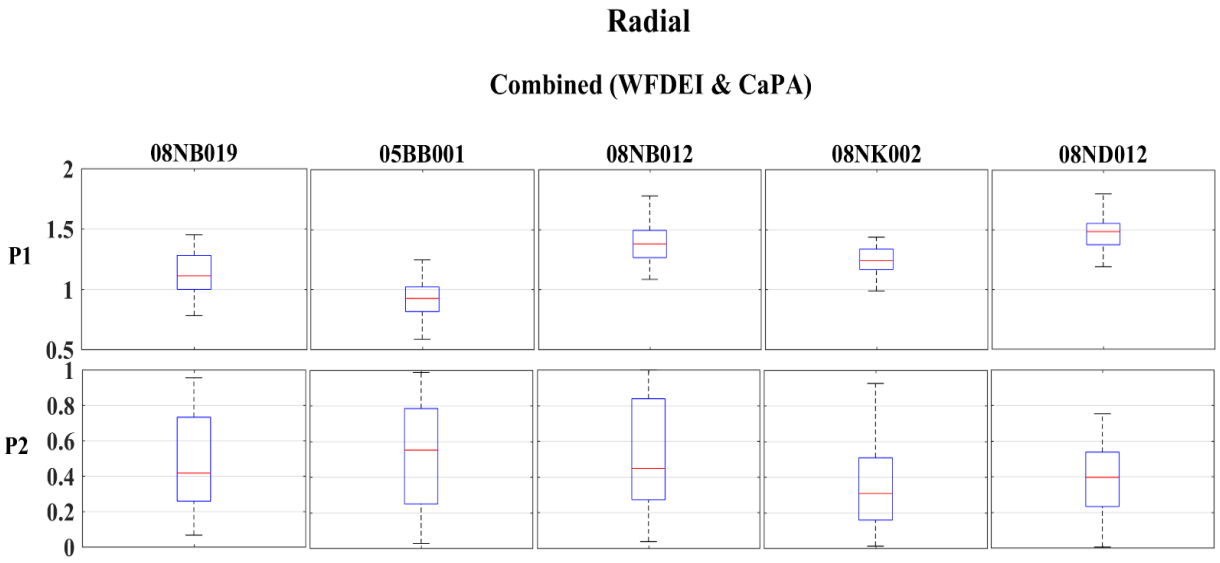

Figure 4.43: Range of precipitation correction factors (P_1 and P_2) for combined data

As can be seen in the above figures, basins with underestimated precipitation are higher in CaPA in comparison with WFDEI since the latter boxplots are more constrained and the median values are closer to 1. CaPA showed the larger bias for three basins out of five, requiring more than one and a half times the correction for basin 08ND012, for instance, in order to approximate total water inputs to the basin.

Figure 4.21 (p. 74) showed that ANUSPLIN had the maximum NSE and NSE-log for basin 08NB012 due to the higher precipitation data it estimated. This result is in agreement with the above figure, which shows that the boxplot of basin 08NB012 related to WFDEI data has the highest distance from 1. The results demonstrated that the higher the estimate for P_1, the lower the calculations for the NSE and NE-Log. For instance, basin 08NK002, with a median P_1 of 1.1, has a median and maximum of 0.79 and 0.82 for NSE, respectively, and 0.79 and 0.85 for NSE-log. Basin 08ND012 has a median P_1 of 1.2; the values are 0.76 and 0.82 for NSE and 0.71 and .0.82 for NSE-log, when WFDEI is used as an input.

Moreover, median and maximum P_1 values of 0.97 and 0.82 for basin 08MB019 indicate that, unexpectedly, overestimation of WFDEI was the reason for the error in streamflow generation by the model. However, WFDIE results in a higher NSE and NSE-log for this basin compared to ANUSPIN, although the latter's average annual estimates were lower than the average

precipitation of WFDEI. Meaning that dynamic of daily WFDEI values (not the total annual amount) were more reasonably representative of real precipitation data compared that those for ANUSPLIN.

When the combined data were adjusted, P_2 spread across the entire value range (figure 4.43), which indicated that one multiplier factor (in this case P_1) could be enough to adjust the precipitation data if they are either used individually or are combined. Secondly, the P_1 values are less constrained. In other words, they are less identifiable compared to those in figure 4.42. The reason for this difference is that one more parameter (P_2) was added to the Monte-Carlo simulation. The higher number of parameters increased model uncertainty and probably reduced the number of identifiable parameters (Shen, Chen, & Chen, 2012).

5 Conclusion

5.1 Summary of study

In this study, we investigated the applicability of the HBV-EC model in simulating streamflow in 25 basins in the Canadian Rocky Mountains. For climate data, we applied three different products to the model: ANUSPLIN, CaPA, and WFDEI. The results of the model showed good agreement between observed and simulated runoff, with the average maximum NSE higher than 0.7 for 14 of the 25 basins.

These three products showed a discrepancy in precipitation and temperature data, more or less, for different basins, with the maximum difference of 600mm/ year and 1.9◦C related to discrepancy of CaPA-ANUSPLIN precipitation and WFDEI-ANUSPLIN temperature data. However, three forcings showed a very good agreement for the smallest basin, 08NP004, which has an area of 92.8km^2.

A more rigorous analysis of hydro-climate data and modeling results were carried out on five selected basins: 08NB019, 05BB001, 08NB012, 08NK002, and 08ND012. Average weekly climate data illustrated that basins 08ND012 and 08NB019 have the highest precipitation values, occurring mostly in winter as snow. These two basins also generated the largest average streamflow during the year and with the same peak timing in weeks 23 and 26.

For these five basins, the uncertainty of hydrological model parameters and forcing data were also investigated. Uncertainties of the model were characterized using the Monte-Carlo simulation, and two cutoff methods – “Radial” and “Cut” – were used to select the behavioral parameter sets. “Radial” picked up 50 parameter sets within a distance of Pareto front to the origin. “Cut” chose parameter sets having NSE and NSE-Log of a minimum of 0.5 and BIAS of less than a value so that eventually 50 parameter sets were selected. Model performance of behavioral parameter sets showed that to distinguish between behavioral and non-behavioral parameters, “Radial” is more stable and reliable than “Cut” since it showed more constrained boxplots of NSE and NSE-Log and with higher median values. However, “Cut” was determined to be more appropriate in

selecting the behavioral parameters regarding the BIAS objective function which returns to the variable values of BIAS were used for parameters selection in this approach.

The identifiability of behavioral parameters showed that among all 13 parameters (11 model and two precipitation correction factor parameters), P1, DC, Kf /Ks (the only parameter identified each time) were well-defined and varied within smaller ranges, more or less. The degree of variability depended on the basin and forcing data. However, most of the parameters could not be identified and good simulations could be achieved over a wide range of parameter values. Non-identifiability of parameters can result from over-parameterization, model structure errors, or missing processes within the model. It has been argued that the problem of identifying a unique parameter set and model variant is not an issue for practical model applications. In other words, different parameter sets and model variants are equally suitable to simulate runoff during a calibration period, and any one of these sets may be applied. However, using different parameter sets may largely limit the use of models for other purposes such as parameter regionalization. Although the applicability of the HBV-EC model has been evaluated in various basins with encouraging results, caution is recommended when using this model for studying the impact of climate or land-use changes and for describing basin hydrology. To conclude, this study showed that when applying the HBV-EC conceptual hydrological model, uncertainty of the model parameters and its impacts on model predictions have to be considered. Future research is needed to promote recommendations and procedures suitable for operational use.

To identify the impact of forcing data uncertainty on streamflow simulations, three climate data sets were input into the model. The magnitude of error for streamflow simulations varied depending on the catchment conditions and the forcing data employed. The best results of objective functions showed that WFDEI had the best reliability and was more capable of estimating accurate climate data for three basins (08NB019, 08ND012, and 08NK002) of the five selected. For two other basins (05BB001 and 08NB012), CaPA and ANUSPLIN resulted in higher NSE and NSE-Log since they tended to estimate higher average precipitation for those areas. Therefore, the higher the precipitation simulated by the product, the better the performance using NSE and NSE-Log criteria. This outcome demonstrated that all three climate products underestimated precipitation for almost all five basins; therefore, a multiplier correction factor (P_1 ranging from 0.5 to 2) was applied to adjust the precipitation data (only CaPA and WFDEI data). The results

showed that both WFDEI and CaPA precipitation data required the correction factor to represent the accurate input water, although this factor is more pronounced for CaPA than for WFDEI. The median values of P_1 for behavioral parameter sets were calculated as 1.39, 0.9, 1.36, 1.23, and 1.6 for CaPA, while they were 0.83, 0.93, 1.4, 1.10, and 1.23 for WFDEI, corresponding to basins 08NB019, 05BB001, 08NB012, 08NK002, and 08ND012, respectively.

5.2 Recommendations

- The sub-period calibration method developed by Gharari et al. (2013) can be applied to analyze the temporal changes in the parameter identifiability and calibration over the period of study for all 25 basins. The method involves calibrating the model independently on different sub-periods and selecting the parameter sets that are more time consistent across all sub-periods.

- This analysis framework can be further extended to other uncertainty sources, including uncertainty from evapotranspiration, along with different objective functions (e.g., RMSE). Since parameter identifiability is sensitive to the choice of cutoff threshold method, other approaches can be applied to investigate uncertainties.

- Sensitivity analysis of parameters is key in identifying dominant parameters that control model behavior. Therefore, to better understand model/parameter uncertainties, it is recommended that a reliable sensitivity analysis be applied to model parameters (Razavi & Gupta 2015).

- It is recommended that a more comparative study be carried out including more complex models for cold regions (such as CRHM, Pomeroy et al. 2007) to investigate whether they preform similarly to the results on this thesis. It should be note that the available input data is one the main crucial criteria to select the model. Therefore if the required data for different models (especially physically-based ones) can be obtained, a comparative study would be a useful approach to assess whether adding complexity will necessarily lead to improved performance of hydrological modelling in the Canadian Rocky catchments and to what extent.

References

Adam, J. C., & Lettenmaier, D. P. (2003). Adjustment of global gridded precipitation for systematic bias. *Journal of Geophysical Research: Atmospheres*, *108*(D9), 4257. https://doi.org/10.1029/2002JD002499

Aghakouchak, A., & Habib, E. (2010). Application of a Conceptual Hydrologic Model in Teaching Hydrologic Processes. *International Journal of Engineering Education*, *26*(4), 963–973. https://doi.org/0949-149X/91

Alarcon, V., McAnally, W., Ervin, G., & Brooks C. (2010).Using MODIS Land-Use/Land-Cover Data and Hydrological Modeling for Estimating Nutrient Concentrations. *Springer-Verlag Berlin Heidelberg, ICCSA Part I, LNCS 6016, Springer-Verlag Berlin Heidelberg,* 501-514.

Andermann, C., Bonnet, S., & Gloaguen, R. (2011). Evaluation of precipitation data sets along the Himalayan front. *Geochemistry, Geophysics, Geosystems*, *12*(7). https://doi.org/10.1029/2011GC003513

Artan, G., Gadain, H., Smith, J. L., Asante, K., Bandaragoda, C. J., & Verdin, J. P. (2007). Adequacy of satellite derived rainfall data for stream flow modeling. *Natural Hazards*, *43*(2), 167–185. https://doi.org/10.1007/s11069-007-9121-6

ASCE. (1993). Criteria for evaluation of watershed models, ASCE task committee on definition of criteria for evaluation of watershed models of the watershed management, irrigation, and drainage division. *Journal of Irrigation and Drainage Engineering*, *119*(3), 429. https://doi.org/10.1061/(ASCE)0733-9437(1993)119:3(429)

Bales, R. C., Molotch, N. P., Painter, T. H., Dettinger, M. D., Rice, R., & Dozier, J. (2006). Mountain hydrology of the western United States. *Water Resources Research*, *42*(8). https://doi.org/10.1029/2005WR004387

Bárdossy, a., & Das, T. (2006). Influence of rainfall observation network on model calibration and application. *Hydrology and Earth System Sciences Discussions*, *3*(6), 3691–3726.

Barnes, C. J. (1995). The art of catchment modeling: What is a good model? Environment International, 21(5), 747–751. https://doi.org/10.1016/0160-4120(95)00082-V https://doi.org/10.5194/hessd-3-3691-2006

Barry, R. G. (2006). The status of research on glaciers and global glacier recession: a review. *Progress in Physical Geography*, *30*(3), 285–306. https://doi.org/10.1191/0309133306pp478ra

Behrangi, A., Khakbaz, B., Jaw, T. C., AghaKouchak, A., Hsu, K., & Sorooshian, S. (2011). Hydrologic evaluation of satellite precipitation products over a mid-size basin. *Journal of Hydrology*, *397*(3–4), 225–237. https://doi.org/10.1016/j.jhydrol.2010.11.043

Benke, K. K., Lowell, K. E., & Hamilton, A. J. (2008). Parameter uncertainty, sensitivity analysis and prediction error in a water-balance hydrological model. *Mathematical and Computer Modelling*, 47(11–12), 1134–1149. https://doi.org/10.1016/j.mcm.2007.05.017

Benninga, H. F. (2015). Performance and limitations of ensemble river flow forecasts, (master's thesis). University of Twente, Faculty of Engineering Technology, Department of Water Engineering & Management. Retrieved from http://essay.utwente.nl/68100/1/Benninga, H.F. 1076523 openbaar.pdf

Bergström, S. (1976). Development and application of a conceptual runoff model for Scandinavian catchments. *SMHI RHO 7, Norrköping*.

Bergström, S. (1992). The HBV model - its structure and applications. *Swedish Meteorological and Hydrological Institute, SMHI 4, Norrköping.*

Bergström S. (1995). In: Computer models of watershed hydrology, Water Resources Publications, Higland Ranch, Colorado, USA. 443–476.

Beven, K. (1993). Prophecy, reality and uncertainty in distributed hydrological modelling. *Advances in Water Resources*, *16*(1), 41–51. https://doi.org/10.1016/0309-1708(93)90028-E

Beven, K. (2006). A manifesto for the equifinality thesis.*Journal of Hydrology*, *320*(1-2), 18–36. https://doi.org/10.1016/j.jhydrol.2005.07.007

Beven, K., & Binley, A. (1992). The future of distributed models: Model calibration and uncertainty prediction. *Hydrological Processes*, *6*(3), 279–298. https://doi.org/10.1002/hyp.3360060305

Biemans, H., Hutjes, R. W. A., Kabat, P., Strengers, B. J., Gerten, D., & Rost, S. (2009). Effects of Precipitation Uncertainty on Discharge Calculations for Main River Basins. *Journal of Hydrometeorology*, *10*(4), 1011–1025. https://doi.org/10.1175/2008JHM1067.1

Blasone, R. (2007). Parameter Estimation and Uncertainty Assessment in Hydrological Modelling (Ph.D. thesis). Institute of Environment & Resources, Technical University of Denmark.

Bohrn, S. K. (2012). Climate change impact assessment and uncertainty analysis of the hydrology of a northern, data-sparse catchment using multiple hydrological models (M.Sc thesis), Faculty of Graduate Studies, The University of Manitoba

Boluwade, A., Zhao, K.-Y., Stadnyk, T. A., & Rasmussen, P. (2017). Towards Validation of the Canadian Precipitation Analysis (CaPA) for Hydrologic Modeling Applications in the Canadian Prairies. *Journal of Hydrology*. https://doi.org/10.1016/j.jhydrol.2017.05.059

Bonsal, B. R., Aider, R., Gachon, P., & Lapp, S. (2013). An assessment of Canadian prairie drought: Past, present, and future. *Climate Dynamics*, *41*(2), 501–516. https://doi.org/10.1007/s00382-012-1422-0

Borah, D. K., & Bera, M. (2003). Watershed-scale hydrologic and nonpoint-source pollution models: review of mathematical bases. *Ransactions of the ASAE*, *46*(6), 1553–1566. https://doi.org/Article

Box, G. E. P., & Hunter, J. S. (1961). The 2^{k-p} Fractional Factorial Designs. *Technometrics*, *3*(3), 311–351. https://doi.org/10.1080/00401706.1961.10489951

Brandt, M, Bergstrom, S, & Gardelin, M. (1988). Modelling the Effects of Clearcutting on Runoff--Examples from Central Sweden. *AMBIO AMBOCX*, *Springer*, *17*(5), 307–313. Retrieved from http://www.jstor.org/stable/4313486

Braun, J. N., & Renner, C. B. (1992). Application of a conceptual runoff model in different physiographic regions of Switzerland. *Hydrological Sciences Journal*, *37*(3), 217–231. https://doi.org/10.1080/02626669209492583

Butts, M. B., Payne, J. T., Kristensen, M., & Madsen, H. (2004). An evaluation of the impact of model structure on hydrological modelling uncertainty for streamflow simulation. *Journal of Hydrology*, *298(1-4)*, 242–266. https://doi.org/10.1016/j.jhydrol.2004.03.042

Canadian Hydraulics Centre. (2010). Green Kenue Reference Manual. Ottawa, Ontario: National Research Council.

Chernos, M., MacDonald, R.J., & Craig; J., (2016). Current and future projections of glacier contribution to streamflow in the upper Athabasca River Basin. The Canadian Collaborative Research Network (CCRN), Advances in Cold Regions Hydrology.

Cho, J., Bosch, D., Lowrance, R., Strickland, T., & Vellidis, G. (2009). Effect of spatial distribution of rainfall on temporal and spatial uncertainty of SWAT output. *Transactions of the ASABE*, *52*(1998), 1545–1555. https://doi.org/10.13031/2013.29143

Chow,V. (1964), Handbook of applied hydrology. *McGraw-Hill*. New York.

Christiaens, K., & Feyen, J. (2002). Constraining soil hydraulic parameter and output uncertainty of the distributed hydrological MIKE SHE model using the GLUE framework. *Hydrological Processes*, *16*(2), 373–391. https://doi.org/10.1002/hyp.335

Cleugh, H. A., Leuning, R., Mu, Q., & Running, S. W. (2007). Regional evaporation estimates from flux tower and MODIS satellite data. *Remote Sensing of Environment*, *106*(3), 285–304. https://doi.org/10.1016/j.rse.2006.07.007

Cruff, R. W., & Thompson, T. H. (1967). A Comparison of Methods of Estimating Potential Evapotranspiration Frcom Climatological Data in Arid and Subhumid Environments. (Geological Survey), *Water-Supply Paper 1839-M, United States Government Printing Office Washington*.

Cunderlik, J. M., & Ouarda, T. B. M. J. (2010). Trends in the timing and magnitude of floods in

Canada. *Journal of Hydrology*, *375*(3–4), 471–480. https://doi.org/10.1016/j.jhydrol.2009.06.050

Dakhlaoui, H., Bargaoui, Z., & Bárdossy, A. (2012). Toward a more efficient Calibration Schema for HBV rainfall-runoff model. *Journal of Hydrology, 444–445*, 161–179. https://doi.org/10.1016/j.jhydrol.2012.04.015

D. N. Moriasi, J. G. Arnold, M. W. Van Liew, R. L. Bingner, R. D. Harmel, & T. L. Veith. (2007). Model Evaluation Guidelines for Systematic Quantification of Accuracy in Watershed Simulations. *Transactions of the ASABE, 50*(3), 885–900. https://doi.org/10.13031/2013.23153

De Ruyver, R. (2004). DEM optimization for hydrological modelling using SRTM for the Pantanal region, Brazil (M.Sc thesis). *Water Resources and Environmental Management Programme*, International Institute for Goe Informmation science and Earthobseravation.

Deb, K. (2001). Multi-Objective Optimization Using Evolutionary Algorithms. *John Wiley & Sons, LTD*. New York, USA, https://doi.org/10.1109/TEVC.2002.804322

DeBeer, C. M., & Pomeroy, J. W. (2009). Modelling snow melt and snowcover depletion in a small alpine cirque, Canadian Rocky Mountains. *Hydrological Processes, 23(18)*, 2584–2599. https://doi.org/10.1002/hyp.7346

Del Giudice, D., Albert, C., Rieckermann, J., & Reichert, P. (2016). Describing the catchment-averaged precipitation as a stochastic process improves parameter and input estimation. *Water Resources Research*, *52*(4), 3162–3186. https://doi.org/10.1002/2015WR017871

Devia, G. K., Ganasri, B. P., & Dwarakish, G. S. (2015). A Review on Hydrological Models. *Aquatic Procedia, 4*, 1001–1007. https://doi.org/10.1016/j.aqpro.2015.02.126

Dornes, P. F., Tolson, B. A., Davison, B., Pietroniro, A., Pomeroy, J. W., & Marsh, P. (2008). Regionalisation of land surface hydrological model parameters in subarctic and arctic environments. *Physics and Chemistry of the Earth, 33*(17–18), 1081–1089. https://doi.org/10.1016/j.pce.2008.07.007

Dupont, F., Chittibabu, P., Fortin, V., Rao, Y. R., & Lu, Y. (2012). Assessment of a NEMO-based hydrodynamic modelling system for the Great Lakes. *Water Quality Research Journal of Canada*, *47*(3–4), 198–214. https://doi.org/10.2166/wqrjc.2012.014

Efstratiadis, A., & Koutsoyiannis, D. (2010). One decade of multi-objective calibration approaches in hydrological modelling: a review. *Hydrological Sciences Journal*, *55*(1), 58–78. https://doi.org/10.1080/02626660903526292

El Hassan, A. A., Sharif, H. O., Jackson, T., & Chintalapudi, S. (2013). Performance of a conceptual and physically based model in simulating the response of a semi-urbanized watershed in San Antonio, Texas. *Hydrological Processes*, *27*(24), 3394–3408. https://doi.org/10.1002/hyp.9443

El-Kadi, A. I. (1989). Watershed models and their applicability to conjunctive use management.. Jawra. *Journal of the American Water Resources Association*, 25(1), 125–137. https://doi.org/10.1111/j.1752-1688.1989.tb05673.x

Ellis, C. R., Pomeroy, J. W., Brown, T., & MacDonald, J. (2010). Simulation of snow accumulation and melt in needleleaf forest environments. *Hydrology and Earth System Sciences*, *14*(6), 925–940. https://doi.org/10.5194/hess-14-925-2010

Eum, H. Il, Dibike, Y., Prowse, T., & Bonsal, B. (2014). Inter-comparison of high-resolution gridded climate data sets and their implication on hydrological model simulation over the Athabasca Watershed, Canada. *Hydrological Processes*, *28*(14), 4250–4271. https://doi.org/10.1002/hyp.10236

Eum, H. Il, Gachon, P., Laprise, R., & Ouarda, T. (2012). Evaluation of regional climate model simulations versus gridded observed and regional reanalysis products using a combined weighting scheme. *Climate Dynamics*, *38*(7–8), 1433–1457. https://doi.org/10.1007/s00382-011-1149-3

FAO. (1991). The Digitized Soil Map of the World. World Soil Resources Report 67, Rome.

FAO. (1971-1981). The FAO-Unesco Soil Map of the World. Legend and 9 volumes. Unesco, Paris.

Fang, X., & Pomeroy, J. W. (2007). Snowmelt runoff sensitivity analysis to drought on the Canadian prairies. In *Hydrological Processes* (Vol. 21, pp. 2594–2609). https://doi.org/10.1002/hyp.6796

Fenicia, F., McDonnell, J. J., & Savenije, H. H. G. (2008). Learning from model improvement: On the contribution of complementary data to process understanding. *Water Resources Research*, *44*(6). https://doi.org/10.1029/2007WR006386

Finger, D., Vis, M., Huss, M., & Seibert, J. (2015). The value of multiple data set calibration versus model complexity for improving the performance of hydrological models in mountain catchments. *Water Resources Research*, 51(4), 1939–1958. https://doi.org/10.1002/2014WR015712

Fleming, S., Cunderlik, J., Jenkinson, W., Thiemann, M., & Lence, B. (2010). A "horse race" intercomparison of process-oriented watershed models for operational river forecasting, *Canadian Water Resources Association Annual Conference*, Vancouver, Canada.

Fortin, V., Roy, G., Donaldson, N., & Mahidjiba, A. (2015). Assimilation of radar quantitative precipitation estimations in the Canadian Precipitation Analysis (CaPA). *Journal of Hydrology*, *531*, 296–307. https://doi.org/10.1016/j.jhydrol.2015.08.003

Fountain, A. G. (1996). Effect of Snow and Firn Hydrology on the Physical and Chemical Characteristics of Glacial Runoff. *Hydrological Processes*, *10*(4), 509–521. https://doi.org/10.1002/(SICI)1099-1085(199604)10:4<509::AID-HYP389>3.0.CO;2-3

Fountain, A. G., & Tangborn, W. V. (1985). The Effect of Glaciers on Streamflow Variations. *Water Resources Research*, *21*(4), 579–586. https://doi.org/10.1029/WR021i004p00579

Freer, J., Beven, K., & Ambroise, B. (1996). Bayesian estimation of uncertainty in runoff prediction and the value of data: An application of the GLUE approach. *Water Resources Research*. https://doi.org/10.1029/96WR03723

Fu, S., Sonnenborg, T. O., Jensen, K. H., & He, X. (2011). Impact of Precipitation Spatial Resolution on the Hydrological Response of an Integrated Distributed Water Resources Model. *Vadose Zone Journal*, *10*(1), 25. https://doi.org/10.2136/vzj2009.0186

Gan, Y., Duan, Q., Gong, W., Tong, C., Sun, Y., Chu, W., … Di, Z. (2014). A comprehensive evaluation of various sensitivity analysis methods: A case study with a hydrological model. *Environmental Modelling and Software*, 51, 269–285. https://doi.org/10.1016/j.envsoft.2013.09.031

Gardelin, M., & Lindstrom, G. (1997). Priestley-Taylor evapotranspiration in HBV-simulations. *Nordic Hydrology*, *28*(4–5), 233–246.

Gharari, S., Hrachowitz, M., Fenicia, F., & Savenije, H. H. G. (2013). An approach to identify time consistent model parameters: Sub-period calibration. *Hydrology and Earth System Sciences*, *17*(1), 149–161. https://doi.org/10.5194/hess-17-149-2013

Gordon, S., Sharp, M., Hubbard, B., Smart, C., Ketterling, B., & Willis, I. (1998). Seasonal reorganization of subglacial drainage inferred from measurements in boreholes. *Hydrological Processes*, *12*(1), 105–133. https://doi.org/10.1002/(SICI)1099-1085(199801)12:13.3.CO;2-R

Gray, D. M. (1964). Physiographic Characteristics and the Runoff Pattern. *Proceedings of Hydrology Symposium*, (4), 146–164.

Groisman, P. Y., Karl, T. R., Knight, R. W., & Stenchikov, G. L. (1994). Changes of snow cover, temperature, and radiative heat balance over the Northern Hemisphere. *Journal of Climate*, *7*(11), 1633–1656. https://doi.org/10.1175/1520-0442(1994)007<1633:COSCTA>2.0.CO;2

Gupta, H. V., Sorooshian, S., & Yapo, P. O. (1998). Toward improved calibration of hydrologic models: Multiple and noncommensurable measures of information. *Water Resources Research*, *34*(4), 751–763. https://doi.org/10.1029/97WR03495

Gupta, H. V., Sorooshian, S., & Yapo, P. O. (1999). Status of Automatic Calibration for Hydrologic Models: Comparison with Multilevel Expert Calibration. *Journal of Hydrologic Engineering*, *4*(2), 135–143. https://doi.org/10.1061/(ASCE)1084-0699(1999)4:2(135)

Gupta, H. V, Sorooshian, S., Hogue, T. S., & Boyle, D. P. (2003). Advances in automatic calibration of watershed models. *Water Science and Application*, *6*, 9–28.

https://doi.org/10.1029/WS006p0009

Habib, E., Haile, A. T., Sazib, N., Zhang, Y., & Rientjes, T. (2014). Effect of bias correction of satellite-rainfall estimates on runoff simulations at the source of the Upper Blue Nile. *Remote Sensing*, *6*(7), 6688–6708. https://doi.org/10.3390/rs6076688

Haile, E., & Assefa, M. (2012). The Impact of Land Use Change on the Hydrology of the Angereb Watershed, Ethiopia. *International Journal of Water Sciences*, *1*(4), 7 pages. https://doi.org/10.5772/56266

Hamilton, A. S., Hutchinson, D. G., & Moore, R. D. (2001). Estimation of winter streamflow using a conceptual hydrological model: a case study, Wolf Creek, Yukon Territory. *Proceedings 11th Workshop on River Ice. River ice processes within a changing environment.* Canada Committee on River Ice Processes and the Environment. CGU-HS. Ottawa, Canada. May. https://doi.org/10.1061/(ASCE)0887-381X(2000)14

Hamilton, A. S., Hutchinson, D. G., & Moore, R. D. (2000). Estimating Winter Streamflow Using Conceptual Streamflow Model. *Journal of Cold Regions Engineering*, *14*(4), 158–175. https://doi.org/10.1061/(ASCE)0887-381X(2000)14:4(158)

Hamon, W. R. (1961). Estimating potential evapotranspiration (B.Sc thesis). Department of Civil and Sanitary Engineering Massachusetts Institute of Technology. Retrieved from http://dspace.mit.edu/handle/1721.1/79479%5Cnhttp://dspace.mit.edu/bitstream/1721.1/79479/2/32827649-MIT.pdf%5Cnhttp://dspace.mit.edu/handle/1721.1/79479#files-area

Harder, P., Pomeroy, J. W., & Westbrook, C. J. (2015). Hydrological resilience of a Canadian Rockies headwaters basin subject to changing climate, extreme weather, and forest management. *Hydrological Processes*, *29*(18), 3905–3924. https://doi.org/10.1002/hyp.10596

Harlin J., Kung C.S. (1992). Parameter uncertainty and simulation of design floods in Sweden, *Journal of Hydrology (Amsterdam), 137 (1),* 209–230.

Harding, R., Best, M., Blyth, E., Hagemann, S., Kabat, P., Tallaksen, L. M., Warnaars, T., Wiberg, D., Weedon ,GP., Lanen, H.V., Ludwig, F., & Haddeland, I. (2011). WATCH:

Current Knowledge of the Terrestrial Global Water Cycle. *Journal of Hydrometeorology*, *12*(6), 1149–1156. https://doi.org/10.1175/JHM-D-11-024.1

Harding, R. J., & Pomeroy, J. W. (1996). The energy balance of the winter boreal landscape. *Journal of Climate*, *9*(11), 2778–2787. https://doi.org/10.1175/1520-0442(1996)009<2778:TEBOTW>2.0.CO;2

Hayes, D. C., & Young, R. L. (2005). Comparison of Peak Discharge and Runoff Characteristic Estimates from the Rational Method to Field Observations for Small Basins in Central Virginia. *USGS Scientific Investigations Report 2005-5254 (U. S. Geological Survey)*, Cooperation with the Virginia Department of Transportation. https://doi.org/Scientific Investigation Report 2005-5254

Heerma, K. (2013). Hydrological modeling of a Mongolian River basin under current and changed climate conditions using permafrost conceptualizations. M.Sc thesis, Master thesis Civil Engineering and Management, University of Twente. Retrieved from http://essay.utwente.nl/62666/

Hironobu Sugiyama, Varawoot Vudhivanich, Andrew C. Whitaker, and K. L. (2003). Stochastic Flow Duration Curves for Evaluation of Flow Regimes in Rivers. *Journal of the American Water Resources Association (JAWRA)*, *39*(1), 47–58. https://doi.org/10.1111/j.1752-1688.2003.tb01560.x

Hirshfield, F. (2008). The impact of climate change and harvest of mountain pine beetle stands on streamflow in northern British Columbia (M.Sc. thesis). Environmental Sciense. University of Northern British Columbia.

Hock, R. (2005). Glacier melt: a review of processes and their modelling. *Progress in Physical Geography*, *29*(3), 362–391. https://doi.org/10.1191/0309133305pp453ra

Honti, M., Stamm, C., & Reichert, P. (2013). Integrated uncertainty assessment of discharge predictions with a statistical error model. *Water Resources Research*, *49*(8), 4866–4884. https://doi.org/10.1002/wrcr.20374

Hopkinson, R. F., Mckenney, D. W., Milewska, E. J., Hutchinson, M. F., Papadopol, P., &

Vincent, A. L. A. (2011). Impact of aligning climatological day on gridding daily maximum-minimum temperature and precipitation over Canada. *Journal of Applied Meteorology and Climatology*, *50*(8), 1654–1665. https://doi.org/10.1175/2011JAMC2684.1

Houska, T., Multsch, S., Kraft, P., Frede, H.-G., & Breuer, L. (2014). Monte Carlo-based calibration and uncertainty analysis of a coupled plant growth and hydrological model. *Biogeosciences*, *11*(7), 2069–2082. https://doi.org/10.5194/bg-11-2069-2014

Hrachowitz, M., Savenije, H. H. G., Blöschl, G., McDonnell, J. J., Sivapalan, M., Pomeroy, J. W., … Cudennec, C. (2013). A decade of Predictions in Ungauged Basins (PUB) - a review. *Hydrological Sciences Journal*, *58*(6), 1198–1255. https://doi.org/10.1080/02626667.2013.803183

Hutchinson, M. F. (1995). Interpolating mean rainfall using thin plate smoothing splines. *International Journal of Geographical Information Systems*, *9*(4), 385–403. https://doi.org/10.1080/02693799508902045

Hutchinson, M. F., & Bischof, R. H. (1983). New method for estimating the spatial distribution of mean seasonal and annual rainfall applied to the Hunter Valley, New South Wales. *Australian Meteorological Magazine, Canberra*, *31*(3), 179–184. Retrieved from http://search.proquest.com/docview/18352905?accountid=28205

Hutchinson, M. F., & Gessler, P. E. (1994). Splines - more than just a smooth interpolator. *Geoderma*, *62*(1–3), 45–67. https://doi.org/10.1016/0016-7061(94)90027-2

Iizumi, T., Okada, M., & Yokozawza, M. (2014). A meteorological forcing data set for global crop modeling: Development, evaluation, and intercomparison. *Journal of Geophysical Research*, *119*(2), 363–384. https://doi.org/10.1002/2013JD020130.

Iman, R. L., & Conover, W. J. (1980). Small sample sensitivity analysis techniques for computer models, with an application to risk assessment. *Communications in Statistics - Theory and Methods*, *9*(17), 1749–1842. https://doi.org/10.1080/03610928008827996

Jia, L., & Stone, M. (2015). Toward improved evaluation of large scale hydrologic models :

estimation and quantification of parameter uncertainty (Ph.D thesis), School of Engineering ETDs, The University of New Mexico.

Jia, Q. Y., & Sun, F. H. (2012). Modeling and forecasting process using the HBV model in Liao river delta. Procedia Environmental Sciences, 13, 122–128. https://doi.org/10.1016/j.proenv.2012.01.012

Jost, G., Moore, R. D., Menounos, B., & Wheate, R. (2012). Quantifying the contribution of glacier runoff to streamflow in the upper Columbia River Basin, Canada. *Hydrology and Earth System Sciences*, *16*(3), 849–860. https://doi.org/10.5194/hess-16-849-2012

Justice, C. O., Townshend, J. R. G., Vermote, E. F., Masuoka, E., Wolfe, R. E., Saleous, N., … Morisette, J. T. (2002). An overview of MODIS Land data processing and product status. *Remote Sensing of Environment 83(1-2),* 3-15. https://doi.org/10.1016/S0034-4257(02)00084-6

Karl, T. R., Knight, R. W., & Plummer, N. (1995). Trends in high-frequency climate variability in the twentieth century. *Nature*, *377*(6546), 217–220. https://doi.org/10.1038/377217a0

Kavetski, D., Kuczera, G., & Franks, S. W. (2006). Bayesian analysis of input uncertainty in hydrological modeling: 2. Application. *Water Resources Research*, *42*(3). https://doi.org/10.1029/2005WR004376

Keesman, K., & van Straten, G. (1989). Identification and prediction propagation of uncertainty in models with bounded noise. *International Journal of Control*, *49*(6), 2259–2269. https://doi.org/10.1080/00207178908559771

Kewlani, G., & Iagnemma, K. (2008). A stochastic response surface approach to statistical prediction of mobile robot mobility. *2008 IEEE/RSJ International Conference on Intelligent Robots and Systems, IROS*, 2234–2239. https://doi.org/10.1109/IROS.2008.4651187

Khu, S.-T., & Werner, M. G. F. (2003). Reduction of Monte-Carlo simulation runs for uncertainty estimation in hydrological modelling. *Hydrology and Earth System Sciences*, *7*, 680–692. https://doi.org/10.5194/hess-7-680-2003

Kidd, C., Bauer, P., Turk, J., Huffman, G. J., Joyce, R., Hsu, K.-L., & Braithwaite, D. (2012). Intercomparison of High-Resolution Precipitation Products over Northwest Europe. *Journal of Hydrometeorology*, *13*(1), 67–83. https://doi.org/10.1175/JHM-D-11-042.1

Kouwen, N. (2011). WATFLOOD/WATROUTE Hydrological model routing & flow forecasting system. Waterloo, Ontario, Canada: University of Waterloo.

Krause, P., & Boyle, D. P. (2005). Advances in Geosciences Comparison of different efficiency criteria for hydrological model assessment. *Advances In Geosciences*, *5*(89), 89–97. https://doi.org/10.5194/adgeo-5-89-2005

Krogh, S. A., Pomeroy, J. W., & McPhee, J. (2015). Physically Based Mountain Hydrological Modeling Using Reanalysis Data in Patagonia. *Journal of Hydrometeorology*, *16*(1), 172–193. https://doi.org/10.1175/JHM-D-13-0178.1

Kuczera, G., & Parent, E. (1998). Monte Carlo assessment of parameter uncertainty in conceptual catchment models: The Metropolis algorithm. *Journal of Hydrology*, *211*(1–4), 69–85. https://doi.org/10.1016/S0022-1694(98)00198-X

Kuczera, G., & Williams, B. J. (1992). Effect of rainfall errors on accuracy of design flood estimates. *Water Resources Research*, *28*(4), 1145–1153. https://doi.org/10.1029/91WR03002

Kundu, P. M., & Olang, L. O. (2011). The impact of land use change on runoff and peak flood discharges for the Nyando River in Lake Victoria drainage basin, Kenya. *WIT Transactions on Ecology and the Environment*, *153*, 83–94. https://doi.org/10.2495/WS110081

Kundzewicz, Z. W., & Kaczmarek, Z. (2000). Coping with hydrological extremes. *Water International*, *25*(1), 66–75. https://doi.org/10.1080/02508060008686798

Langenbrunner, B., & Neelin, J. D. (2017). Multiobjective constraints for climate model parameter choices: Pragmatic Pareto fronts in CESM1. *Journal of Advances in Modeling Earth Systems*, *9*(5), 2008–2026. https://doi.org/10.1002/2017MS000942

Lauer, D. T., Morain, S. a, & Salomonson, V. V. (1997). The Landsat Program : Its Origins,

Evolution, and Impacts. *Photogrammetric Engineering & Remote Sensing*, *63*(7), 831–838. Retrieved from http://info.asprs.org/publications/pers/97journal/july/1997_jul_831-838.pdf

Legates, D. R., & McCabe, G. J. (1999). Evaluating the use of "goodness-of-fit" measures in hydrologic and hydroclimatic model validation. *Water Resources Research*, *35*(1), 233–241. https://doi.org/10.1029/1998WR900018

Lehmann, P., Hinz, C., McGrath, G., Tromp-van Meerveld, H. J., & McDonnell, J. J. (2007). Rainfall threshold for hillslope outflow: an emergent property of flow pathway connectivity. *Hydrology and Earth System Sciences*, *11*(2), 1047–1063. https://doi.org/10.5194/hessd-3-2923-2006

Lespinas, F., Fortin, V., Roy, G., Rasmussen, P., & Stadnyk, T. (2015). Performance Evaluation of the Canadian Precipitation Analysis (CaPA). *Journal of Hydrometeorology*, *16*(5), 2045–2064. https://doi.org/10.1175/JHM-D-14-0191.1

Li, L., Ngongondo, C. S., Xu, C.-Y., & Gong, L. (2013). Comparison of the global TRMM and WFD precipitation datasets in driving a large-scale hydrological model in southern Africa. *Hydrology Research*, *44*(5), 770. https://doi.org/10.2166/nh.2012.175

Li, L., Xu, C. Y., Zhang, Z., & Jain, S. K. (2014). Validation of a new meteorological forcing data in analysis of spatial and temporal variability of precipitation in India. *Stochastic Environmental Research and Risk Assessment*, *28*(2), 239–252. https://doi.org/10.1007/s00477-013-0745-7

Lindström, G., M., Gardelin, M., Persson (1994) Conceptual modelling of evapotranspiration for simulations of climate change effects, Swedish Meteorological Hydrological Institute, SMHI S-601 76 NorrkoÈping, Sweden. SMHI Report Hydrology 10, 25 pp

Lindström, G., Johansson, B., Persson, M., Gardelin, M., & Bergström, S. (1997). Development and test of the distributed HBV-96 hydrological model. *Journal of Hydrology*, *201*(1–4), 272–288. https://doi.org/10.1016/S0022-1694(97)00041-3

Liu, J., Zhang, C., Kou, L., & Zhou, Q. (2017). Effects of Climate and Land Use Changes on Water Resources in the Taoer River. *Advances in Meteorology, 2017*.

https://doi.org/10.1155/2017/1031854

Liu, X., Liu, F. M., Wang, X. X., Li, X. D., Fan, Y. Y., Cai, S. X., & Ao, T. Q. (2017). Combining rainfall data from rain gauges and TRMM in hydrological modelling of Laotian data-sparse basins. *Applied Water Science*, *7*(3), 1487–1496. https://doi.org/10.1007/s13201-015-0330-y

Loukas, A., Vasiliades, L., & Dalezios, N. R. (2002). Potential climate change impacts on flood producing mechanisms in southern British Columbia, Canada using the CGCMA1 simulation results. *Journal of Hydrology*, *259*(1–4), 163–188. https://doi.org/10.1016/S0022-1694(01)00580-7

Lu, J., Sun, G., McNulty, S. G., & Amatya, D. M. (2005). A COMPARISON OF SIX POTENTIAL EVAPOTRANSPIRATION METHODS FOR REGIONAL USE IN THE SOUTHEASTERN UNITED STATES. *Journal of the American Water Resources Association*, *41*(3), 621–633. https://doi.org/10.1111/j.1752-1688.2005.tb03759.x

Madsen, H. (2000). Automatic calibration of a conceptual rainfall–runoff model using multiple objectives. *Journal of Hydrology*, *235*(3), 276–288. https://doi.org/10.1016/S0022-1694(00)00279-1

Mahat, V., & Anderson, A. (2013). Impacts of climate and catastrophic forest changes on streamflow and water balance in a mountainous headwater stream in Southern Alberta. *Hydrology and Earth System Sciences*, 17(12), 4941–4956. https://doi.org/10.5194/hess-17-4941-2013

Mailhot, J., B??lair, S., Charron, M., Doyle, C., Joe, P., Abrahamowicz, M., … Tong, L. (2010). Environment Canada's experimental numerical weather prediction systems for the Vancouver 2010 winter olympic and paralympic games. *Bulletin of the American Meteorological Society*, *91*(8), 1073–1085. https://doi.org/10.1175/2010BAMS2913.1

Manithaphone Mahaxay, Wanchai Arunpraparut, Yongyut Trisurat, & Nipon Tangtham. (2016). Calibration of Hydrological Streamflow Modeling Using MODIS. *Journal of Geological Resource and Engineering*, *4*(1), 49–55. https://doi.org/10.17265/2328-2193/2015.01.007

Marshall, S. J., White, E. C., Demuth, M. N., Bolch, T., Wheate, R., Menounos, B., … Shea, J. M. (2011). Glacier Water Resources on the Eastern Slopes of the Canadian Rocky Mountains. *Canadian Water Resources Journal*, *36*(2), 109–134. https://doi.org/10.4296/cwrj3602823

Masih, I., Maskey, S., Uhlenbrook, S., & Smakhtin, V. (2011). Assessing the Impact of Areal Precipitation Input on Streamflow Simulations Using the SWAT Model. *Journal of the American Water Resources Association*, *47*(1), 179–195. https://doi.org/10.1111/j.1752-1688.2010.00502.x

McKay, M. D., W. J. Conover & R. J. Beckman. (1979). A Comparison of Three Methods for Selecting Values of Input Variables in the Analysis of Output from a Computer Code. *Technometrics 21(2),* 239-245.

Mengistu, S. G., & Spence, C. (2016). Testing the ability of a semidistributed hydrological model to simulate contributing area. *Water Resources Research*, *52*(6), 4399–4415. https://doi.org/10.1002/2016WR018760

Merritt, W. S., Alila, Y., Barton, M., Taylor, B., Cohen, S., & Neilsen, D. (2006). Hydrologic response to scenarios of climate change in sub watersheds of the Okanagan basin, British Columbia. *Journal of Hydrology*, *326*(1–4), 79–108. https://doi.org/10.1016/j.jhydrol.2005.10.025

Minville, M., Cartier, D., Guay, C., Leclaire, L.-A., Audet, C., Le Digabel, S., & Merleau, J. (2014). Improving process representation in conceptual hydrological model calibration using climate simulations. *Water Resources Research*, *50*(6), 5044–5073. https://doi.org/10.1002/2013WR013857

Miranda, R. D. Q., Galvíncio, J. D., Moura, M. S. B. De, Jones, C. A., & Srinivasan, R. (2017). Reliability of MODIS Evapotranspiration Products for Heterogeneous Dry Forest: A Study Case of Caatinga. *Advances in Meteorology*, *2017*. https://doi.org/10.1155/2017/9314801

Mohamoud, Y. M. (2008). Prediction of daily flow duration curves and streamflow for ungauged catchments using regional flow duration curves. *Hydrological Sciences Journal*, *53*(4),

706–724. https://doi.org/10.1623/hysj.53.4.706

Monteith, J. L. (1965). Evaporation and environment. *Symposia of the Society for Experimental Biology, 19*, 205–234. https://doi.org/10.1613/jair.301

Moore, R. D. (1992). the Influence of Glacial Cover on the Variability of Annual Runoff, Coast Mountains, British Columbia, Canada. *Canadian Water Resources Journal*, *17*(2), 101–109. https://doi.org/10.4296/cwrj1702101

Moore, R. D. (1993). Application of a conceptual streamflow model in a glacierized drainage basin. *Journal of Hydrology*, *150*(1), 151–168. https://doi.org/10.1016/0022-1694(93)90159-7

Moore, R. D., & Demuth, M. N. (2001). Mass balance and streamflow variability at Place Glacier, Canada, in relation to recent climate fluctuations. *Hydrological Processes*, *15*(18), 3473–3486. https://doi.org/10.1002/hyp.1030

Moore, R. D., Fleming, S. W., Menounos, B., Wheate, R., Fountain, A., Stahl, K., … Jakob, M. (2009). Glacier change in western North America: Influences on hydrology, geomorphic hazards and water quality. *Hydrological Processes, 23(1),* 42-61. https://doi.org/10.1002/hyp.7162

Moradkhani, H., & Sorooshian, S. (2008). General review of rainfall-runoff modeling: Model calibration, data assimilation, and uncertainty analysis. In Book *Hydrological Modelling and the Water Cycle* ,1–24. DOI:10.1007/978-3-540-77843-1_1

Moriasi, D., & Gitau, M. (2015). Hydrologic and Water Quality Models: Performance Measures and Evaluation Criteria. *Transactions of the ASABE*, *58*(6), 1763–1785. https://doi.org/10.13031/trans.58.10715

Morris, M. D. (1991). Factorial sampling plans for preliminary computational experiments. *Technometrics, 33(2)*, 161–174. https://doi.org/10.1080/00401706.1991.10484804

Moulin, L., Gaume, E., & Obled, C. (2008). Uncertainties on mean areal precipitation: assessment and impact on streamflow simulations. *Hydrology and Earth System Sciences*

Discussions, *5*(4), 2067–2110. https://doi.org/10.5194/hessd-5-2067-2008

Moussa, R., & Chahinian, N. (2009). Comparison of different multi-objective calibration criteria using a conceptual rainfall-runoff model of flood events. *Hydrology and Earth System Sciences*, 519–535. https://doi.org/Hydrol. Earth Syst. Sci., 13, 519–535, 2009

Mu, Q., Heinsch, F. A., Zhao, M., & Running, S. W. (2007). Development of a global evapotranspiration algorithm based on MODIS and global meteorology data. *Remote Sensing of Environment*, *111*(4), 519–536. https://doi.org/10.1016/j.rse.2007.04.015

Mu, Q., Jones, L. A., Kimball, J. S., McDonald, K. C., & Running, S. W. (2009). Satellite assessment of land surface evapotranspiration for the pan-Arctic domain. *Water Resources Research*, *45*(9). https://doi.org/10.1029/2008WR007189

Mu, Q., Zhao, M., & Running, S. W. (2011). Improvements to a MODIS global terrestrial evapotranspiration algorithm. *Remote Sensing of Environment*, *115*(8), 1781–1800. https://doi.org/10.1016/j.rse.2011.02.019

Muhammed, A. H. (2012). Satellite Based Evapotranspiration Estimation and Runoff Simulation : a Topmodel Application To the Gilgel Abay Catchment , Ethiopia (M.Sc thesis), Faculty of Geo-Information Science and Earth Observation. The University of Twente.

Muleta, M. K. (2012). Model Performance Sensitivity to Objective Function during Automated Calibrations. *Journal of Hydrologic Engineering*, *17*(6), 756–767. https://doi.org/10.1061/(ASCE)HE.1943-5584.0000497

Nachtergaele, F. (1999). From the Soil Map of the World To the Digital Global Soil and Terrain Database: 1960-2002. *Handbook of Soil Science. CRC Press, Boca Raton*, 1–19. Retrieved from http://www.itc.nl/personal/rossiter/docs/wrb/soilmapworld.pdf

Nandakumar, N., & Mein, R. G. (1997). Uncertainty in rainfall-runoff model simulations and the implications for predicting the hydrologic effects of land-use change. *Journal of Hydrology*, *192(1–4)*, 211–232. https://doi.org/10.1016/S0022-1694(96)03106-X

Nash, J. E., & Sutcliffe, J. V. (1970). River flow forecasting through conceptual models part I - A discussion of principles. *Journal of Hydrology*, *10*(3), 282–290. https://doi.org/10.1016/0022-1694(70)90255-6

National Water Research Institute, Threats to water availability in Canada. 2004. Environment Canada, , Burlington, Ontario. 3,128

NRCan: Regional, national and international climate modeling.2014. Available at: http://cfs.nrcan.gc.ca/projects/3?lang=en_CA

NRCan: Characterization and Monitoring Change of Canada's Land Surface. 2008. Available at: http://www.nrcan.gc.ca/earth-sciences/land-surface-vegetation/land-cover/north-american-landcover/9146

Nkiaka, E., Nawaz, N., & Lovett, J. (2017). Evaluating Global Reanalysis Datasets as Input for Hydrological Modelling in the Sudano-Sahel Region. *Hydrology*, *4*(1), 13. https://doi.org/10.3390/hydrology4010013

Ontario stormwater Management Planning & Design Manual, 2003, Ontario Ministry of the Environment.

Oudin, L., Hervieu, F., Michel, C., Perrin, C., Andréassian, V., Anctil, F., & Loumagne, C. (2005). Which potential evapotranspiration input for a lumped rainfall-runoff model? Part 2 - Towards a simple and efficient potential evapotranspiration model for rainfall-runoff modelling. *Journal of Hydrology*, *303*(1–4), 290–306. https://doi.org/10.1016/j.jhydrol.2004.08.026

Oudin, L., Perrin, C., Mathevet, T., Andréassian, V., & Michel, C. (2006). Impact of biased and randomly corrupted inputs on the efficiency and the parameters of watershed models. *Journal of Hydrology*, *320*(1–2), 62–83. https://doi.org/10.1016/j.jhydrol.2005.07.016

Ouyang, S., Puhlmann, H., Wang, S., von Wilpert, K., Sun, O. J., Allen, R., … Wang, Y. (2014). Parameter uncertainty and identifiability of a conceptual semi-distributed model to simulate hydrological processes in a small headwater catchment in Northwest China. *Ecological Processes*, *3*(1), 14. https://doi.org/10.1186/s13717-014-0014-9

Owen, a B. (1992). Orthogonal Arrays for Computer Experiments, Integration and Visualization. *Statistica Sinica*, 2(2), 439-452. https://doi.org/10.2307/24304869

Papadopoulos, C. E., & Yeung, H. (2001). Uncertainty estimation and Monte Carlo simulation method. *Flow Measurement and Instrumentation*, *12*(4), 291–298. https://doi.org/10.1016/S0955-5986(01)00015-2

Pareto, V. (1896). The New Theories of Economics. *Journal of Political Economy*, *5*(4), 485–502. https://doi.org/10.1086/250454

Parker, R., Arnold, J. G., Barrett, M., Burns, L., Carrubba, L., Neitsch, S. L., … Srinivasan, R. (2007). Evaluation of three watershed-scale pesticide environmental transport and fate models. *Journal of the American Water Resources Association*, *43*(6), 1424–1443. https://doi.org/10.1111/j.1752-1688.2007.00101.x

Paturel, J. E., Servat, E., & Vassiliadis, A. (1995). Sensitivity of conceptual rainfall-runoff algorithms to errors in input data -case of the GR2M model. *Journal of Hydrology*, *168*(1–4), 111–125. https://doi.org/10.1016/0022-1694(94)02654-T

Pearce, A. J. (1990). Streamflow Generation Processes: An Austral View. *Water Resources Research*, *26*(12), 3037–3047. https://doi.org/10.1029/WR026i012p03037

Pellicciotti, F., Buergi, C., Immerzeel, W. W., Konz, M., & Shrestha, A. B. (2012). Challenges and Uncertainties in Hydrological Modeling of Remote Hindu Kush–Karakoram–Himalayan (HKH) Basins: Suggestions for Calibration Strategies. *Mountain Research and Development*, *32*(1), 39–50. https://doi.org/10.1659/MRD-JOURNAL-D-11-00092.1

Penman, H. L. (1948). Natural Evporation from Open Water, Bare Soil and Grass. *The Royal Society*, *193*(1032), 120–145. https://doi.org/10.1098/rspa.1948.0037

Pennelly, C., Reuter, G., & Flesch, T. (2014). Verification of the WRF model for simulating heavy precipitation in Alberta. *Atmospheric Research*, *135–136*, 172–192. https://doi.org/10.1016/j.atmosres.2013.09.004

Pietroniro, A., Fortin, V., Kouwen, N., Neal, C., Turcotte, R., Davison, B., … Pellerin, P. (2007).

Using the MESH modelling system for hydrological ensemble forecasting of the Laurentian Great Lakes at the regional scale. *Hydrology and Earth System Sciences*, *3*(4), 1279–1294. https://doi.org/10.5194/hess-11-1279-2007

Pokhrel, P., Gupta, H. V., & Wagener, T. (2008). A spatial regularization approach to parameter estimation for a distributed watershed model. *Water Resources Research*, *44*(12). https://doi.org/10.1029/2007WR006615

Pomeroy, J., Macdonald, M. K., Debeer, C. M., & Brown, T. (2009). Modelling Alpine Snow Hydrology in the Canadian Rocky Mountains. *77th Western Snow Conference*, 9, Canmore, Canada.

Pomeroy, J., Fang, X., & Ellis, C. (2012). Sensitivity of snowmelt hydrology in Marmot Creek, Alberta, to forest cover disturbance. *Hydrological Processes*, *26*(12), 1892–1905. https://doi.org/10.1002/hyp.9248

Pomeroy, J. W., Fang, X., & Rasouli, K. (2015). Sensitivity of snow processes to warming in the Canadian Rockies. *72nd Eastern Snow Conference*, Sherbrooke, Quebec, Canada, 22–33. 9-11 June.

Pomeroy, J. W., & Gray, D. M. (1995). Snowcover Accumulation, Relocation and Management. *Hydrological Sciences Journal*, 40(1). 125. https://doi.org/10.1080/02626669509491396

Pomeroy, J. W., Gray, D. M., Brown, T., Hedstrom, N. R., Quinton, W. L., Granger, R. J., & Carey, S. K. (2007). The cold regions hydrological model : a platform for basing process representation and model structure on physical evidence. *Hydrological Processes*, *21*, 2650–2667. https://doi.org/10.1002/hyp

Pomeroy, J. W., Parviainen, J., Hedstrom, N., & Gray, D. M. (1998). Coupled modelling of forest snow interception and sublimation. *Hydrological Processes*, *12*(15), 2317–2337. https://doi.org/10.1002/(SICI)1099-1085(199812)12:15<2317::AID-HYP799>3.0.CO;2-X

Pomeroy, J.W., Gray, D.M., Brown, T., Hedstrom, N.R., Quinton, W.L., Granger, R.J., & Carey, S.K., 2007. The cold regions hydrological process representation and model: a platform for basing model structure on physical evidence. *Hydrol. Process*. 21 (19), 2650–2667.

Price, K., Purucker, S. T., Kraemer, S. R., Babendreier, J. E., & Knightes, C. D. (2014). Comparison of radar and gauge precipitation data in watershed models across varying spatial and temporal scales. *Hydrological Processes*, *28*(9), 3505–3520. https://doi.org/10.1002/hyp.9890

Priestley, C. H. B., & Taylor, R. J. (1972). On the Assessment of Surface Heat Flux and Evaporation Using Large-Scale Parameters. *Monthly Weather Review*, *100*(2), 81–92. https://doi.org/10.1175/1520-0493(1972)100<0081:OTAOSH>2.3.CO;2

Przeczek, K., Déry S., Menounos B., & Moore D. (2009). Field Testing and Comparison of Four Snowmelt Model Approaches in the Quesnel Highlands, Interior British Columbia. *Proceedings of the 77th Annual Western Snow Conference.*

Raat, K. J., Vrugt, J. a., Bouten, W., & Tietema, A. (2004). Towards reduced uncertainty in catchment nitrogen modelling: quantifying the effect of field observation uncertainty on model calibration. *Hydrology and Earth System Sciences*, *8*(4), 751–763. https://doi.org/10.5194/hess-8-751-2004

Rabiti, C., Alfonsi, A., Cogliati, J., Mandelli, D., Kinoshita, R., & Sen, S. (2015). RAVEN User Manual, Revision 1. Idaho National Laboratory, Battelle Energy Alliance for the United States Department of Energy.

Razavi, T. (2014). Streamflow Estimation in Ungauged Watersheds (Ph.D thesis), Department of Civil Engineering and the School of Graduate Studies of McMaster University.Hamilton, Canada.

Razavi, S., & Gupta, H.V. (2015), What do we mean by sensitivity analysis? The need for comprehensive characterization of ‘‘global’’ sensitivity in Earth and Environmental systems models, *Water Resour. Res.*, 51, 3070–3092, doi:10.1002/2014WR01652

Razavi, S., & Gupta, H. V., (2016a), A new framework for comprehensive, robust, and efficient global sensitivity analysis: 1. Theory, *Water Resources Research*, 51, doi:10.1002/2015WR017558

Razavi, S., & Gupta, H. V. (2016b). A new framework for comprehensive, robust, and efficient

global sensitivity analysis: 2. Application. Water Resources Research, 52(1), 440-455.

Reid, I.A., & Charbonneau, J. (1979). Glaciers surveys in Alberta. IWD Report Series 65. *Water Resources Branch*, Inland Waters Directorate, Environment Canada, Ottawa, Canada.

Rodenhuis, D. R., Bennett, K. E., Werner, A. T., Murdock, T. Q., & Bronaugh, D. (2007). Hydro-climatology and Future Climate Impacts in British Columbia (Climate Overview). *Pacific Climate Impacts Consortium*. University of Victoria, British Columbia, Canada

Sælthun N.R. (1996). The "Nordic" HBV model. Description and documentation of the model version developed for the project Climate Change and Energy Production. NVE publication (7). *Water Resources and Energy Administration*. Oslo, Norwegian.

Sandink, D., Kovacs, P., Oulahen, G., & McGillivray, G. (2010). Making Flood Insurable for Canadian Homeowners: A Discussion Paper. *Institute for Catastrophic Loss Reduction & Swiss Reinsurance Company Ltd*, (November). University of Toronto, Toronto, Canada

Sangvaree, W., & Yevjevich, V. (1977). Effects of Forest and Agricultural Land Use on Flood Unit Hydrographs. *Hydrology Papers 92*, (92), 32. Colorado State University, Colorado, U.S.

Saltelli, A. (1999). Sensitivity analysis: Could better methods be used? Journal of Geophysical Research, 104(D3), 3789. https://doi.org/10.1029/1998JD100042

Searcy, J. K. (1959). Manual of Hydrology: Part 2. Low-Flow Techniques - Flow-Duration Curves. *Geological Survey Water-Supply Paper 1542-A*, 33. https://doi.org/10.1002/047147844X.sw321

Seibert, J. (1997). Estimation of Parameter Uncertainty in the HBV Model. *Nordic Hydrology*, *28*(1982), 247–262. https://doi.org/10.2166/nh.1997.015

Seibert, J. (1999). Regionalisation of parameters for a conceptual rainfall-runoff model. *Agricultural and Forest Meteorology, 98–99*, 279–293. https://doi.org/10.1016/S0168-1923(99)00105-7

Servat, E., & Dezetter, A. (1991). Selection of calibration objective fonctions in the context of rainfall-ronoff modelling in a Sudanese savannah area. *Hydrological Sciences Journal*, *36*(4), 307–330. https://doi.org/10.1080/02626669109492517

Sheikholeslami, R., & Razavi, S. (2017). Progressive Latin Hypercube Sampling: An efficient approach for robust sampling-based analysis of environmental models. *Environmental Modelling & Software*, *93*, 109–126. https://doi.org/10.1016/j.envsoft.2017.03.010

Sheikholeslami, R., Yassin, F., Lindenschmidt, K.-E., & Razavi, S. (2017). Improved understanding of river ice processes using global sensitivity analysis approaches. *Journal of Hydrologic Engineering*, *22*(11), 1–11. https://doi.org/10.1061/(ASCE)HE.1943-5584.0001574

Shen, Z. Y., Chen, L., & Chen, T. (2012). Analysis of parameter uncertainty in hydrological and sediment modeling using GLUE method: A case study of SWAT model applied to Three Gorges Reservoir Region, China. *Hydrology and Earth System Sciences*, *16*(1), 121–132. https://doi.org/10.5194/hess-16-121-2012

Shi, Y., Davis, K. J., Zhang, F., Duffy, C. J., & Yu, X. (2014). Parameter estimation of a physically based land surface hydrologic model using the ensemble Kalman filter: A synthetic experiment. *Water Resources Research*, *50*(1), 706–724. https://doi.org/10.1002/2013WR014070

Sikorska, A. E., Scheidegger, A., Banasik, K., & Rieckermann, J. (2012). Bayesian uncertainty assessment of flood predictions in ungauged urban basins for conceptual rainfall-runoff models. *Hydrology and Earth System Sciences*, *16*(4), 1221–1236. https://doi.org/10.5194/hess-16-1221-2012

Singh, A., Rudra, R., & Gharabaghi, B. (2012). Evaluation of CANWET model for hydrologic simulations for upper Canagagigue Creek watershed in southern Ontario. *Csbe-Scgab.Ca*, *54*, 7–18. Retrieved from http://www.csbe-scgab.ca/docs/journal/54/C12014.pdf

Singh, V. P., & Woolhiser, D. A. (2002). Mathematical Modeling of Watershed Hydrology. *Journal of Hydrologic Engineering*, *7*(4), 270–292. https://doi.org/10.1061/(ASCE)1084-

0699(2002)7:4(270)

Sivapalan, M. (2003). Prediction in ungauged basins: a grand challenge for theoretical hydrology. *Hydrological Processes*, *17*(15), 3163–3170. https://doi.org/10.1002/hyp.5155

Sobol, I. (1967). On the distribution of points in a cube and the approximate evaluation of integrals. *USSR Computational Mathematics and Mathematical Physics, 7 (4).* https://doi.org/10.1016/0041-5553(67)90144-9

Sobol, I. M. (1993). Sensitivity Estimates for Nonlinear Mathematical Models. *Mathematical Modeling and Computational Experiment*. https://doi.org/1061-7590/93/04407-008

Sombroek, W. G. (1989). Geographic quantification of soils and changes in their properties, in Soils and the Greenhouse Effect, edited by A. F. Bouwman. *John Wiley, New York.* 35-59.

Son, K., & Sivapalan, M. (2007). Improving model structure and reducing parameter uncertainty in conceptual water balance models through the use of auxiliary data. *Water Resources Research*, *43*(1). https://doi.org/10.1029/2006WR005032

Song, K., Wang, Z., Liu, Q., Lu, D., Yang, G., & Zeng, L. (2009). Land use/land cover (LULC) characterizaitoin with MODIS time series data in the Amu River Basin, 2009 IEEE International Geoscience and Remote Sensing Symposium,5. University of Cape Town Cape Town, South Africa, 12-17 July.

Sorooshian, S., Duan, Q. Y., & Gupta, V. K. (1993). Calibration of Rainfall-Runoff Models - Application of Global Optimization to the Sacramento Soil-Moisture Accounting Model. *Water Resources Research*, *29*(4), 1185–1194. https://doi.org/10.1029/92WR02617

Spiegelhalter, K. (2010). Modelling the coupled influence of climate and glacier change on discharge (M.Sc thesis). Institute of Hydrology, Albert-Ludwigs-University of Freiburg, Germany.

Stahl, K., Moore, R. D., Shea, J. M., Hutchinson, D., & Cannon, A. J. (2008). Coupled modelling of glacier and streamflow response to future climate scenarios. *Water Resources Research*, *44*(2). https://doi.org/10.1029/2007WR005956

Stewart, I. T., Cayan, D. R., & Dettinger, M. D. (2005). Changes toward earlier streamflow timing across western North America. *Journal of Climate*, *18*(8), 1136–1155. https://doi.org/10.1175/JCLI3321.1

Stillman, S. T. (1996). A comparison of three automated precipitation simulation models : ANUSPLIN, MTCLIM-3D, and PRISM (M.Sc thesis), Earth Sciences, Montana State University, Montana, U.S.

Storr, D. (1967). Precipitation variation in a small forested watershed. 35th Annual Western Snow Conference, april 1967. Boise, U.S. https://westernsnowconference.org/sites/westernsnowconference.org/PDFs/1967Storr.pdf

Sullivan, C. (2002). Calculating a Water Poverty Index. *World Development*, *30*(7), 1195–1210. https://doi.org/10.1016/S0305-750X(02)00035-9

Sun, X., Mein, R. G., Keenan, T. D., & Elliott, J. F. (2000). Flood estimation using radar and raingauge data. *Journal of Hydrology*, *239*(1–4), 4–18. https://doi.org/10.1016/S0022-1694(00)00350-4

Tennant, C., & Menounos, B. (2013). Glacier change of the Columbia Icefield, Canadian Rocky Mountains, 1919-2009. *Journal of Glaciology*, *59*(216), 671–686. https://doi.org/10.3189/2013JoG12J135

Tesemma, Z. K., Wei, Y., Peel, M. C., & Western, A. W. (2015). The effect of year-to-year variability of leaf area index on Variable Infiltration Capacity model performance and simulation of runoff. *Advances in Water Resources*, *83*, 310–322. https://doi.org/10.1016/j.advwatres.2015.07.002

Thornthwaite, C. W. (1948). An Approach toward a Rational Classification of Climate. *Geographical Review*, *38*(1), 55. https://doi.org/10.2307/210739

Todini, E. (2009). Predictive uncertainty assessment in real time flood forecasting. *Uncertainties in Environmental Modelling and Consequences for Policy Making*, 205–228. https://doi.org/10.1007/978-90-481-2636-1_9

Tsonis, A. A. (1996). Widespread increases in low-frequency variability of precipitation over the past century. *Nature*, *382*(6593), 700–703. https://doi.org/10.1038/382700a0

Tsonis, A. A. (2004). Is Global Warming Injecting Randomness Into the Climate System ? *Distribution*, *85*(38), 361–364. https://doi.org/10.1029/2001JB000269.Roberts

Tuo, Y., Duan, Z., Disse, M., & Chiogna, G. (2016). Evaluation of precipitation input for SWAT modeling in Alpine catchment: A case study in the Adige river basin (Italy). *Science of the Total Environment*, *573*, 66–82. https://doi.org/10.1016/j.scitotenv.2016.08.034

Uhlenbrook, S., Seibert, J., Leibundgut, C., & Rodhe, A. (1999). Prediction uncertainty of conceptual rainfall-runoff models caused by problems in identifying model parameters and structure. *Hydrological Sciences Journal*, *44*(5), 779–797. https://doi.org/10.1080/02626669909492273

Uhlenbrook, S., & Wenninger, J. (2006). Identification of flow pathways along hillslopes using electrical resistivity tomography (ERT). In *Predictions in Ungauged Basins: Promise and Progress*, (Proceedings of symposium S7 held during the Seventh IAHS Scientific Assembly at Foz do Iguaçu, Brazil, (April 2005). 303, 15–20.

Uppala, S. M., KÅllberg, P. W., Simmons, A. J., Andrae, U., Bechtold, V. D. C., Fiorino, M., … Woollen, J. (2005). The ERA-40 re-analysis. *Quarterly Journal of the Royal Meteorological Society*, *131*(612), 2961–3012. https://doi.org/10.1256/qj.04.176

USDA Natural Resources Conservation Service. Hydrology. In *National Engineering Handbook*; USDA Soil Conservation Service: Washington, DC, USA, 1972; Chapter 21.

Valeo, C., Xiang, Z., Bouchart, F. J.-C., Yeung, P., & Ryan, M. C. (2007). Climate Change Impacts in the Elbow River Watershed. *Canadian Water Resources Journal*, *32*(4), 285–302. https://doi.org/10.4296/cwrj3204285

Vanderhoof, M. K., & Williams, C. A. (2015). Persistence of MODIS evapotranspiration impacts from mountain pine beetle outbreaks in lodgepole pine forests, south-central rocky mountains. *Agricultural and Forest Meteorology*, *200*, 78–91.

https://doi.org/10.1016/j.agrformet.2014.09.015

Venturini, V., Islam, S., & Rodriguez, L. (2008). Estimation of evaporative fraction and evapotranspiration from MODIS products using a complementary based model. *Remote Sensing of Environment*, *112*(1), 132–141. https://doi.org/10.1016/j.rse.2007.04.014

Vinukollu, R. K., Wood, E. F., Ferguson, C. R., & Fisher, J. B. (2011). Global estimates of evapotranspiration for climate studies using multi-sensor remote sensing data: Evaluation of three process-based approaches. *Remote Sensing of Environment*, *115*(3), 801–823. https://doi.org/10.1016/j.rse.2010.11.006

Vivoni, E. R., Di Benedetto, F., Grimaldi, S., & Eltahir, E. A. B. (2008). Hypsometric control on surface and subsurface runoff. Water Resources Research, 44(12). https://doi.org/10.1029/2008WR006931

Vogel, R. M., & Fennessey, N. M. (1995). Flow duration curves II: a review of applications in water resources planning. *Journal of the American Water Resources Association*, *31*(6), 1029–1039. https://doi.org/10.1111/j.1752-1688.1995.tb03419.x

Vrugt, J. A., Gupta, H. V., Bastidas, L. A., Bouten, W., & Sorooshian, S. (2003). Effective and efficient algorithm for multiobjective optimization of hydrologic models. *Water Resources Research*, *39*(8). https://doi.org/10.1029/2002WR001746

Wada, Y., Van Beek, L. P. H., Wanders, N., & Bierkens, M. F. P. (2013). Human water consumption intensifies hydrological drought worldwide. *Environmental Research Letters*, *8*(3). https://doi.org/10.1088/1748-9326/8/3/034036

Wagener, T., & Gupta, H. V. (2005). Model identification for hydrological forecasting under uncertainty. *Stochastic Environmental Research and Risk Assessment*, *19*(6), 378–387. https://doi.org/10.1007/s00477-005-0006-5

Walker, W. E., Harremoës, P., Rotmans, J., van der Sluijs, J. P., van Asselt, M. B. A., Janssen, P., & Krayer von Krauss, M. P. (2003). Defining Uncertainty: A Conceptual Basis for Uncertainty Management in Model-Based Decision Support. *Integrated Assessment*, *4*(1), 5–17. https://doi.org/10.1076/iaij.4.1.5.16466

Wallach, D. (2006). Evaluating Crop Models. In: Wallach, D., Makowski, D. and Jones, J.W., Eds., Working with Dynamic Crop Models Evaluation, Analysis, Parameterization, and Applications, Elsevier, Amsterdam, 11-54.

Wang, X., & Melesse, A. (2005). Evaluation of the SWAT model's snowmelt hydrology in a northwestern Minnesota watershed. *Transactions of the ASAE*, *48*(4), 1–18. https://doi.org/10.1002/hyp.7457

Weedon, G. P., Balsamo, G., Bellouin, N., Gomes, S., Best, M. J., & Viterbo, P. (2014). The WFDEI meteorological forcing data set: WATCH Forcing data methodology applied to ERA-Interim reanalysis data. *Water Resources Research*, *50*(9), 7505–7514. https://doi.org/10.1002/2014WR015638

Wheater, H., & Gober, P. (2013). Water security in the Canadian Prairies: science and management challenges. *Philosophical Transactions of the Royal Society A: Mathematical, Physical and Engineering Sciences*, *371*(2002).https://doi.org/10.1098/rsta.2012.0409

Whitfield, P. H. (2012). Floods in future climates: A review. *Journal of Flood Risk Management*, 5(4), 336-365. https://doi.org/10.1111/j.1753-318X.2012.01150.x

Whitfield, P. H., Cannon, A. J., & Reynolds, C. J. (2002). Modelling Streamflow in Present and Future Climates: Examples from the Georgia Basin, British Columbia. *Canadian Water Resources Journal*, *27*(4), 427–456. https://doi.org/10.4296/cwrj2704427

Willmott, C. J. 1981. On the validation of models. *Physical Geography*, *2(2)*, 184-194.

Winsemius, H. C. (2009). Satellite data as complementary information for hydrological modelling (Ph.D thesis), Water Resources Section, Faculty of Civil Engineering and Geosciences, Delft University of Technology, Delft, Netherlands.

Wong, J. S., Razavi, S., Bonsal, B. R., Wheater, H. S., & Asong, Z. E. (2017). Inter-comparison of daily precipitation products for large-scale hydro-climatic applications over Canada. *Hydrology and Earth System Sciences*, *21*(4), 2163–2185. https://doi.org/10.5194/hess-21-2163-2017

Xu, C. (2002). Textbook of Hydrologic Models (Eddition 2002). Department of Earth Sciences

Hydrology, Uppsala University. Uppsala, Sweden.

Xu, T. & Hutchinson, M. (2011) ANUCLIM Version 6.1 User Guide. The Australian National University, Fenner School of Environment and Society, Canberra.

Yan, H., Nix, H. A., Hutchinson, M. F., & Booth, T. H. (2005). Spatial interpolation of monthly mean climate data for China. *International Journal of Climatology*, *25*(10), 1369–1379. https://doi.org/10.1002/joc.1187

Yang, Y., Wang, G., Wang, L., Yu, J., & Xu, Z. (2014). Evaluation of gridded precipitation data for driving SWAT model in area upstream of three gorges reservoir. *PLoS ONE*, *9*(11). https://doi.org/10.1371/journal.pone.0112725

Zeweldi, D. a., Gebremichael, M., & Downer, C. W. (2011). On CMORPH Rainfall for Streamflow Simulation in a Small, Hortonian Watershed. *Journal of Hydrometeorology*, *12*(3), 456–466. https://doi.org/10.1175/2010JHM1270.1

Zhao, K. (2013). Validation of the Canadian Precipitation Analysis (CaPA) for Hydrological Modelling in the Canadian Prairies (M.Sc thesis). Department of Civil Engineering University of Manitoba, Winnipeg, Canada.

6 APPENDIX

Table 6.1: Average temperature (T) and annual precipitation (P, mm/year)

	ANUSPLIN		CaPA		WFDEI	
Basin ID	**P**	**T**	**P**	**T**	**P**	**T**
08NP004	794.31	2.41	829.24	2.67	759.23	2.39
08NK002	701.28	1.35	647.79	1.12	781.73	-0.06
08NG065	723.54	1.73	592.73	1.04	555.14	0.12
08ND012	1081.41	0.68	1000.43	0.18	1297.92	-0.25
08NB019	1177.64	0.37	835.41	-0.29	1363.83	-1.32
08NA002	831.7	0.75	574.97	0.39	631.47	-0.23
08KB003	661.43	1.3	1263.22	0.99	814.58	1.56
08KA005	745.61	-0.07	825.52	-0.9	646.35	0.32
08NB014	1066.13	0.39	880.14	-0.76	1339.09	-0.43
08NB012	797.41	-0.58	719.42	-1.94	684.91	-1.69
08LB038	897.18	1.14	1095.74	0.42	1040.19	0.76
07FB006	581.93	0.95	835.81	0.83	796.88	0.59
07FB003	563.48	1.16	765.41	1.01	791.38	0.75
07AA001	677.54	-0.33	599.74	-1.42	590.36	-0.41
07EC002	584.7	-0.06	875.06	-0.11	512.15	-0.26
07EC004	582.45	-0.48	757.98	-0.67	505.35	-0.74
07ED003	544.43	1.12	729.79	1.37	578.75	0.83
07EE007	580.51	1.89	1082.39	1.67	839.91	1.38
05AA008	628.66	2.68	573.08	2.32	821.46	1.33
05AA022	758.18	2.88	701.26	2.68	769.98	1.61
05AA023	607.99	2.59	552.64	2.45	749.38	0.77
05BB001	591.56	-0.51	594.57	-1.34	568.51	-2.16
05BG006	613.55	1.51	517.6	1.01	583.59	-0.41
05BL022	677.35	0.71	594.66	0.54	722.03	-1.28
05DA007	786.29	-0.97	744.94	-2.1	690.22	-1.9

Table 6.2: Runoff ratio of basins for different climate products

Basin ID	ANUSPLIN	CaPA	WFDEI
08NP004	0.84	0.8	0.88
08NK002	0.69	0.75	0.62
08NG065	0.64	0.78	0.83
08ND012	1.18	1.28	0.98
08NB019	0.98	1.38	0.85
08NA002	0.62	0.9	0.82
08KB003	2	1.05	1.62
08KA005	1.2	1.08	1.38
08NB014	1.26	1.53	1.01
08NB012	1.14	1.26	1.33
08LB038	1.38	1.13	1.19
07FB006	1.37	0.95	1
07FB003	1.25	0.92	0.89
07AA001	0.25	0.28	0.28
07EC002	0.9	0.6	1.03
07EC004	1	0.77	1.16
07ED003	0.79	0.59	0.74
07EE007	1.65	0.89	1.14
05AA008	0.61	0.67	0.47
05AA022	0.79	0.86	0.78
05AA023	0.47	0.51	0.38
05BB001	0.87	0.87	0.91
05BG006	0.37	0.43	0.39
05BL022	0.56	0.64	0.53
05DA007	1.02	1.08	1.16